

République Algérienne Démocratique et Populaire  
Ministère de l'Enseignement Supérieur et de la Recherche Scientifique



Ecole Nationale Polytechnique  
Département d'Electronique

Laboratoire des Dispositifs de Communication  
et de Conversion Photovoltaïque



# PhD Thesis in Electronics

Presented by:

**BENNIA Rachid**

Entitled

---

## Power Optimization in Partially Shaded PV Arrays using the Hybrid PSO-CS Metaheuristic Algorithm

---

Members of jury:

Mr. Hicham BOUSBIA-SALAH	MCA - (ENP)	President
Mr. Cherif LARBES	Pr – (ENP)	Supervisor
Mrs. Faiza BELHACHAT	MCA – (ENSTA)	Co-Supervisor
Mr. Mourad ADNANE	Pr – (ENP)	Examinator
Mrs. Linda HASSAINE	DR – (CDER)	Examinator
Mrs. Sabrina TITRI	MRA – (CDTA)	Examinator

**ENP 2025**



République Algérienne Démocratique et Populaire  
Ministère de l'Enseignement Supérieur et de la Recherche Scientifique



المدرسة الوطنية المتعددة التقنيات  
Ecole Nationale Polytechnique

Ecole Nationale Polytechnique  
Département d'Electronique

Laboratoire des Dispositifs de Communication  
et de Conversion Photovoltaïque



# PhD Thesis in Electronics

Presented by:

**BENNIA Rachid**

Entitled

---

## Power Optimization in Partially Shaded PV Arrays using the Hybrid PSO-CS Metaheuristic Algorithm

---

Members of jury:

Mr. Hicham BOUSBIA-SALAH	MCA - (ENP)	President
Mr. Cherif LARBES	Pr – (ENP)	Supervisor
Mrs. Faiza BELHACHAT	MCA – (ENSTA)	Co-Supervisor
Mr. Mourad ADNANE	Pr – (ENP)	Examinator
Mrs. Linda HASSAINE	DR – (CDER)	Examinator
Mrs. Sabrina TITRI	MRA – (CDTA)	Examinator

**ENP 2025**

République Algérienne Démocratique et Populaire  
Ministère de l'Enseignement Supérieur et de la Recherche Scientifique



Ecole Nationale Polytechnique  
Département d'Electronique

Laboratoire des Dispositifs de Communication  
et de Conversion Photovoltaïque



# Thèse de Doctorat en Electronique

Option: Electronique

Présentée par:

**BENNIA Rachid**

---

## Optimisation de la Puissance des Champs Photovoltaïques Partiellement Ombragés par l'Algorithme Meta-heuristique Hybride PSO-CS

---

Membres du jury:

M. Hicham BOUSBIA-SALAH	MCA – (ENP)	Président
M. Cherif LARBES	Pr – (ENP)	Directeur de thèse
Mme. Faiza BELHACHAT	MCA – (ENSTA)	Co-Directeur de thèse
M. Mourad ADNANE	Pr – (ENP)	Examineur
Mme. Linda HASSAINE	DR – (CDER)	Examineur
Mme. Sabrina TITRI	MRA – (CDTA)	Examineur

**ENP 2025**



## ملخص

تقدم هذه الأطروحة مساهمة في دراسة وتحسين الطاقة المولدة من الأنظمة الكهروضوئية المعرضة للتظليل الجزئي من خلال استغلال الخوارزميات الذكية لاستخلاص أقصى طاقة ممكنة. في حالة التظليل الجزئي، تتميز المنحنيات البيانية للألواح الكهروضوئية بعدة نقاط قصوى مما يمثل عائقا للخوارزميات التقليدية استخراج أقصى قدرة ممكنة باعتبارها تتميز بحلول موضعية. في نفس السياق، تعتبر الخوارزميات الذكية المتقدمة بديلا مناسباً غير أنها لا تخلو من بعض النقص حيث يحتمل أن تقترب إلى الحد الأقصى المحلي نتيجة بعض سيناريوهات التظليل المعقدة أو بسبب سوء برمجة المعاملات أثناء تغير المناخ، مما يتسبب في خسائر هائلة في الطاقة. لتفادي هذه الصعوبات قمنا بتقديم وتصميم برنامج هجين ذكي يجمع بين خوارزمية تحسين سرب الجسيمات (PSO) وخوارزمية تحسين الوقواق (CSA) القادر على تتبع الاستطاعة القصوى في حالات التظليل الجزئي والتغير السريع للأحوال الجوية. يتميز الحل الهجين المقترح باستغلال نقاط قوة كل خوارزمية على حدى مع التقليل من عيوبهما، مما يعزز الاستغلال الأمثل للأنظمة الكهروضوئية. كما يتميز البرنامج المقترح بتحسين الأداء العام مع الوصول إلى القيمة القصوى في وقت قياسي ويتميز أيضا بسرعة الاستجابة والثبات أثناء التغيرات المناخية المفاجئة وهذا بفضل وظيفة إعادة الضبط المندمجة في النظام الخاص بنا. تم اختبار وحدة التحكم الهجينة المقترحة مع أنظمة كهروضوئية مرتبة على التسلسل وعلى التوازي بأحجام متعددة في ظل سيناريوهات تظليل مختلفة. وكانت النتائج التي تم الحصول عليها مرضية للغاية من حيث الكفاءة والاستقرار ووقت التقارب. تظهر هذه النتائج أن وحدة التحكم الهجينة الخاصة بنا تساهم بشكل كبير في حل مشكلة تحسين الطاقة، وبالتالي توفير حل مناسب وفعال لإدارة الأنظمة الكهروضوئية الخاضعة للتظليل الجزئي أو التغيرات السريعة في الظروف المناخية.

### الكلمات المفتاحية:

الأنظمة الكهروضوئية، التحسين، التظليل الجزئي، تتبع نقطة الاستطاعة العظمى، الخوارزميات الذكية، الخوارزميات الهجينة.

## Résumé

Cette thèse présente une contribution à l'étude et à l'optimisation de l'énergie générée des champs photovoltaïques (PV) soumis à un ombrage partiel (PS) en exploitant les algorithmes méta-heuristiques pour la poursuite du point de puissance maximale (MPP). Dans ces conditions, les caractéristiques de sortie P-V et I-V d'un champ photovoltaïque sont multimodales. Les techniques MPPT conventionnelles sont inadéquates dans ces situations et convergent souvent vers un maximum local ce qui cause des pertes énormes en énergie. En plus, les algorithmes méta-heuristiques peuvent présenter des difficultés de convergence sous certains scénarios d'ombrages complexes ou dû à un mauvais ajustement des paramètres lors des changements climatiques. D'où, l'objectif de notre travail est de présenter et concevoir une approche hybride méta-heuristique intelligente combinant l'algorithme d'optimisation par essaim particulaire (PSO) et l'algorithme d'optimisation du coucou (CSA) capable de poursuivre la puissance maximale globale. Cette approche hybride exploite les atouts de chaque algorithme tout en réduisant leurs inconvénients, ce qui favorise une optimisation maximale. Les avantages de l'approche méta-heuristique hybride proposée incluent, entre autres, des performances améliorées, un temps de convergence réduit et une robustesse remarquable aux changements climatiques grâce à la fonction de réinitialisation intégrée dans notre système MPPT. Le contrôleur hybride MPPT proposé a été testé avec des configurations PV séries et séries-parallèles de tailles multiples sous scénarios d'ombrages variés. Les résultats obtenus ont été très satisfaisants en termes d'efficacité, de stabilité et de temps de convergence. Ces résultats montrent que notre contrôleur MPPT hybride contribue de manière significative à résoudre le problème d'optimisation de puissance, fournissant ainsi une solution adéquate et efficace pour la gestion des systèmes PV soumis à un ombrage partiel ou à des changements rapides des conditions climatiques.

### Mots clés :

Système photovoltaïque, optimisation, ombrage partiel, MPPT, algorithmes méta-heuristiques, PSO, CS, hybride.

## Abstract

This thesis presents a contribution to the study and optimization of the energy generated by photovoltaic (PV) arrays subjected to partial shading (PS) applying meta-heuristic algorithms to track the global maximum power point (GMPP). Under PSC, the P-V and I-V output characteristics of a photovoltaic array are multimodal. Conventional MPPT techniques are mostly local searches and thus cannot guarantee global optimality resulting in significant power losses. Additionally, metaheuristic algorithms, might converge to a local maximum power point (LMPP) rather than the global maximum (GMPP) under certain complex shading scenarios or when their parameters are not adjusted precisely to mitigate the PS effect. In this context, this thesis presents an intelligent hybrid approach combining two Swarm Intelligence metaheuristic algorithms namely, Particle Swarm Optimization (PSO) and Cuckoo Search Algorithm (CSA). This hybrid approach enhances the strengths of each algorithm while minimizing their drawbacks when used separately, which improves significantly the PV system output. The proposed hybrid meta-heuristic approach overcomes the shortcomings of conventional techniques and many similar Swarm Intelligence (SI) approaches; it comes with improved performance as well as reduced convergence time and remarkable robustness to weather changes due to the reset function integrated within the proposed MPPT system.

The proposed hybrid MPPT controller has been validated using series and series-parallel PV configurations of different dimensions under various shading scenarios. The obtained results were very satisfactory in terms of efficiency, stability and convergence time. We can conclude that the proposed hybrid MPPT controller contributes significantly in optimizing the power output of PV systems affected by PS or rapid change of weather circumstances.

### Keywords:

Photovoltaic system, optimization, partial shading, MPPT, meta-heuristic algorithms, PSO, CS, hybrid.

*I dedicate this work to all my family members, especially to the cherished memory of my beloved mother, whose love and wisdom have guided me throughout my life. Though she is no longer with us, her spirit inspires and motivates me in every endeavor. This achievement stands as a tribute to her enduring legacy and the profound impact she has had on shaping who I am today.*

*I also dedicate this work to the loving memory of my wife, who has been my constant source of inspiration and strength. Although, she left us forever; her spirit guides and motivates me. This work is a testament to her enduring legacy and her profound impact on my life.*

*Finally, to my beloved children: Hamoud, Khalilou, and Anfoula.*



## **Power Optimization in Partially Shaded PV Arrays using the Hybrid PSO-CS Metaheuristic Algorithm**

## ACKNOWLEDGMENT

This thesis has been conducted at the Laboratory of Communication Devices and Photovoltaic Conversion of the National Polytechnic School Department of Electronics (ENP) - Algiers.

Initially, I would like to extend my deepest gratitude to my project supervisors, Professor Cherif Larbes and Doctor Faiza Belhachat, for their invaluable help, unwavering support, and insightful guidance throughout my research journey. Their expertise and encouragement have been pivotal in overcoming challenges and achieving my research work. Their mentorship has enhanced my academic and professional growth and inspired a passion for continuous learning.

I also want to express my sincere gratitude to the President of the jury, Dr. BOUSBIA-SALAH Hicham from the National Polytechnic School, and the members of the jury, Prof. ADNANE Mourad from the National Polytechnic School (ENP), Dr. HASSAINE Linda from: The Renewable Energy Development Center (CDER) and Dr. TITRI Sabrina from: The Center for Development of Advanced Technologies (CDTA) for accepting to be members of the jury and for their precious time, insightful comments, and valuable suggestions and analysis of the present work.

Yet importantly, I would like to take this opportunity to express my appreciation and gratitude to my colleagues at the University of Bordj Bou Arréridj: Dr. Naoui Amar, Dean of the Faculty of Technology of the University of BBA, Dr. Yousfi Abderrahim, Head of the department of electronics at the University of BBA, Dr. Saidani Okba, Dr. Zerrouki Raouf and Dr. Talbi Billel for their support and encouragement during my research journey.

Finally, I express my deepest appreciation and gratitude to everyone who contributed directly or indirectly to the completion of this work.

**Rachid BENNIA**

## TABLE OF CONTENTS

<a href="#">List of Figures</a>	
<a href="#">List of Tables</a>	
<a href="#">List of Acronyms</a>	
<a href="#">General introduction</a>	14
<b><a href="#">Chapter 1: Photovoltaic energy systems concepts and shading mitigation techniques</a></b>	<b>19</b>
1.1 <a href="#">Introduction</a>	20
1.2 <a href="#">Overview of photovoltaic generation systems</a>	20
1.3 <a href="#">Photovoltaic cells technologies</a>	21
1.4 <a href="#">Photovoltaic cells and photovoltaic modules</a>	26
1.4.1 <a href="#">Open circuit voltage and short circuit current</a>	27
1.4.2 <a href="#">Maximum Power Point</a>	27
1.4.3 <a href="#">Efficiency</a>	28
1.4.4 <a href="#">Fill Factor</a>	28
1.5 <a href="#">Effect of solar irradiance and temperature on the PV module</a>	28
1.5.1 <a href="#">Irradiance effect</a>	29
1.5.2 <a href="#">Temperature effect</a>	29
1.5.3 <a href="#">Spectral effect</a>	30
1.6 <a href="#">PV array modeling</a>	30
1.6.1 <a href="#">Single-diode model</a>	30
1.6.2 <a href="#">Two-diode model</a>	31
1.6.3 <a href="#">Multi-diode PV model</a>	32
1.7 <a href="#">DC-DC converters</a>	33
1.7.1 <a href="#">Buck converter</a>	34
1.7.2 <a href="#">Boost converter</a>	37
1.7.3 <a href="#">Buck-Boost converter</a>	39
1.8 <a href="#">Effect of partial shading on PV system performance</a>	41
1.9 <a href="#">Partial shading mitigation techniques</a>	45
1.9.1 <a href="#">PV system topologies</a>	46
1.9.1.1 <a href="#">Bypass and blocking diodes</a>	46
1.9.1.2 <a href="#">PV system architectures</a>	48
1.9.1.3 <a href="#">PV array configuration</a>	50

1.9.1.4 <a href="#">PV array reconfiguration</a> .....	51
1.9.2. <a href="#">MPPT techniques</a> .....	54
1.10 <a href="#">Conclusion</a> .....	55
<b><a href="#">Chapter 2: Maximum power point tracking techniques via metaheuristic approaches</a></b> .....	56
2.1 <a href="#">Introduction</a> .....	57
2.2 <a href="#">MPPT principle</a> .....	57
2.3 <a href="#">Challenges facing MPPT techniques</a> .....	57
2.4 <a href="#">Conventional MPPT techniques</a> .....	59
2.4.1 <a href="#">On-line techniques</a> .....	59
2.4.1.1 <a href="#">Perturb-and-Observe (P&amp;O) technique</a> .....	60
2.4.1.2 <a href="#">Incremental Conductance (InCond) technique</a> .....	60
2.4.2 <a href="#">Off-line techniques</a> .....	62
2.4.2.1 <a href="#">Fractional Open Circuit Voltage (FOCV) technique</a> .....	62
2.4.2.2 <a href="#">Fractional Short Circuit Current (FSCC) technique</a> .....	62
2.5 <a href="#">Maximum power extraction from the photovoltaic system under partial shading</a> <a href="#">Conditions</a> .....	62
2.6 <a href="#">Metaheuristic MPPT techniques</a> .....	65
2.6.1 <a href="#">Swarm intelligence-based MPPT techniques</a> .....	66
2.6.1.1 <a href="#">Particle Swarm Optimization-based MPPT</a> .....	66
2.6.1.2 <a href="#">Ant Colony Optimization Algorithm</a> .....	68
2.6.1.3 <a href="#">Artificial Bee Colony</a> .....	70
2.6.2 <a href="#">Evolutionary-based MPPT techniques</a> .....	72
2.6.2.1 <a href="#">Genetic Algorithm</a> .....	72
2.6.2.2 <a href="#">Differential Evolution Algorithm</a> .....	73
2.6.3 <a href="#">Nature Inspired-based MPPT techniques</a> .....	75
2.6.3.1 <a href="#">Cuckoo Search</a> .....	75
2.6.3.2 <a href="#">Grey Wolf Optimization technique</a> .....	78
2.6.3.3 <a href="#">Flower Pollination Algorithm</a> .....	81
2.6.3.4 <a href="#">Firefly Algorithm</a> .....	82
2.6.3.5 <a href="#">Bat Algorithm</a> .....	83
2.7 <a href="#">Hybrid-based MPPT techniques</a> .....	86
2.7.1 <a href="#">Hybrid soft computing – soft computing algorithm</a> .....	86

2.7.2	<a href="#">Hybrid soft computing-conventional</a>	90
2.7.2.1	<a href="#">Steps of the algorithm</a>	90
2.7.2.1.1	<a href="#">PSO method</a>	90
2.7.2.1.2	<a href="#">PO method</a>	91
2.8	<a href="#">Overview of recent hybrid MPPT techniques in PV systems subjected to PSCs</a>	93
2.9	<a href="#">Conclusion</a>	98
<b><a href="#">Chapter 3: Proposed hybrid MPPT algorithm for PV systems subjected to partial shading conditions</a></b>		<b>99</b>
3.1	<a href="#">Introduction</a>	100
3.2	<a href="#">Simulation of the PV array characteristics under partial shading</a>	100
3.3	<a href="#">Overview of used MPPT techniques</a>	103
3.3.1	<a href="#">PSO-based MPPT algorithm</a>	103
3.3.2	<a href="#">Cuckoo Search via Levy Flights</a>	104
3.3.2.1	<a href="#">Levy Flights</a>	105
3.4	<a href="#">Proposed hybrid PSO-CS-based MPPT technique (SHA)</a>	106
3.4.1	<a href="#">SHA-based MPPT details</a>	107
3.4.2	<a href="#">Convergence and initialization criteria</a>	108
3.5	<a href="#">Description of the proposed PV system</a>	109
3.6	<a href="#">Results and discussion</a>	111
3.6.1	<a href="#">Tracking performance under standard test conditions</a>	112
3.6.2	<a href="#">Tracking performance under rapid change in irradiance</a>	115
3.6.3	<a href="#">Performance comparison with other MPPT techniques</a>	117
3.6.4	<a href="#">Tracking performance for a parallel configuration</a>	121
3.6.5	<a href="#">Tracking performance for the second set of shading profiles</a>	122
3.6.6	<a href="#">Statistical analysis</a>	124
3.6.7	<a href="#">Comparative study</a>	125
3.7	<a href="#">Conclusion</a>	129
<a href="#">General conclusion</a>		130
<a href="#">Bibliography</a>		133
<a href="#">Publications</a>		147

## LIST OF FIGURES

<a href="#"><u>Fig. 1.1: (a) Typical solar cell - (b) Structure of a typical PV cell</u></a> .....	21
<a href="#"><u>Fig. 1.2: Equivalent circuit of a single PV diode model</u></a> .....	22
<a href="#"><u>Fig. 1.3: Equivalent circuit of a two-diode PV model</u></a> .....	22
<a href="#"><u>Fig. 1.4: (a) A silicon ingot - (b) Polycrystalline Solar Panels (Poly-SI)</u></a> .....	23
<a href="#"><u>Fig. 1.5: Thin-Film Solar Cells (TFSC)</u></a> .....	24
<a href="#"><u>Fig. 1.6: Tandem/silicon stacked solar cell module</u></a> .....	24
<a href="#"><u>Fig. 1.7: Different solar concentrators for Concentrated Photovoltaic (CPV) system</u></a> .....	25
<a href="#"><u>Fig. 1.8: PV cell, PV module, and PV array</u></a> .....	26
<a href="#"><u>Fig. 1.9 (a) Cadmium telluride (CdTe) PV array - (b) Monocrystalline PV array</u></a> .....	26
<a href="#"><u>Fig. 1.10: Current-Voltage characteristic (<math>I_{pv}</math>-<math>V_{pv}</math>) for a solar cell</u></a> .....	27
<a href="#"><u>Fig. 1.11: Current-Voltage and Power-Voltage characteristics for a solar cell</u></a> .....	28
<a href="#"><u>Fig. 1.12: Irradiance effect on output of the PV module</u></a> .....	29
<a href="#"><u>Fig. 1.13: Temperature effect on output of the PV module</u></a> .....	30
<a href="#"><u>Fig. 1.14: Equivalent circuit of a multi-diode PV model</u></a> .....	31
<a href="#"><u>Fig. 1.15: Equivalent circuit of a two-diode PV model</u></a> .....	32
<a href="#"><u>Fig. 1.16: Equivalent circuit of a multi-diode PV model</u></a> .....	33
<a href="#"><u>Fig. 1.17: Electrical circuit of the Buck converter</u></a> .....	35
<a href="#"><u>Fig. 1.18: Ideal output control characteristic curve for the buck converter</u></a> .....	36
<a href="#"><u>Fig. 1.19: Electrical circuit of a boost converter</u></a> .....	38
<a href="#"><u>Fig. 1.20: Boost converter's voltage gain</u></a> .....	38
<a href="#"><u>Fig. 1.21: Electrical circuit of a buck-boost converter</u></a> .....	40
<a href="#"><u>Fig. 1.22: P-V characteristic of PV module under PSC</u></a> .....	42
<a href="#"><u>Fig. 1.23: I-V characteristic of PV module under PSC</u></a> .....	42
<a href="#"><u>Fig. 1.24: I-V and P-V characteristics of PV module under various shading patterns</u></a> .....	44
<a href="#"><u>Fig. 1.25: Partial shading mitigation techniques</u></a> .....	45
<a href="#"><u>Fig. 1.26: PV array with the bypass and blocking diodes</u></a> .....	46
<a href="#"><u>Fig. 1.27: (a) Burns in PV module due to hotspots (b) Bypass diodes</u></a> .....	47
<a href="#"><u>Fig. 1.28: Bypass diodes effects on P-V characteristic</u></a> .....	47
<a href="#"><u>Fig. 1.29: PV system architectures (a) centralized (b) series-connected MIC</u></a>	

<a href="#"><u>(c) parallel-connected MIC (d) micro-inverters (e) interleaved DC–DC converter</u></a> .....	48
<a href="#"><u>Fig. 1.30: PV array configurations: (a) SP (b) TCT (c) BL and (d) HC</u></a> .....	50
<a href="#"><u>Fig. 1.31: Adaptive reconfiguration technique process</u></a> .....	53
<a href="#"><u>Fig. 1.32: PV system integrated with MPPT</u></a> .....	54
<a href="#"><u>Fig. 2.1: Challenges facing MPPT Techniques</u></a> .....	58
<a href="#"><u>Fig. 2.2: MPPT control system</u></a> .....	59
<a href="#"><u>Fig. 2.3: Flow chart of the Perturb &amp; Observe method</u></a> .....	60
<a href="#"><u>Fig. 2.4: Incremental Conductance Flow chart</u></a> .....	61
<a href="#"><u>Fig. 2.5: Influence of the load resistance on the operating point</u></a> .....	63
<a href="#"><u>Fig. 2.6: Influence of the irradiance on the MPP</u></a> .....	63
<a href="#"><u>Fig. 2.7: Multi-MPP due to PS effect</u></a> .....	64
<a href="#"><u>Fig. 2.8: Classification of MPPT-based Metaheuristic Algorithms</u></a> .....	65
<a href="#"><u>Fig. 2.9: Flowchart of PSO-based tracker</u></a> .....	68
<a href="#"><u>Fig. 2.10: Flowchart of the ACO Algorithm</u></a> .....	69
<a href="#"><u>Fig. 2.11: Flowchart of the Artificial Bee Colony Algorithm</u></a> . ....	71
<a href="#"><u>Fig. 2.12: Flowchart of the GA-based MPPT</u></a> .....	73
<a href="#"><u>Fig. 2.13: Flowchart of the DE algorithm</u></a> .....	74
<a href="#"><u>Fig. 2.14: Flowchart of the CS-based MPPT tracker</u></a> .....	77
<a href="#"><u>Fig. 2.15: Leadership pyramids</u></a> .....	79
<a href="#"><u>Fig. 2.16: Flowchart of the GWO Algorithm</u></a> .....	80
<a href="#"><u>Fig. 2.17: Flowchart of the Bat Algorithm</u></a> .....	85
<a href="#"><u>Fig. 2.18: Hunting procedure of the GWO technique</u></a> .....	88
<a href="#"><u>Fig. 2.19: Flowchart of the GWO-PSO Algorithm</u></a> .....	89
<a href="#"><u>Fig. 2.20: Hybrid PSO-PO Algorithm</u></a> .....	92
<a href="#"><u>Fig. 3.1: P-V characteristic under partial shading conditions</u></a> .....	101
<a href="#"><u>Fig. 3.2: P-V characteristics for the first set of PS profiles under 4S and 4S2P configurations</u></a> .....	102
<a href="#"><u>Fig. 3.3: P-V characteristics for the second set of PS profiles under 8S, 10S and 12S configurations</u></a> .....	103
<a href="#"><u>Fig. 3.4: Levy's flights in consecutive 50 steps</u></a> .....	105
<a href="#"><u>Fig. 3.5: Flowchart of SHA-based MPPT</u></a> .....	108



<a href="#"><u>Fig. 3.6: Proposed MPPT PV system along with PV array series configurations (n=4, 8, 10 and 12).</u></a>	109
<a href="#"><u>Fig. 3.7: Search process (Pest and Gbest) for the SHA under STC (G=1000 W/m<sup>2</sup>, T= 25°C).</u></a>	113
<a href="#"><u>Fig. 3.8: Selection process for SHA under STC</u></a>	113
<a href="#"><u>Fig. 3.9: SHA performance under STC. (G=1000 W/m<sup>2</sup>, T= 25°C).</u></a>	114
<a href="#"><u>Fig. 3.10: SHA performance under rapid change in irradiance</u></a>	116
<a href="#"><u>Fig. 3.11: Search process (Pest and Gbest) for SHA under rapid change in irradiance.....</u></a>	117
<a href="#"><u>Fig. 3.12: Performance comparison of SHA with other techniques under shading profile 1.</u></a>	117
<a href="#"><u>Fig. 3.13: SHA performance under shading profile 2</u></a>	119
<a href="#"><u>Fig. 3.14: SHA performance under shading profile 3</u></a>	120
<a href="#"><u>Fig. 3.15: Performance of SHA under shading profile 4 (4S2P).</u></a>	121
<a href="#"><u>Fig. 3.16: Performance of SHA, PSO and CS under 8S configuration.</u></a>	122
<a href="#"><u>Fig. 3.17: Performance of SHA, PSO and CS under 10S configuration.</u></a>	123
<a href="#"><u>Fig. 3.18: Performance of SHA, PSO and CS under 12S configuration.</u></a>	123
<a href="#"><u>Fig. 3.19: Graphical representation of average convergence time and average static efficiency for the first set of shading profiles.</u></a>	127
<a href="#"><u>Fig. 3.20: Graphical representation of average convergence time and static efficiency for the second set of shading profiles.</u></a>	128

## LIST OF TABLES

<b><u>Table. 1.1</u></b> PV cells' characteristics .....	<b>25</b>
<b><u>Table. 1.2</u></b> PV module configurations under different patterns .....	<b>43</b>
<b><u>Table. 1.3</u></b> Comparisons of the PV system architectures .....	<b>49</b>
<b><u>Table. 1.4</u></b> Benefits and shortcomings of different PV array configurations .....	<b>51</b>
<b><u>Table. 1.5</u></b> Advantages and disadvantages of the PV array reconfigurations .....	<b>54</b>
<b><u>Table. 3.1</u></b> First set of detailed profiles of PS used in this study.....	<b>101</b>
<b><u>Table. 3.2</u></b> Second set of detailed profiles of PS used in this study.....	<b>102</b>
<b><u>Table. 3.3</u></b> TP250 MBZ PV module parameters at STC.....	<b>110</b>
<b><u>Table. 3.4</u></b> Detailed algorithm parameters.....	<b>110</b>
<b><u>Table. 3.5</u></b> Performance comparison of the SHA with other methods for the first set of shading profiles.....	<b>122</b>
<b><u>Table. 3.6</u></b> Performance comparison of the SHA with other methods for the second set of shading profiles.....	<b>124</b>
<b><u>Table. 3.7</u></b> Statistical analysis of SHA against PSO and CS.....	<b>125</b>
<b><u>Table. 3.8</u></b> Performance comparison of the SHA with other SI-based MPPT techniques for the first set of shading profiles.....	<b>126</b>

## LIST OF ACRONYMS

RES: Renewable Energy Sources	IGWO: Improved GWO
PV : Photovoltaic	ACO: Ant Colony Optimization
GMPP: Global Maximum Power Point	ABC: Artificial Bee Colony
GP: Global peak	Pbest: Particle best
LP: Local peak	Gbest: Global best
LMPP: Local Maximum Power Point	$\omega$ : The inertia weight
MPP: Maximum power point	c1: Cognitive coefficient
MPPT: Maximum Power Point Tracking	c2: Social coefficient
PSC: Partial Shading Condition	d : Particle position
PS: Partial shading	v: Particle velocity
P-V: Power Voltage characteristic	r1, r2 : Random numbers from the range [0,1].
I-V: Current Voltage characteristic	$\oplus$ : Entry-wise multiplication
P&O: Perturb & observe method	$\lambda$ : Levy flight parameter
CS: Cuckoo search	$\alpha$ : Lévy multiplying coefficient
PSO: Particle swarm optimization	$u$ and $v$ : Normal distributions
SHA: Smart Hybrid Algorithm.	I <sub>pv</sub> : Photovoltaic current
STC: Standard Test Conditions	V <sub>pv</sub> : Photovoltaic voltage
I <sub>0</sub> : Diode saturation current	P <sub>pv</sub> : Photovoltaic power
V <sub>t</sub> : Thermal voltage	P <sub>a</sub> : probability
k: Boltzmann constant	P <sub>max</sub> : Maximum power
a: The ideality factor	V <sub>oc</sub> (V): Open-circuit voltage
N <sub>s</sub> : Number of series Cells per string	V <sub>mp</sub> (V): Voltage at MPP
T: The module's temperature in Kelvin.	I <sub>mp</sub> (A): Current at MPP
PWM: Pulse width modulation	I <sub>sc</sub> (A): Short circuit current
DC-DC: Direct Current to Direct Current conversion	DC: Duty Cycle
CCM: Continuous conduction mode	$\eta_{Static}$ : Static efficiency
DCM: Discontinuous conduction mode	$\eta_{Dynamic}$ : Dynamic efficiency
PVGS: Photovoltaic generation system.	GWO: Grey Wolf Optimization
CI: Computational Intelligence	PS-FW: Particle Swarm – Fire Works
FLC: Fuzzy Logic Control	DM-JAYA: Modified deterministic Jaya
ANN: Artificial Neural Networks	FW: Fire Works Algorithm
GA: Genetic Algorithm	FF: Fire Fly Algorithm
AI: Artificial Intelligence	Inc: Incremental Conductance
NA-PSO: New Adaptive PSO	Bat: Bat Algorithm
DE: Differential Evolution	FFA: Fusion Fire Fly Algorithm

### **General introduction**

Many governments worldwide have made renewable energy sources (RES) a key priority due to the massive rise in energy demand and the volatility of the fossil fuel market. RES have risen to the top of the global priority list because of the enormous increase in energy consumption and the instability of the fossil fuel market. Governments actively advocate them owing to the worldwide concern over CO<sub>2</sub> emissions from one side and their virtues from the other, leading to widespread adoption. A substantial amount of the energy sources utilized in both developed and emerging nations can be attributed to the combustion of fossil fuels. In developing countries, approximately 90% of the total heat is derived from oil, coal, and natural gas. Similarly, in developed countries, this figure stands at around 65% [1]. However, it is essential to note that these finite resources are expected to be depleted within the next few centuries [2]. These resources are widely recognized for their significant environmental, ecological, and health effects [3]. As a result, scientists and governments are increasingly directing their efforts toward improving energy efficiency and exploring various alternatives before resources are completely depleted.


RES have emerged as the primary solution in our pursuit of sustainable power [4]. They are often called the "energy sources of the future" due to their potential to meet the increasing global energy demands. The correlation between economic growth and energy demand is so robust that any economic theory would deem it essential to include this component in the equation for growth. RES are energy flows and resources that are continuously regenerated and may be extracted for use without causing a significant negative impact on the environment, leading to their worldwide adoption [5]. Several nations are establishing ambitious goals to strengthen and explore their RES, recognizing their unlimited availability and significant contribution to reducing pollution.


The positive impact of RES is reflected in the protection of ecosystems and the improvement of the environment. RES also play a vital role in preventing the greenhouse effect and addressing the global warming problem caused by the use of fossil fuels [6]. According to the International Energy Agency (IEA), renewable energy will contribute about 90% of global power production by 2050 to attain net zero gas emissions. RES include solar [7], wind [8], hydroelectric [9], geothermal [10], and biomass energy [11]. Unlike fossil fuels, renewable energy sources are


considered sustainable and environmentally friendly, as they are not finite and do not contribute significantly to greenhouse gas emissions. RES are characterized by the following key points:


- Solar energy is generated from sunlight using PV cells; it is becoming more popular owing to its decreasing cost and diversity in uses, ranging from household to large-scale solar plants.
- Wind energy is harnessed by transforming the kinetic energy of wind into electrical energy via turbines. Wind power has seen substantial expansion and is considered one of the most economically efficient methods of producing green power.
- Hydroelectric energy is generated by exploiting the energy of moving water, usually by constructing dams. It is important to acknowledge that well-established technology plays a crucial role in generating substantial electricity in numerous countries.
- Geothermal Energy employs the internal Earth's heat to produce electricity. It is particularly effective in areas with volcanic activity.
- Biomass Energy is obtained from organic matter, including plant and animal waste. Biomass may be transformed into biofuels or used directly for heating and generating energy.

RES are distinguished by their immense potential and benefits compared to traditional energy sources [12]. Some notable attributes include:

 Environmental Impact: It significantly reduces carbon emissions and air pollutants, enhancing public health and mitigating climate change.

 Economic Advantages: The renewable energy industry generates employment possibilities, thus contributing to economic prosperity.

 Renewable energy is crucial in enhancing national energy security by varying energy sources and decreasing dependence on imported fuels.

 Sustainability: Renewable energy sources are abundant and regenerated naturally, making them a long-term energy solution.

RES include mainly these important types: stand-alone, grid-connected, and hybrid systems [13]. Solar energy is regarded as one of the most promising renewable energy sources. PV arrays are installed worldwide to convert solar irradiation into useful energy. Various configurations are used to connect PV modules to obtain the required power ratings for any application [14]. However,

the PV output characteristic is significantly affected by climatic conditions. When PV modules are subjected to uniform irradiation, the resulting power-voltage (P-V) curve is characterized by a single peak representing the maximum power point [15]. When partial shading (PS) happens, the P-V characteristic becomes multi-modal due to the incorporated bypass diodes. Under this situation, this characteristic shows several maxima with many local maximum power points (LMPPs) and one global maximum power point (GMPP) [16], which necessitates finding a way to extract the optimum power delivered by the PV system. PS is a critical issue that substantially diminishes the overall efficiency of the system [17]; it is acknowledged as the main source of energy losses in PV power systems. Under PSCs, the panel exposed to shading absorbs the power provided by other modules; it acts as a charge rather than a generator, resulting in the "hot spot" effect [18]. Studies have indicated that PS can significantly reduce system yield, ranging from 10% to 70% [19]. The severity and type of shading pattern influence this variation. This dilemma motivated us to develop a metaheuristic algorithm based on swarm intelligence to monitor efficiently the global maximum power (GMP) delivered by the PV system. The primary objective of this thesis is to propose an efficient hybrid MPPT controller to improve the efficiency of photovoltaic systems when exposed to PSCs. While traditional MPPT techniques work well under uniform conditions, their efficiency drops significantly when PS is present [20]. To circumvent this issue, a significant interest is dedicated by researchers to the MPPT techniques based on SI, particularly particle swarm optimization (PSO) [21] and Cuckoo Search (CS) [22,23], which are powerful optimization techniques used to address various engineering optimization problems with several peaks and can handle effectively the partial shading issues.

Nevertheless, we have noted a research gap in developing hybrid approaches that integrate these two algorithms to improve MPPT performance across diverse environmental circumstances, particularly under PSCs. This work fills this gap by introducing a novel hybrid algorithm called Smart Hybrid Algorithm (SHA). The proposed approach combines these two algorithms to produce a powerful optimizer that circumvents the common shortcomings of conventional MPPT techniques and provides a robust MPPT monitor to address the PS issue in PV systems effectively.

To fulfill the objective of this thesis, a comprehensive evaluation is carried out to justify our algorithm's viability. To verify the robustness and suitability of the proposed approach in tracking the GMPP, multiple performance tests are conducted in both homogeneous and

nonhomogeneous weather conditions. Tests are performed using diverse PV connections including, the 4S, 8S, 10S, 12S, and 4S2P PV configurations. The introduced SHA is compared to well-known similar MPPT techniques in terms of steady-state efficiency, dynamic efficiency, and convergence time; the obtained results demonstrate the proposed method's superiority and robustness in tracking and monitoring the GMPP.

This thesis is organized into three chapters. Their contents are outlined as follows:

**Chapter 1:** This chapter presents an overview of the photovoltaic system. Additionally, solar cell technology and its working principles, including the effect of temperature and irradiance on PV cell performance, are introduced. Special attention is given to PV array modeling due to the importance of precise modeling in system accuracy. Moreover, electrical power converters are thoroughly discussed due to their crucial importance in photovoltaic energy systems. Finally, the impact of partial shading on PV systems is presented, including its mitigation through PV system design topologies, which is considered owing to the inherited features in optimizing the generated power in PV systems.

**Chapter 2:** Deals with the most recently developed metaheuristic approaches to harvest and monitor the GMPP in PV systems subjected to PS issues, highlighting the effectiveness of metaheuristic-based MPPT techniques in addressing partial shading issues. The necessary theory of these techniques and a discussion of their characteristics are presented. The MPPT principle and the challenges facing MPPT techniques are introduced. Hybrid MPPT techniques are presented, their different types are introduced and discussed thoroughly due to their vital importance. Since our approach is based on hybridizing two metaheuristic algorithms, the key features of Cuckoo Search (CS) and Particle Swarm Optimization (PSO) are presented. Furthermore, the formulation of MPPT as an optimization problem is addressed, and the application of each proposed technique for MPPT is discussed.

**Chapter 3:** Presents the developed hybrid PSO-CS algorithm (SHA). The necessary theory and the working principle are introduced. The system simulations in the Matlab/Simulink environment are put forward. The suggested technique is examined thoroughly using several tests under STC, PSCs, and rapid irradiance change to validate the robustness and performance of the proposed approach in tracking the GMPP. Eight shading profiles in conjunction with two PV array configurations, 4S, 8S, 10S, 12S and 4S2P are addressed. The proposed hybrid algorithm is

benchmarked against PSO, CS, and PO algorithms. A performance comparison is carried out against well-known SI-based MPPT algorithms.

Finally, a conclusion is drawn in order to highlight the key contributions of this research work. Additionally, some potential avenues for future research are presented.



## Chapter 1

---

# PHOTOVOLTAIC ENERGY SYSTEMS CONCEPTS AND SHADING MITIGATION TECHNIQUES

---

## Contents

---

1.1 <a href="#">Introduction</a> .....	20
1.2 <a href="#">Overview of photovoltaic generation systems</a> .....	20
1.3 <a href="#">Photovoltaic cells technologies</a> .....	21
1.4 <a href="#">Photovoltaic cells and photovoltaic modules</a> .....	26
1.4.1 <a href="#">Open Circuit Voltage and Short Circuit Current</a> .....	27
1.4.2 <a href="#">Maximum Power Point</a> .....	27
1.4.3 <a href="#">Efficiency</a> .....	28
1.4.4 <a href="#">Fill factor</a> .....	28
1.5 <a href="#">Influence of solar irradiance and temperature on the PV module</a> .....	28
1.5.1 <a href="#">Irradiance effect</a> .....	29
1.5.2 <a href="#">Temperature effect</a> .....	29
1.5.3 <a href="#">Spectral effect</a> .....	30
1.6 <a href="#">PV array modeling</a> .....	30
1.6.1 <a href="#">Single-diode model</a> .....	30
1.6.2 <a href="#">Two-diode model</a> .....	31
1.6.3 <a href="#">Multi-diode PV model</a> .....	32
1.7 <a href="#">DC-DC converters</a> .....	33
1.7.1 <a href="#">Buck converter</a> .....	34
1.7.2 <a href="#">Boost converter</a> .....	37
1.7.3 <a href="#">Buck-Boost converter</a> .....	39
1.8 <a href="#">Effect of partial shading on PV system performance</a> .....	41
1.9 <a href="#">Partial shading mitigation techniques</a> .....	45
1.9.1 <a href="#">PV system topologies</a> .....	46
1.9.1.1 <a href="#">Bypass and blocking diodes</a> .....	46
1.9.1.2 <a href="#">PV array configuration</a> .....	48
1.9.1.3 <a href="#">PV system architectures</a> .....	50
1.9.1.4 <a href="#">PV array reconfiguration</a> .....	51
1.9.2. <a href="#">MPPT techniques</a> .....	54
1.10 <a href="#">Conclusion</a> .....	55

## **1.1 Introduction**

In recent years, the global energy landscape has undergone a huge transformation, with an increasing focus on sustainable energy solutions due to rising energy demands and the urgent need to address environmental degradation caused by fossil fuel reliance. Among the many renewable energy options, solar energy stands out due to its abundance and the rapid advancements in solar technology. Solar cells, which convert sunlight into electricity, have been at the forefront of this shift. However, the development of solar technology requires a perfect knowledge of the electrical production of these systems at different levels. This precise estimate can only be made by considering the dramatic effects of shading on the delivered electrical power.

This chapter discusses the following important points: Initially an overview of photovoltaic (PV) generation systems. Next, the photovoltaic cells and modules including the effect of temperature and irradiance. PV array modeling is thoroughly examined, including the effect of partial shading on PV systems. Then, the most used types of DC-DC converters in monitoring the delivered power from PV systems. Finally, Partial shading mitigation techniques are presented.

## **1.2 Overview of photovoltaic generation systems**

The photovoltaic effect was identified in the early 19<sup>th</sup> century. In 1839, a young French scientist, Alexandre Edmond Becquerel, discovered a physical phenomenon or effect that made it possible to convert light into electricity [24]. Nonetheless, owing to elevated manufacturing rates, significant advancement of this technology started only with the semiconductor industry's evolution in the late of the 20<sup>th</sup> century. Solar cells have been considered as an exceptional alternative for energy provision in areas far from the power grid. The development of solar cells for commercial usage in homes has been the subject of intense attention. Furthermore, there has been a noticeable rise in the widespread usage of solar cells in rural regions without infrastructure and energy networks. Electricity generated in these regions is used for water pumping, energy cooling, telecommunications, and other home appliances. [25].

Photovoltaic cells are composed of semiconductor materials like silicon. A thin semiconductor wafer is carefully treated to create an electric field in solar cells, with one side positively charged and the other negatively charged, as shown in [Fig. 1.1](#). When light energy gets in contact with the solar cell, electrons are released from the atoms in the semiconductor material. If both sides of the PV cell are connected, forming an electrical circuit, the generated electrons can

be controlled to form an electric current. This current can then be used to feed a load [26]. A PV cell can be either circular or square in construction. Because of the low voltage generated in a solar cell (less than 1V), several PV cells are coupled in series (for high voltage) and in parallel (for high current) to assemble a PV module for the required output. The power produced by one module is insufficient to meet home or business requirements. To figure out this issue, modules in a photovoltaic array are often linked in series to obtain the desired voltages; then in parallel to enhance current production [27].

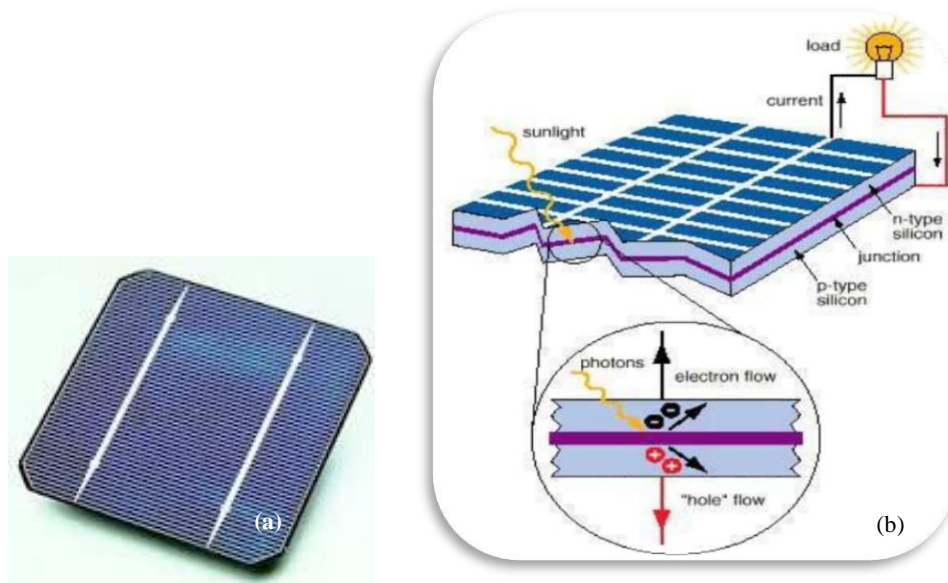


**Fig. 1.1** (a) Typical solar cell (b) Structure of a typical PV cell

### 1.3 Photovoltaic cells technologies

The fundamental element of a PV system is solar cells, which allow the conversion of sunlight energy into direct current. A conventional solar cell is made up of a PN junction in a semiconductor material, similar to a diode. The most widely used semiconductor material in solar cells is silicon. However, the photovoltaic industry employs alternative materials that vary in terms of cost and efficiency. A crystalline-based solar cell incorporates a p-n junction, as shown in Fig. 1.2. The production process includes melting, doping, metallization and texturing. The junction's positive and negative sides generate an electric current when a load is connected. Nonetheless, the voltage produced by an individual p-n junction cell falls below 1V, which is insufficient for many practical uses. Furthermore, it exhibits mechanical fragility and requires lamination and protection for effective application. Solar technology features rapid innovation, and

a solar cell's efficiency continuously increases. Different types of solar cells are found in the market; we can mention the following:

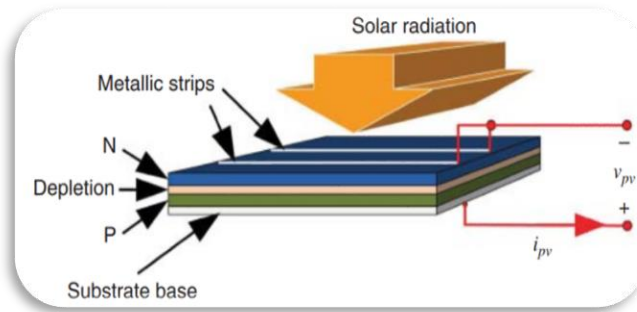


**Fig. 1.2** Typical crystalline PV cell construction

- **Monocrystalline silicon (c-Si):**

[Fig. 1.3](#) illustrates a solar panel composed of monocrystalline solar cells. It is the most widely available cell material; however, its efficiency is limited due to several constraints. Monocrystalline silicon exhibits the highest verified conversion efficiency among all commercial photovoltaic technologies, with a recorded single-junction cell laboratory efficiency of 26.7%, surpassing polycrystalline silicon at 22.3% and established thin-film technologies, including CIGS cells at 21.7%, CdTe cells at 21.0%, and amorphous silicon cells at 10.2%. The highest theoretical efficiency for conventional single-junction cells is 33.16% [28]. Theoretically, an unlimited number of junctions could achieve a maximum efficiency of 86.8% when exposed to highly concentrated sunlight [29]. The most effective laboratory-based examples of conventional crystalline silicon (c-Si) solar cells as of 2024 have efficiencies of up to 27.1%, [30]. In contrast, multi-junction cell examples have shown performance of over 46% under intensive sunlight [31].



**Fig. 1.3** Monocrystalline Solar Panels (Mono-SI)

- **Polycrystalline cells**

It is referred to as polysilicon. The molten silicon is shaped into ingots, as illustrated in [Fig. 1.4](#) (a). Subsequently, it forms various crystalline structures. The conversion efficiency of these cells is slightly reduced compared to the single-crystal cells. “Monocrystalline” and “polycrystalline” silicon modules demonstrate exceptional reliability for outdoor power applications [[32](#)]. [Fig. 1.4](#) (b) shows a solar panel made of polycrystalline solar cells.



**Fig. 1.4 (a) A silicon ingot (b) Polycrystalline Solar Panels (Poly-SI)**

- **Thin film cells (second generation)**

Thin-film solar cell (TFSC), as shown in [Fig. 1.5](#), is made of thin film materials. Thin-film solar cells cost less than crystalline cells. The usually used Thin-film solar cells [[33](#)] are:

1. “Amorphous silicon” (a-Si) and thin-film silicon (TF-Si). Amorphous solar cells' efficiency ranges from 10% to 13%. Their lifespan is less than that of crystalline cells [[34](#)].
2. “Cadmium Telluride” (CdTe) is a crystalline substance composed of cadmium and tellurium, exhibiting an efficiency of approximately 15% [[35](#)].
3. “Copper indium gallium selenide” (CIS or CIGS) consists of copper, indium, gallium, and selenium. It has an efficiency of 16.71% [[36](#)].
4. “A dye-sensitized solar cell” (DSC) comprises a photosensitized anode paired with an electrolyte. The efficiency measures approximately 11.1% [[37](#)].

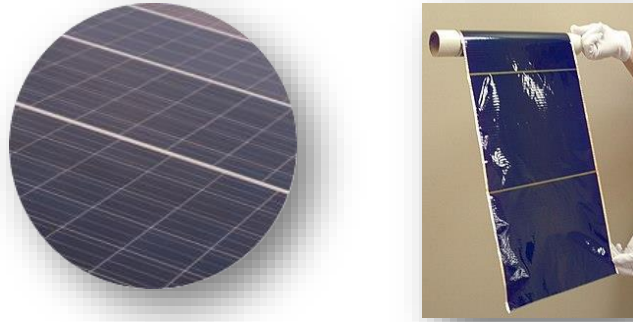


**Fig. 1.5** Thin-Film Solar Cells (TFSC)

- **Additional emerging technologies:**

1. “Organic solar cells” (OSC) consist of thin layers of organic substances. The highest power conversion efficiency was reported to be 11.7% [38].

2. “Tandem or stacked cells”, illustrated in [Fig. 1.6](#), involve various semiconductor materials optimized for distinct spectral ranges, layered atop each other. Tandem solar cells' maximum conversion efficiency is 33.66% [39].

3. “Concentrator cells” utilize reflective and refractive optical devices. This system relies solely on direct radiation and requires an additional sun-tracking mechanism, as illustrated in [Fig. 1.7](#) [40]. Its efficiency is approximately 42.4%.

4. “MIS Inversion Layer cells”: The inner electric field is generated at the interface between a thin oxide layer and a semiconductor.

[Table. 1.1](#) details the characteristics of the different types of PV cells.

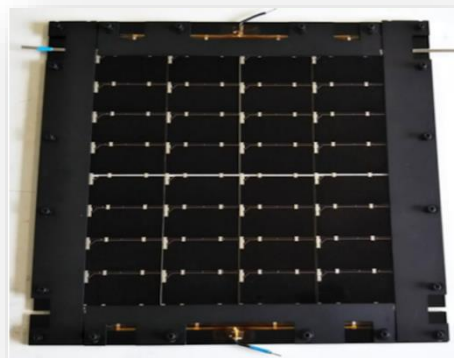


**Fig. 1.6** Tandem/silicon stacked solar cell module

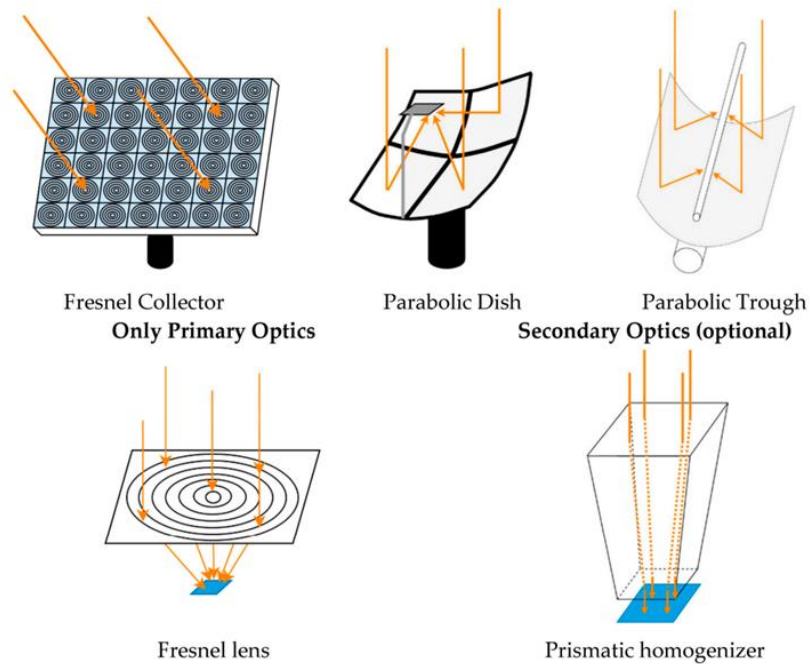


**Fig. 1.7** Different solar concentrators for Concentrated Photovoltaic (CPV) system [41]

**Table. 1.1** PV cells’ characteristics

Solar panel type	Average efficiency	Average lifetime (years)	Merits	Shortcomings
“Polycrystalline”	13-16%	25-30	Less expensive than monocrystalline	Reduced efficiency compared to monocrystalline
“Monocrystalline”	18-24%	25-40	The most effective variant on the market	It costs more than polycrystalline
“Thin-film”	7-13%	10-20	Most flexible choice	Reduced power output
“Transparent”	1-10%	25-35	Integrates seamlessly with window designs	Low performance
“Solar tiles”	10-20%	25-30	Integrates seamlessly with rooftops	Quite costly



#### 1.4 Photovoltaic cells and photovoltaic modules

Numerous cells are coupled in parallel and series circuits to increase the voltage and current to suitable useful values [42]. Solar modules comprise many separate solar cells joined and enclosed in a common support structure. Solar arrays enclose many PV modules connected to obtain the desired power ratings, as illustrated in Fig. 1.8. When similar modules are connected in series, the current remains constant. At the same time, the voltage rises directly to the number of cells in series. Similarly, when identical modules are linked in parallel, the voltage stays constant at the voltage of each module while the current rises proportionally to the number of parallel modules.

Fig. 1.9 (a) shows a PV array made of cadmium telluride (CdTe) solar panels, while Fig. 1.9 (b) shows a PV array made of monocrystalline solar panels.

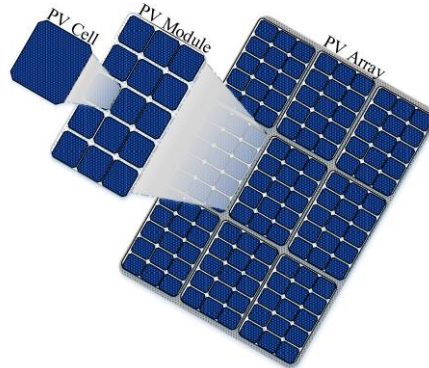


Fig. 1.8 PV cell, PV module, and PV array [43]



(a)

Fig. 1.9 (a) Cadmium telluride (CdTe) PV array



(b)

(b) Monocrystalline PV array



### 1.4.1 Open-circuit voltage and Short-circuit current

“Open circuit voltage” and “short circuit current” are extensively utilized to describe the cell's electrical performance, as shown in [Fig. 1.10](#). The short circuit current ( $I_{sc}$ ) is obtained by shorting the module's output terminals. It corresponds to the current at zero voltage ( $V_{pv} = 0$  V), while the open circuit voltage corresponds to the voltage obtained when no load is connected to the output terminals of the PV module. It is the voltage at zero current ( $I_{pv} = 0$  A). The reference values  $I_{sc-ref}$  and  $V_{oc-ref}$  in the datasheet correspond to those ratings obtained under STC, i.e. ( $G = 1000$  W/m<sup>2</sup> and  $T = 25^\circ\text{C}$ ).

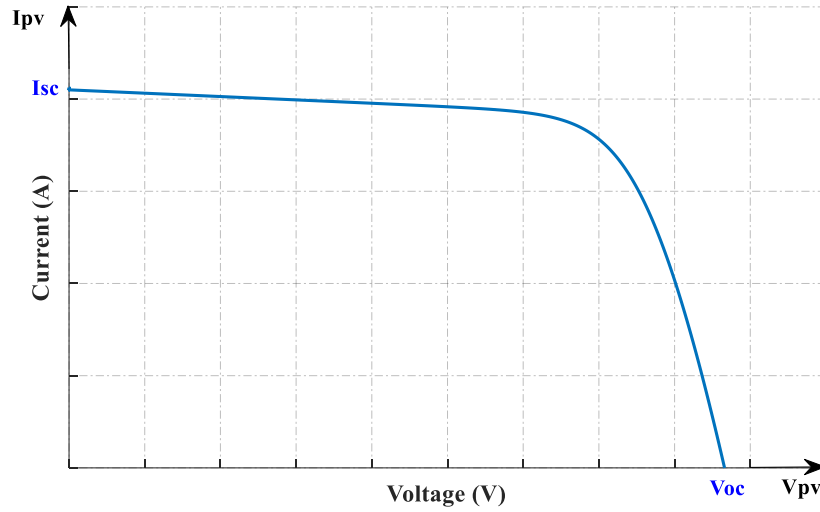


**Fig. 1.10** Current-Voltage characteristic ( $I_{pv}$ - $V_{pv}$ ) for a solar cell

### 1.4.2 Maximum Power Point

The power delivered by a photovoltaic generator is given by:

$$P_{pv} = V_{pv} \cdot I_{pv} \quad (1.1)$$

“Maximum Power Point” (MPP) refers to the point where the PV module generates its maximum output power. Then,  $V_{pv}$  and  $I_{pv}$  are referred to as  $V_{MPP}$  and  $I_{MPP}$ , as shown in [Fig. 1.11](#). At that point,  $P(V_{MPP}, I_{MPP})$ , the power  $P_{pv}$  provided by the photovoltaic generator is maximum and designated  $P_{MPP}$ . We have:

$$P_{MPP} = V_{MPP} \cdot I_{MPP} \quad (1.2)$$

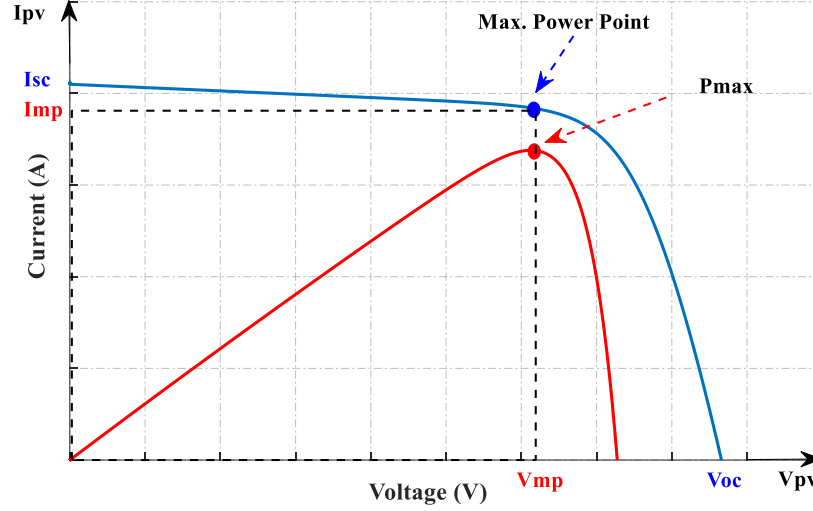


**Fig. 1.11** Current-Voltage (  $I_{pv}$ - $V_{pv}$  ) and Power-Voltage ( $P_{pv}$ - $V_{pv}$ ) characteristics for a solar cell

### 1.4.3 Efficiency

The conversion efficiency of a photovoltaic module refers to the ratio of the electrical energy it generates to the sunlight energy it receives. The definition pertains to the module's output power ratio to the incident light power.

$$\eta = \frac{P_{out}}{P_{in}} = \frac{V_{pv} \cdot I_{pv}}{A_{pv} \cdot G} \quad (1.3)$$

$A_{pv}$  corresponds to the module's or cell's surface, and  $G$  corresponds to the irradiance.

### 1.4.4 Fill Factor

The “fill factor” (FF) refers to the ratio of the maximum power ( $I_{MPP} \cdot V_{MPP}$ ) to the theoretical one ( $I_{SC} \cdot V_{OC}$ ). The MPP values ( $I_{MPP}$ ,  $V_{MPP}$ ) are always less than ( $I_{SC}$ ,  $V_{OC}$ ) because of the series, shunt resistances, and the diode. For commercial solar cells, a typical fill factor exceeds 0.70. The FF is defined as follows:

$$FF = \frac{P_{MPP}}{V_{OC} \cdot I_{SC}} = \frac{V_{MPP} \cdot I_{MPP}}{V_{OC} \cdot I_{SC}} \quad (1.4)$$

## 1.5 Effect of solar irradiance and temperature on the PV module

Photovoltaic panels are anticipated to be the primary solution for fulfilling worldwide energy demand via converting solar energy into electricity. The primary impediment to the extensive implementation of photovoltaic systems is their low efficiency, which is significantly influenced by solar radiation and operating temperature. A comprehensive understanding of

photovoltaic modules' performance, efficiency, and output power and their variations with changes in solar radiation and temperature is essential for determining the best system size and mitigating extra-financial risks. This section examines the impact of operating temperature and solar radiation on the power production of photovoltaic modules.

### 1.5.1 Irradiance effect

Fig. 1.12 illustrates the module's output characteristics ( $I_{pv}$ - $V_{pv}$ ) and ( $P_{pv}$ - $V_{pv}$ ) for different irradiance levels. We observe a significant rise in the  $I_{sc}$  current with increasing irradiance while the voltage  $V_{oc}$  increases slightly. The same behaviour is obtained at the power level, where the generated power is proportional to the irradiance increase, i.e., the efficiency of a PV module or array is better for high irradiance levels. The reference conditions or Standard Test Conditions (STC) are generally chosen with an irradiance of  $1000 \text{ W/m}^2$  and temperature of  $25^\circ\text{C}$ . In practical applications, the irradiance on photovoltaic systems without light concentration tends to be lower, resulting in reduced efficiency than its rated value.

### 1.5.2 Temperature effect

Fig. 1.13 depicts the temperature impact on solar cells; we can observe that as the cell's internal temperature increases, the short circuit current  $I_{sc}$  rises slightly, attributed to improved light absorption resulting from the reduction in gap energy with temperature. However, the open-circuit voltage is inversely proportional to rising temperature. On the other hand, the maximum delivered power exhibits a significant decline as temperature increases. The standard conditions are typically selected for an internal temperature of  $25^\circ\text{C}$ .

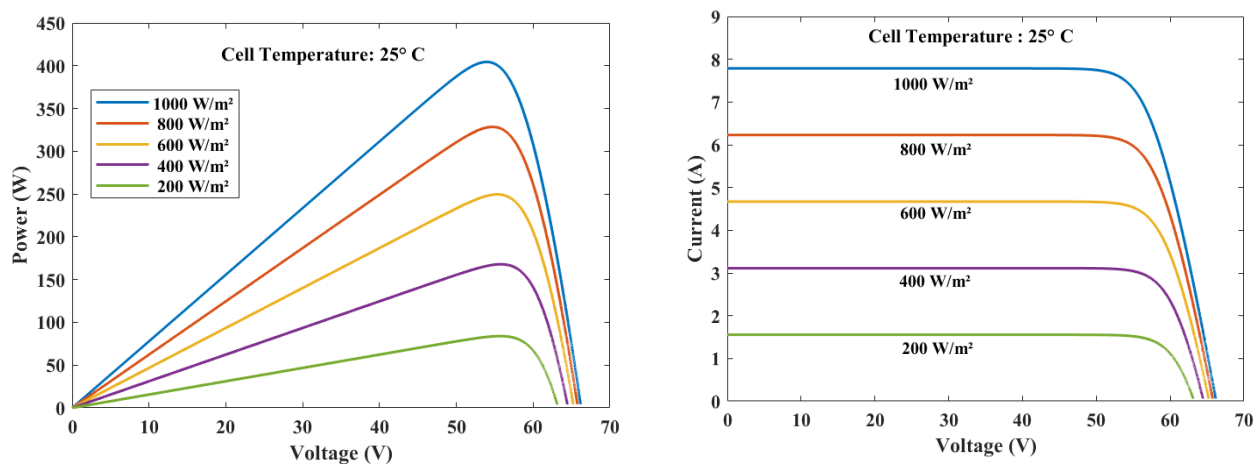


Fig. 1.12 Irradiance effect on output of the PV module

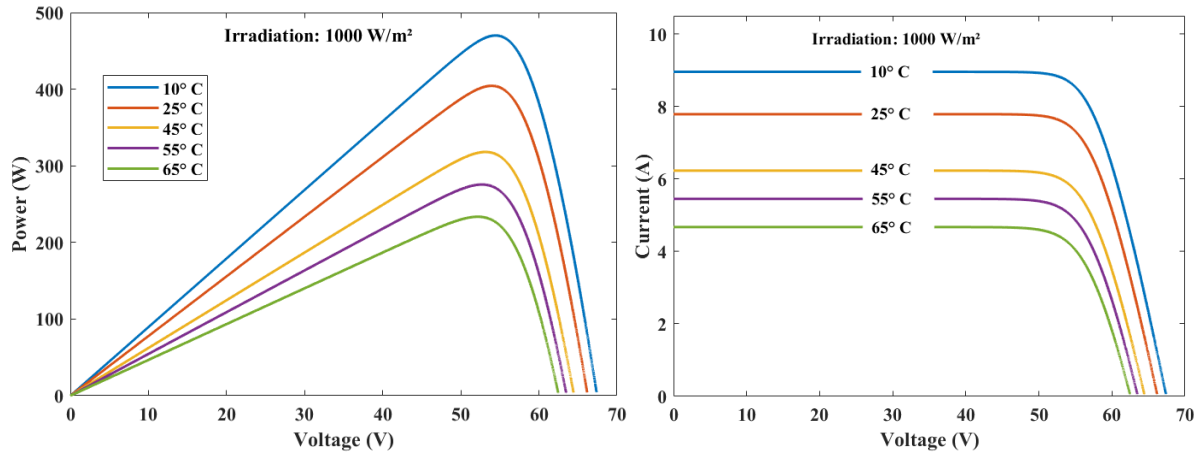


Fig. 1.13 Temperature effect on the output of the PV module

### 1.5.3 Spectral effect

White light may be defined as the combination of radiations, including various wavelengths. Photovoltaic generators exhibit varying efficiency over different wavelengths. Hence, the conventional criteria used for evaluating cells and modules have a limitation on the visible light spectrum. The standard spectrum used in optimizing PV cells is AM 1.5. Nevertheless, in real conditions, the light spectrum can differ, which also influences the efficiency of photovoltaic systems.

### 1.6 PV array modeling

Numerous mathematical models have been proposed in the literature to explain the operation and behaviour of the photovoltaic generator. These models vary in their calculation approach, precision, and number of factors involved in the modeling procedure. The commonly used models are the following:

#### 1.6.1 Single-diode model

Fig. 1.14 depicts the single-diode model of a PV cell [44]. This model is the most prevalent among photovoltaic models, primarily because it utilizes the fewest physical parameters. In this model,  $I_L$  is the internally generated light of the PV cell,  $I_0$  refers to the diode reverse saturation current,  $R_s$  represents the series resistance,  $(a)$  stands for the ideality factor, and  $R_{SH}$  denotes the shunt resistance, which is presumed to be infinite in this model. The four-parameter simplified model requires less computational effort, though its accuracy across various technologies remains

a topic of discussion. It is compatible with module I-V curves throughout a broad spectrum of irradiances, as indicated in [45].

The five-parameter version necessitates the application of numerical methods for resolution [46]. Furthermore, it can be developed utilizing solely the data supplied by manufacturers under standard test conditions (STC:  $G=1000 \text{ W/m}^2$  and  $T=25 \text{ }^\circ\text{C}$ ). The primary equation that characterizes the single-diode model is presented as follows:

$$I = I_L - I_0 \left[ \exp \left( \frac{V + IR_S}{aV_t} \right) - 1 \right] - \frac{V + IR_S}{R_{SH}} \quad (1.5)$$

Where  $I_0$  stands for the diode saturation current,  $(a)$  represents the diode ideality factor, and  $V_t = k.T/q$  is the thermal voltage. The parameter  $k$  refers to the Boltzmann constant ( $1.3806503 \times 10^{-23} \text{ J/K}$ ),  $q$  is the electron charge ( $1.60217646 \times 10^{-19} \text{ C}$ ), and  $T$  is the temperature of the PV module in Kelvin.

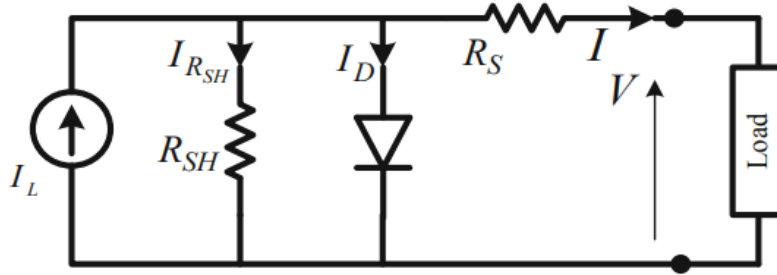


Fig. 1.14 Equivalent circuit of a single PV diode model

### 1.6.2 Two-diode model

The single-diode equation presumes a fixed ideality factor  $(a)$  value. The ideality factor is influenced by the voltage applied across the device in practical scenarios. Under high voltage conditions, when surface and bulk region recombination predominates within the device, the ideality factor approaches unity. The junction experiences significant recombination at lower voltages, leading to an ideality factor that approaches two. The junction recombination is altered by incorporating a second diode parallel to the initial one and adjusting the ideality factor generally to two. The two-diode model represents an enhancement of the single-diode photovoltaic model, incorporating the impact of recombination by adding a parallel diode, as illustrated in Fig. 1.15. The two-diode model consists of a first diode representing diffusion and surface recombination,

while the second diode addresses recombination occurring in the depletion region, particularly prevalent at higher irradiances [47].

Under low irradiance and temperatures, the two-diode photovoltaic model demonstrates superior accuracy in curve characteristics compared to the single-diode model. The two-diode model is particularly recommended for precise modeling under low irradiance conditions [48]. A diverse range of studies has been conducted to develop a mathematical model for photovoltaic cells. The two-diode model has been referenced in numerous studies [49-51]. The primary equation that characterizes the two-diode model is presented as follows:

$$I = I_L - I_{01} \left[ \exp \left( \frac{V + IR_S}{aV_t} \right) - 1 \right] - I_{02} \left[ \exp \left( \frac{V + IR_S}{aV_t} \right) - 1 \right] - \frac{V + IR_S}{R_{SH}} \quad (1.6)$$

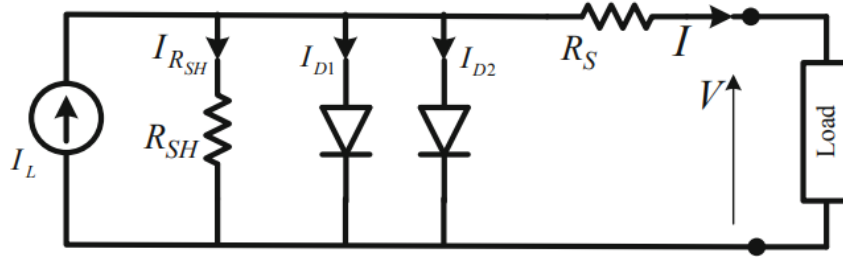


Fig. 1.15 Equivalent circuit of a two-diode PV model

### 1.6.3 Multi-diode PV model

Fig. 1.16 illustrates the equivalent circuit of the multi-diode photovoltaic model. Incorporating additional diodes into the multi-diode PV model enhances its flexibility, allowing for a more accurate representation of the output characteristics of various PV cells [52].

The generalized multi-diode PV model generates an output current  $I$  as given in equation (1.7).

$$I = I_L - \sum_{i=0}^n I_{0,i} \left[ \exp \sum_{j=0}^m \left( \frac{V + IR_S}{a_{ij} N_s V_t} \right) - 1 \right] - \frac{V + IR_S}{R_{SH}} \quad (1.7)$$

Where  $I_L$  is the photocurrent source,  $D_{n,m}$  represents the series and parallel diodes with ( $n$  by  $m$ ) dimension,  $R_S$  stands for the series resistance including the sum of structure resistance, and  $R_{SH}$  is the parallel resistance representing the leakage current.

$I_0$  denotes the diode saturation current,  $(a)$  represents the diode ideality factor,  $V_t = kT/q$  is the thermal voltage,  $N_s$  is the cell's series number per string,  $k$  is the Boltzmann's constant ( $1.3806503 \times 10^{-23} \text{ J/K}$ ),  $q$  is the electron charge ( $1.60217646 \times 10^{-19} \text{ C}$ ), and  $T$  is the module's temperature in Kelvin.

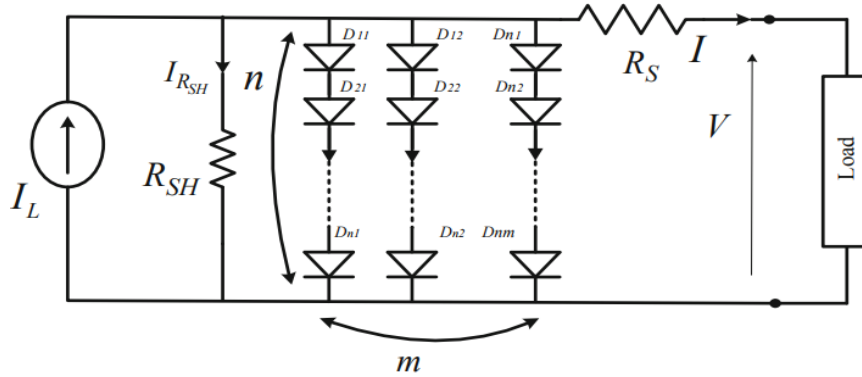


Fig. 1.16 Equivalent circuit of a multi-diode PV model

## 1.7 DC-DC converters

The electrical power converter is a crucial element in photovoltaic energy systems; it adjusts the output power, increasing or decreasing the voltage level to ensure system compliance. Numerous power converter topologies for renewable energy systems have been described and realized in the literature [53]. Switching devices enable the transfer of power from the input to the output. Given that the input is continuous (DC), these devices are often operated at significantly higher frequencies than the line frequency, to levels of several hundred kilohertz. Such converter circuits are referred to as high-frequency DC-DC switching converters or regulators. The switching device used in these converters may be the bipolar junction transistor (BJT), metal-oxide-semiconductor field-effect transistor (MOSFET), or insulated gate bipolar transistor (IGBT). Numerous topologies are often used to realize Switched-Mode Power Supplies (SMPS) [54]. Each topology has distinct characteristics, making it most appropriate for certain applications. To determine the optimal topology for a certain specification, it is crucial to understand its fundamental functioning, benefits, limitations, complexity, and applicable domains. The most often used converters for efficient power conversion in photovoltaic-based power systems are boost,

buck, and buck-boost converters. These topologies' input and output voltages share a common ground, making them non-isolated.

A DC-DC converter may function in either continuous or discontinuous conduction mode. Continuous conduction mode (CCM) is characterized by a continuous current flow through the inductor during the whole switching cycle during steady-state operation. In contrast, discontinuous conduction mode (DCM) is characterized by the inductor current being zero for a segment of the switching cycle. The CCM is favored for its high efficiency and effective use of semiconductor switches and passive components. The DCM can be utilized in applications that demand specific control requirements. These converters are used in renewable energy systems, including standalone, grid-integrated, micro-grids, smart grids, and hybrid energy systems [55]. In these power generation systems, efficient and reliable MPPT algorithms control the converter's output, optimizing energy output from photovoltaic systems in diverse environmental conditions. The choice of any of these generic power converters is contingent upon the particular applications intended.

### **1.7.1 Buck converter**

The buck converter is mainly used as a power converter in photovoltaic-based energy systems. It reduces the input voltage, resulting in an output voltage consistently lower than the input voltage [56]. The buck converter operates in two primary modes: continuous conduction mode and discontinuous conduction mode. Both modes are accountable for supplying power to the connected load. The buck converter is the most basic and efficient power converter type for PV-based power generating systems, making it an excellent option for power designers to include in their systems. The transition of the buck converter's operational mode from CCM to DCM is prompted by shading and non-shading conditions, compromises the system's robustness, and necessitates an effective circuit design and advanced control algorithm to ensure stable and reliable functioning of the photovoltaic-based energy generation system. Environmental fluctuations and climatic circumstances mostly influence the operational mode of the buck converter, diminishing its efficiency and complicating its dependable performance in delivering continuous power to the connected load. [Fig. 1.17](#) illustrates the electrical model of a buck converter.



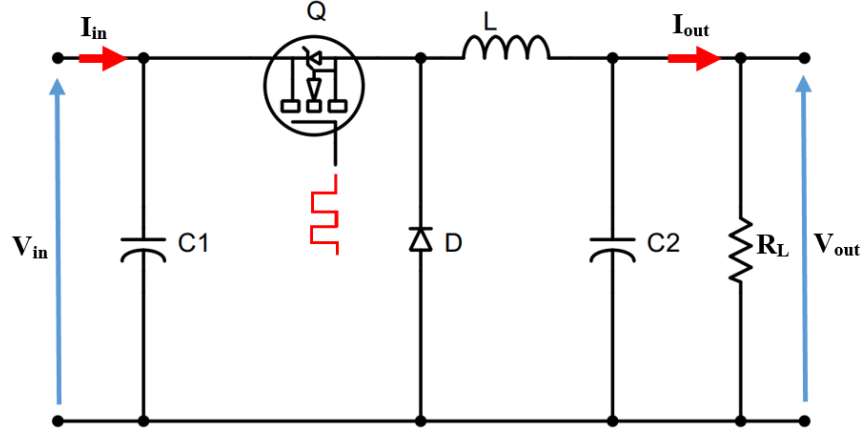


**Fig. 1.17** Electrical circuit of the Buck converter

As illustrated in [Fig. 1.17](#), the DC-DC converter includes a power switch (Q) and a low-pass filter composed of an inductor and a capacitor. It switches between two states every cycle, the ON and OFF states of the switch (Q). A PWM signal drives the switch's gate. The ON state duration is  $(d.T_s)$ , where  $(d)$  is the duty cycle of the PWM signal and  $T_s$  is the switching time. During the switch's ON time, the input supplies energy to both the output load and the inductor (L). During the switch's OFF time, the energy stored within the inductor and capacitor continues to supply the load. Diode D, a freewheeling diode, completes the inductor current path when Q is turned off. The following system of equations shows the converter's governing equations throughout a single switching period:

$$\begin{cases} C_1 \frac{dv_{in}(t)}{dt} = i_{in}(t) - di_L(t) \\ C_2 \frac{dv_{out}(t)}{dt} = i_L(t) - i_{out}(t) \\ L \frac{di_L(t)}{dt} = dv_{in}(t) - v_{out}(t) - R_L i_L(t) \end{cases} \quad (1.8)$$

Where;  $i_{in}(t)$ ,  $i_{out}(t)$  and  $i_L(t)$  are input, output, and inductor currents respectively, whereas;  $v_{in}(t)$ ,  $v_{out}(t)$ , and  $v_L(t)$  are input, output, and inductor voltages respectively. The buck converter's voltage conversion is expressed using the equation (1.9).

$$\frac{V_o}{V_{in}} = D \quad (1.9)$$

Therefore, the buck converter's maximum output voltage gain is 1. Considering equation (1.9) representing the buck converter's voltage gain, we can derive two essential observations:

given that the converter's components (L, C, D, Q) are ideal, they do not dissipate any power, yielding 100% voltage efficiency. The average input and output voltage ratio exhibits a linear control characteristic curve, as seen in [Fig. 1.18](#). By adjusting the duty cycle, D, we can adjust the average output voltage to the appropriate level.

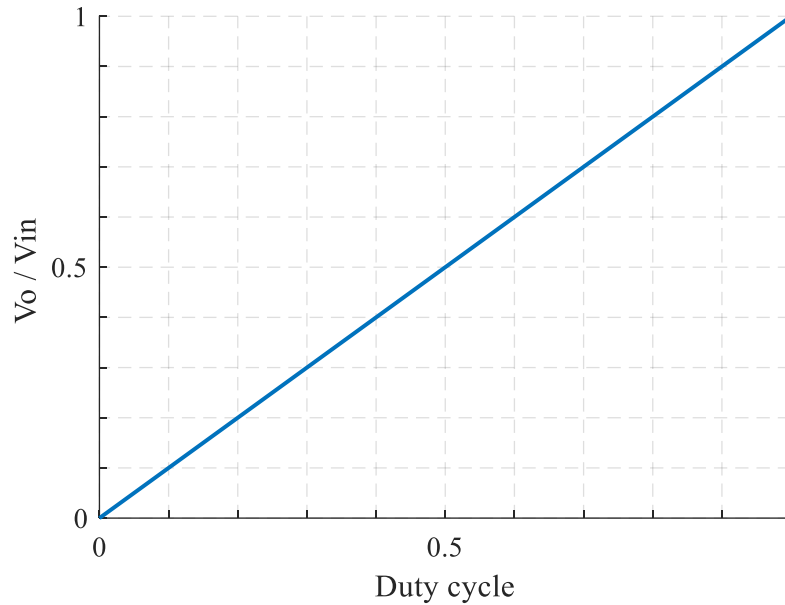


**Fig. 1.18** Ideal output control characteristic curve for the buck converter.

The buck converter's current gain is given by equation (1.10)

$$\frac{I_o}{I_{in}} = \frac{1}{D} \quad (1.10)$$

The average input and output powers must be equal if we take into consideration the conservation principle of power and an ideal converter, then:

$$I_{in} V_{in} = I_o V_o \quad (1.11)$$

$$\frac{I_{in}}{I_o} = \frac{V_o}{V_{in}} = D \quad (1.12)$$

- **Buck converter design parameters**

The output capacitor's value is a critical design parameter as it affects the overall dimensions of the DC-DC converter and the extent of switching frequency ripple attenuation. Consequently, using a larger output capacitor to minimize the AC ripple over the output voltage is standard design practice. Theoretically, as capacitance approaches infinity, the capacitor behaves

as a short circuit to the AC ripple, yielding zero output voltage ripple. Assuming C is finite, a voltage ripple occurs superimposed on the average output voltage. The following equation gives the output voltage ripple:

$$\Delta V_c = \frac{(1 - D)V_o}{8LCf^2} \quad (1.13)$$

The ratio of the ripple to the output voltage is expressed alternatively in equation (1.14)

$$\frac{\Delta V_c}{V_o} = \frac{1 - D}{8LCf^2} \quad (1.14)$$

Eq. 14 refers to the output voltage ripple that indicates regulation. As anticipated, increasing the frequency and the filtering capacitor results in a reduction in voltage ripple. The minimum capacitor and inductor values to maintain the converter in continuous conduction mode (CCM) are specified as follows:

$$C_{min} = \frac{(1 - D)V_o}{8\Delta V_o f^2} \quad (1.15)$$

$$L_{crit} = \frac{(1 - D)R_L}{2f} \quad (1.16)$$

### 1.7.2 Boost converter

The boost converter is widely used for PV-based energy generation systems [57]. It increases the output voltage of the PV panel by altering the duty cycle. The boost converter operates in two modes: CCM and DCM. The corresponding electrical model is shown in [Fig. 1.19](#). This model consists mainly of an input inductor (L), a diode (D), and a power switch (Q) that can be a MOSFET or an IGBT, and a capacitor (C) at the output side. The transistor functions as a switch that is turned ON and OFF by a pulse-width modulated (PMW) control voltage. The boost converter operates as follows: First, the inductor (L) stores the energy from the input source when the MOSFET is switched ON within a period. During the OFF period, the inductor and the output capacitor (C<sub>o</sub>) deliver the stored energy to the load. The diode (D) completes the inductor current path through the output capacitor during the Q<sub>OFF</sub> period. The value of (C<sub>o</sub>) must be as high as possible to supply the load current during the ON period while maintaining the output voltage as constant as possible with minimal ripples. The following system of equations represents the boost converter's dynamics during one switching cycle:

$$\begin{cases} C_1 \frac{dv_{in}(t)}{dt} = i_{in}(t) - i_L(t) \\ C_2 \frac{dv_{out}(t)}{dt} = (1 - d)i_L(t) - i_{out}(t) \\ L \frac{di_L(t)}{dt} = v_{in}(t) - (1 - d)v_{out}(t) - R_L i_L(t) \end{cases} \quad (1.17)$$

Where  $i_{in}(t)$ ,  $i_{out}(t)$ , and  $i_L(t)$  are input, output, and inductor currents, respectively whereas  $v_{in}(t)$ ,  $v_{out}(t)$ , and  $v_L(t)$  are input, output, and inductor voltages respectively.

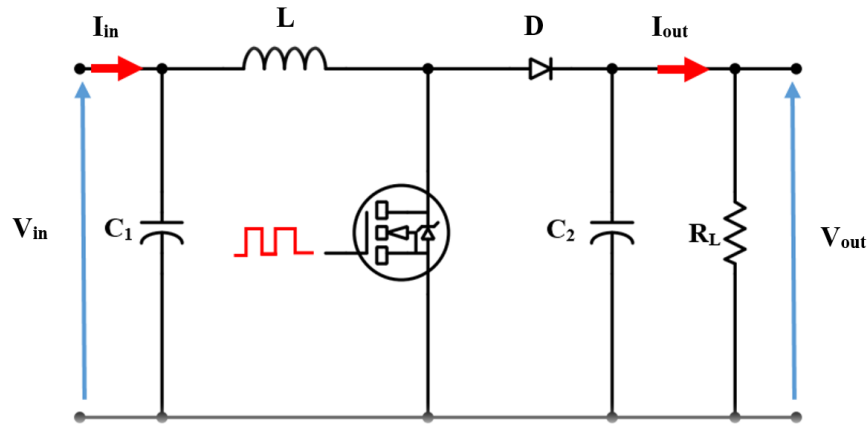


**Fig. 1.19** Electrical circuit of a boost converter.

The boost converter's voltage conversion is as given in eq. (1.18)

$$\frac{V_o}{V_{in}} = \frac{1}{1 - D} \quad (1.18)$$

Equation (1.18) shows that the boost converter's voltage gain is always greater than 1.

[Fig. 1.20](#) shows a plot for the voltage conversion ratio as a function of the duty cycle.

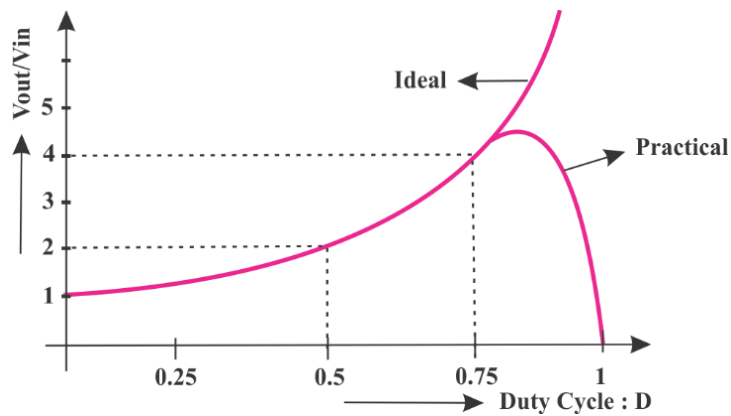


**Fig. 1.20** Boost converter's voltage gain

[Fig. 1.20](#) also includes a practical waveform that illustrates the case where the non-ideal behaviour of the circuit component is taken into consideration. Practically, operating at (D) greater than 0.75 is inadequate due to the inherent losses in the inductor, capacitor, and switch (Q) when operating at OFF periods.

- **Boost converter design parameters**

The inductor's ripple current is as given in eq. (1.19).

$$\Delta I_L = \frac{D(1-D)V_o}{Lf} \quad (1.19)$$

The average input and output powers must be equal if we take into consideration the conservation principle of power and an ideal converter, then:

$$V_{in}I_{in} = V_oI_o \quad (1.20)$$

Which results in:

$$\frac{I_{in}}{I_o} = \frac{V_o}{V_{in}} = \frac{1}{1-D} \quad (1.21)$$

The output ripple voltage is given by:

$$\frac{\Delta V_o}{V_o} = \frac{DT}{RC} = \frac{D}{RCf} \quad (1.22)$$

The critical values of the inductance and capacitance can be calculated using the following equations,

$$L_{crit} = \frac{(1-D)^2 DR}{2f} \quad (1.23)$$

$$C_{min} = \frac{DV_o}{\Delta V_o R_L f} \quad (1.24)$$

### 1.7.3 Buck-Boost converter

The buck-boost converter is widely used in renewable energy technologies, particularly in photovoltaic-based energy generation systems [58]. It increases or decreases the output voltage supplied to the associated load, depending on the specific application requirements. Power is supplied to the connected load in both operating cycles (ON or OFF) of the power switch. Unlike buck and boost converters, this converter produces a negative output voltage when operated

without isolation. The electrical buck-boost converter circuit is shown in Fig. 1.21. The following system represents the equations governing the buck-boost converter for one switching cycle:

$$\begin{cases} C_1 \frac{dv_{in}(t)}{dt} = i_{in}(t) - d * i_L(t) \\ C_2 \frac{dv_{out}(t)}{dt} = -(1 - d)i_L(t) - i_{out}(t) \\ L \frac{di_L(t)}{dt} = dv_{in}(t) + (1 - d)v_{out}(t) - R_L i_L(t) \end{cases} \quad (1.25)$$

Where  $i_{in}(t)$ ,  $i_{out}(t)$ , and  $i_L(t)$  are input, output, and inductor currents, respectively, whereas  $v_{in}(t)$ ,  $v_{out}(t)$ , and  $v_L(t)$  are input, output, and inductor voltages respectively.

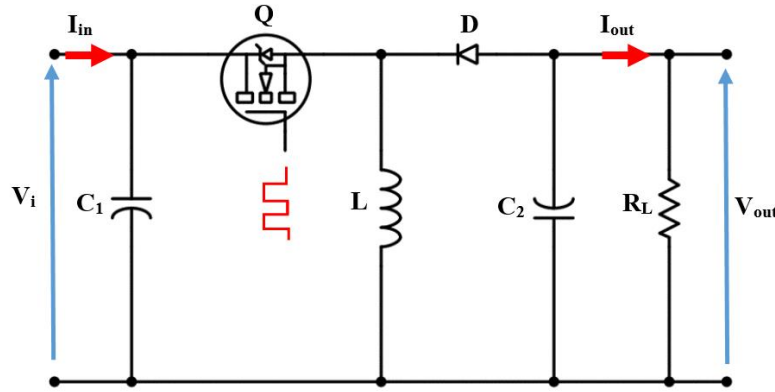


**Fig. 1.21** Electrical circuit of a buck-boost converter.

The voltage gain relationship is expressed in Eq. (1.26).

$$\frac{V_o}{V_{in}} = \frac{D}{1 - D} \quad (1.26)$$

This equation indicates that the output voltage may be either less than or more significant than the input voltage. The following cases are obtained:

$$\begin{cases} D > 0.5 & \text{Boost} \\ D < 0.5 & \text{Buck} \\ D = 0.5 & \text{Unity gain} \end{cases}$$

Applying the conservation principle of power:

$$I_{in}V_{in} = I_oV_o \quad (1.27)$$

We can then obtain:

$$\frac{I_{in}}{I_o} = \frac{V_o}{V_{in}} = \frac{D}{1-D} \quad (1.28)$$

It is observed that, at identical operational frequencies and load resistances, the buck converter exhibits the most significant critical inductor limit as compared to the boost and buck-boost converters. In contrast, the boost converter presents the lowest  $L_{crit}$ , allowing for a broader spectrum of inductor design options.

- **Buck-Boost converter design parameters**

It can be demonstrated that the capacitor current of the buck-boost converter is identical to that of the boost. Consequently, the capacitor ripple voltage is given in eq. (1.29).

$$\frac{\Delta V_o}{V_o} = \frac{D}{RCf} \quad (1.29)$$

The critical values of the inductance and capacitance that maintains the converter in the CCM can be calculated using the following equations:

$$L_{crit} = \frac{R_L(1-D)^2}{2f} \quad (1.30)$$

$$C_{min} = \frac{DV_o}{\Delta V_o R_L f} \quad (1.31)$$

## 1.8 Effect of partial shading on PV system performance

The partial shadowing situation is the primary meteorological factor that affects the efficiency of photovoltaic systems [59-61]. Partial Shading Condition (PSC) may be attributed to several factors, including shade from tree leaves, the presence of birds or their droppings on the cells, or soft shading caused by adjacent structures, installations, or fleeting clouds. Upon the occurrence of PSC, the ensuing outcomes are as follows:

1. The shaded area allows currents to exceed their “short-circuit” current in the opposite direction, thus functioning in a consuming mode instead of a generating mode, which can be mitigated by installing blocking diodes. [62].
2. The partially shaded array exhibits multiple peaks [63-65] in its P–V characteristic and conventional monitoring methods are inadequate for tracking the maximum output power in such scenarios [66].

3. In the event of extreme reverse bias voltage resulting from high shading levels, the inner diode of the PV module presents significant resistance, leading to an “open circuit” throughout the complete PV module. This condition can create a hot spot, potentially damaging the diode itself [62].

With increasing shading on the module, the system exhibits several maximum power points, complicating the determination of the true global peak for conventional trackers [67, 68]. This scenario can result in oscillations around the MPP or other unintended behaviours, as illustrated in Fig. 1.22 and Fig. 1.23.

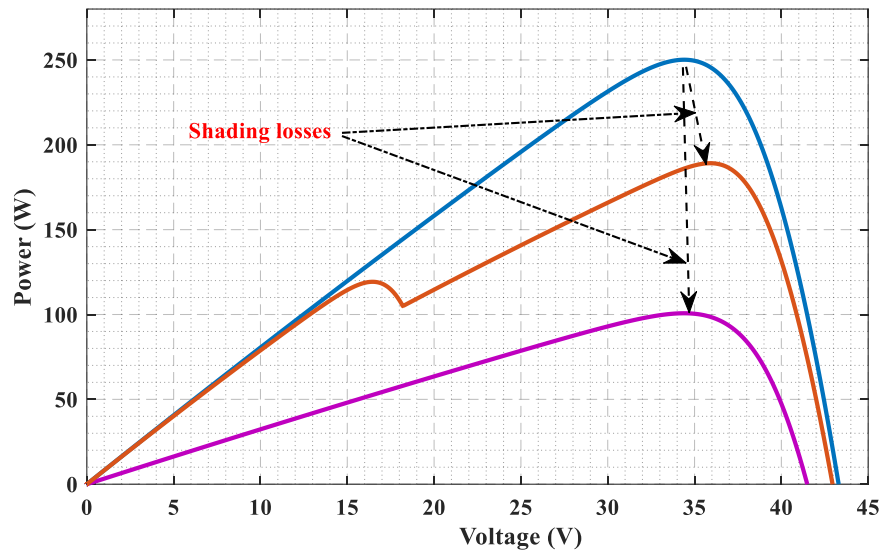


Fig. 1.22 P-V characteristic of PV module under PSC

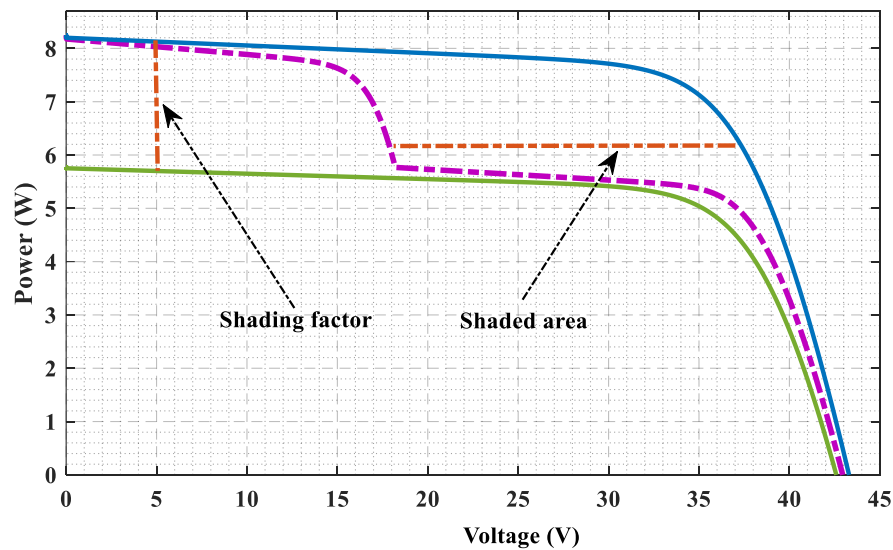


Fig. 1.23 I-V characteristic of PV module under PSC



Ambient temperature and solar irradiance are key determinants of a photovoltaics system's output voltage and current. The former component affects the voltage, while the subsequent parameter influences the current. The PV output voltage and current are critical in determining the maximum power point [69]. Power production is directly proportional to the amount of solar irradiance. Based on Table 1.2 and its corresponding P-V and I-V curves depicted in Fig. 1.24, it is evident that there is only one optimal point at which the maximum power is delivered to the PV system.

In large-scale PV systems, PV modules are arranged in series-parallel configurations. However, some modules perform poorly due to numerous factors, such as clouds, shade, and low solar irradiance. Partial shadowing condition refers to the situation in which an array experiences insufficient irradiance. This phenomenon introduces multiple peaks on the output characteristics of the photovoltaic array, as shown in Fig. 1.24 [70]. The highest point among these peaks is the “global maximum power point” (GMPP). The remaining maxima are named “local maximum power points” (LMPPs). The amplitude and location of LMPPs depend on the structure of photovoltaic modules and the shading patterns [71]. Employing advanced optimization methods to achieve the GMPP under PSCs is essential [72]. This phenomenon occurs because traditional MPPT methods fail to achieve convergence to the GMPP [73].

**Table 1.2** PV module configurations under different patterns.

Pattern	Irradiance (KW/m <sup>2</sup> )				Power Peaks (W)
STC	1	1	1	1	<b>500.2</b>
PSC1	1	0.5	1	1	<b>369.3</b> 292.0
PSC2	1	0.7	0.1	1	238.4 <b>287.3</b> 60.67

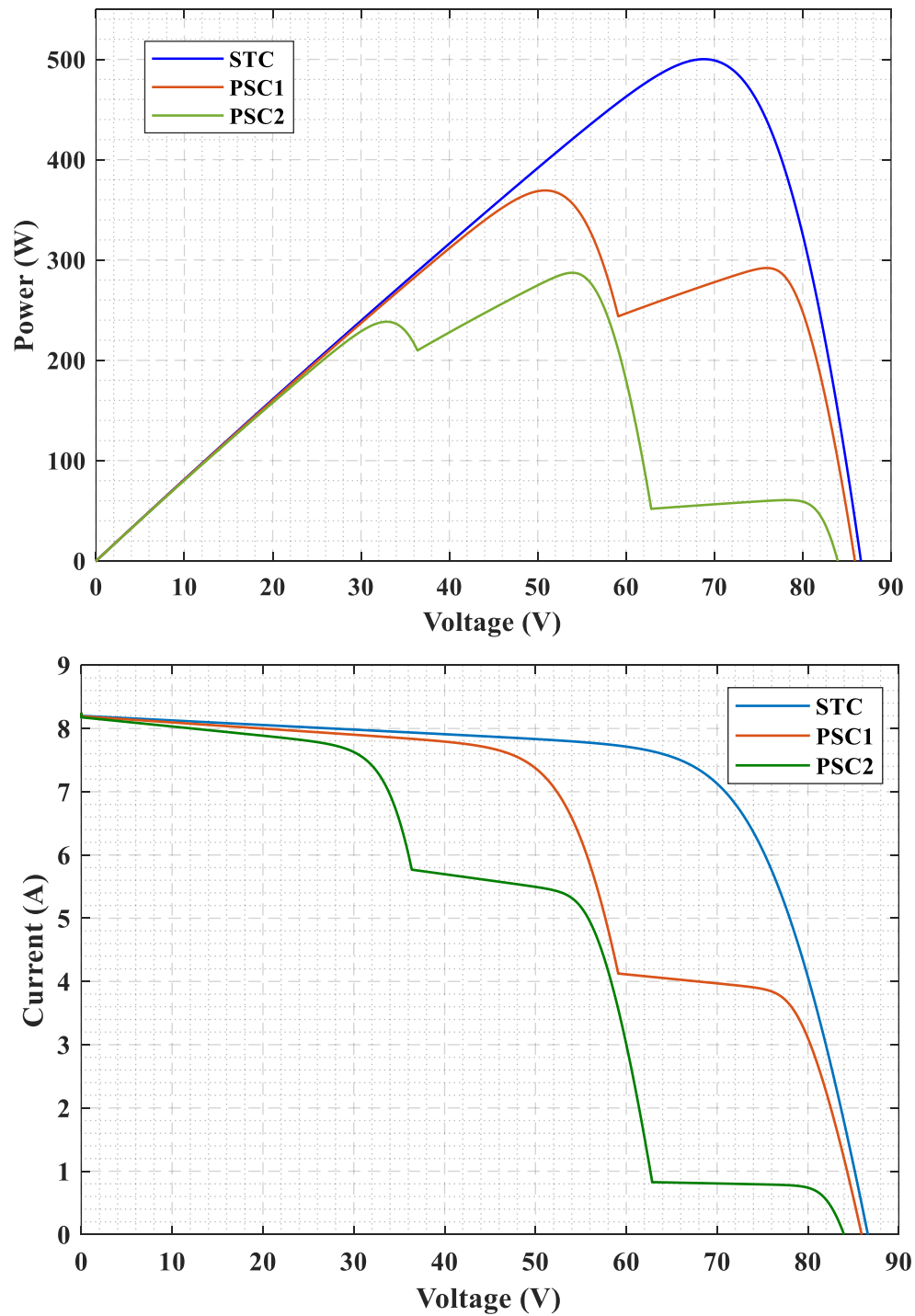


Fig. 1.24 I-V and P-V characteristics of PV module under various shading patterns

## 1.9 Partial shading mitigation techniques

PS mitigation methods are classified into two primary groups: “PV system design topologies” and “MPPT techniques”, as illustrated in Fig. 1.25. The design topologies of photovoltaic systems encompass “bypass and blocking diodes”, “PV system architectures”, “PV array configurations”, and “PV array reconfiguration”. Whereas, MPPT techniques include Conventional, Soft Computing and Hybrid approaches.

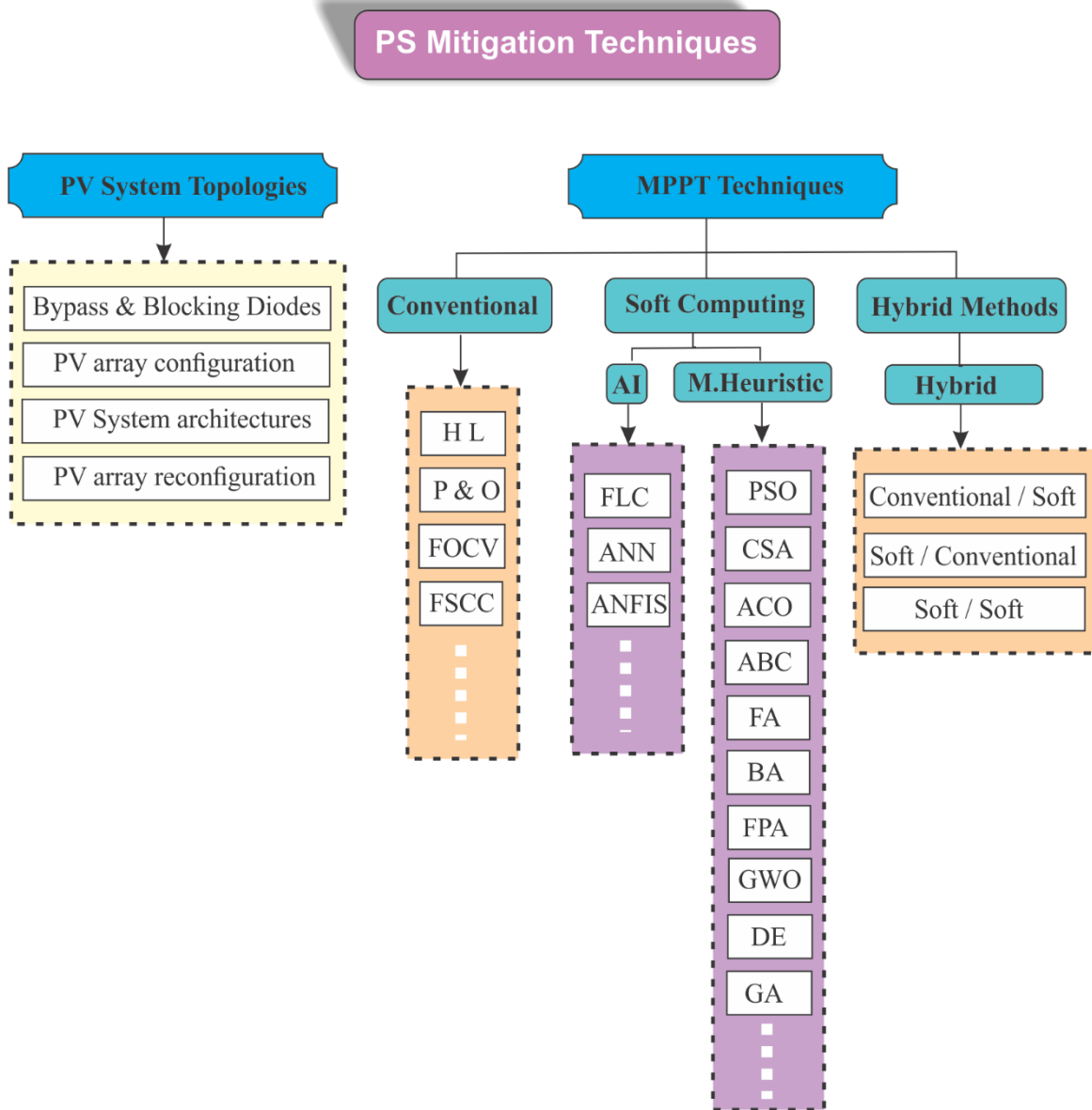


Fig. 1.25 Partial shading mitigation techniques

## 1.9.1 PV system topologies

### 1.9.1.1 Bypass and blocking diodes

“Bypass diodes” are installed in parallel with the photovoltaic module, whereas the “blocking diode” is coupled in series with the PV array to inhibit opposite current flow through shaded modules, as shown in [Fig. 1.26](#). Under standard conditions, the bypass diode is reversely biased; however, it conducts in non-uniform or PS conditions. The bypass diode serves two fundamental functions [74], outlined as follows:

- Ensuring the protection of the photovoltaic module against potential “hot spot” issues and thermal breakdowns that may arise, as illustrated in [Fig. 1.27](#) (a).
- Minimizes the reverse voltage drop of the shaded cells in the modules exposed to shading, thereby constraining the shading voltage drop to the diode’s reverse voltage (0.4–0.7 V).

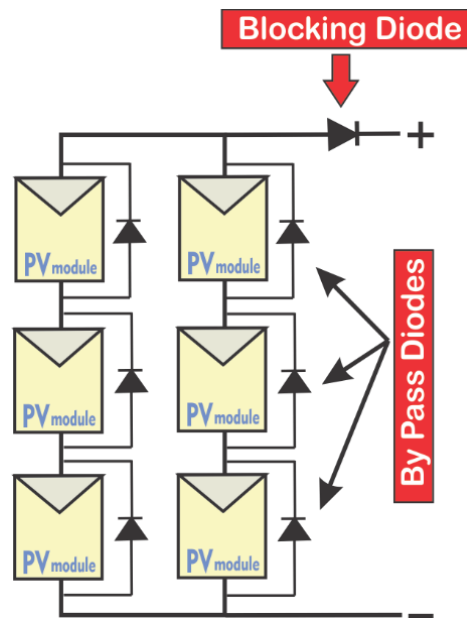


**Fig. 1.26** PV array along with the bypass and blocking diodes

Each photovoltaic module must have one or more antiparallel bypass diodes to safeguard the shaded cells from heat degradation as shown in [Fig. 1.27](#) (b). The current produced by the unshaded photovoltaic cells is conducted through bypass diodes, mitigating the shading impact and preventing degradation of the photovoltaic system.

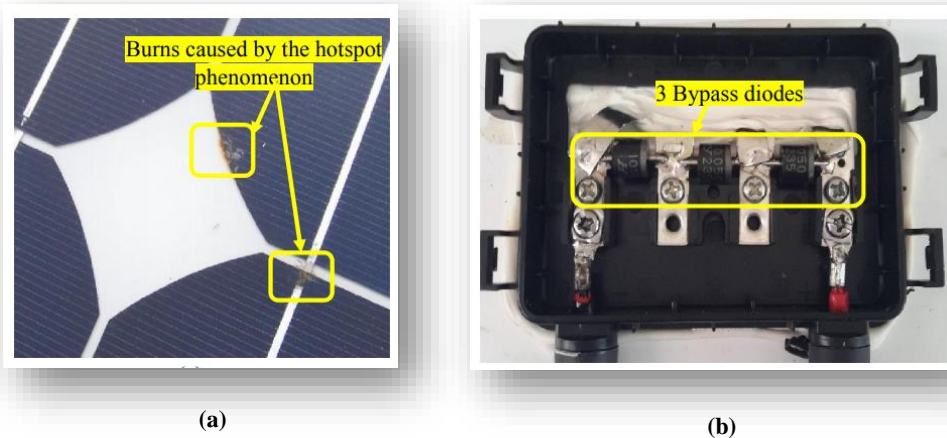


**Fig. 1.27** (a) Burns in PV module due to hotspots (b) Bypass diodes

Bypass diodes are critical components in photovoltaic systems, since they enhance performance by preventing power loss in shaded conditions. When a portion of a solar panel is shaded, the bypass diode allows the current to bypass the affected cells, ensuring that the unshaded sections continue to generate power. This effectively mitigates the "hot spot" phenomenon, which can damage the panel. Nevertheless, this method significantly alters the P-V characteristics of photovoltaic arrays, resulting in several Local Maximum Power Points (LMPP), which complicates the identification of the Global Maximum Power Point (GMPP), as shown in [Fig. 1.28](#). While bypass diodes offer major benefits regarding protection and longevity, their implementation is not without challenges. For instance, they can reduce the overall output power under PSCs, as the energy harvested from shaded cells is lost entirely or partially. Additionally, incorporating bypass diodes adds complexity and potential points of failure in the system. Thus, while they are beneficial for maintaining performance, careful design consideration is necessary to balance their advantages and disadvantages.

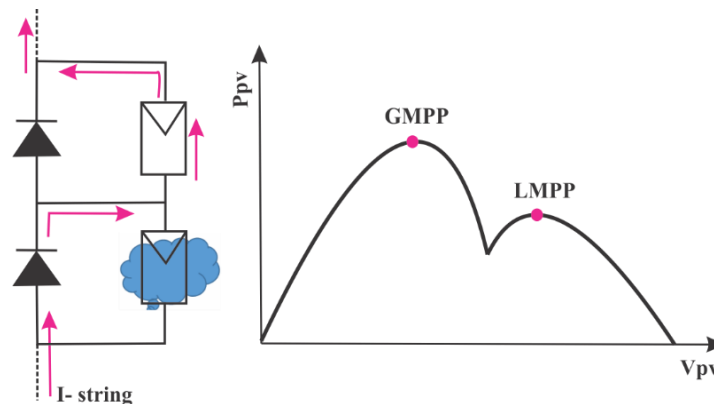


**Fig. 1.28** Bypass diodes effects on P-V characteristic

### 1.9.1.2 PV system architectures

PV system architectures involve designing and building photovoltaic modules. Various PV architectures can monitor the global power peak of individual PV modules. Therefore, photovoltaic designs that allow Maximum Power Point Tracking for each module will be more suited for partial shade. However, this characteristic will increase the total cost of the system. PV system architectures can be categorized into “centralized architecture”, “series-connected micro-converters”, “parallel-connected micro-converters”, “micro-inverters”, and “interleaved DC-DC converters”, as shown in Fig. 1.29 [75]. The benefits and shortcomings of various PV system architectures about PS are presented in Table 1.3.

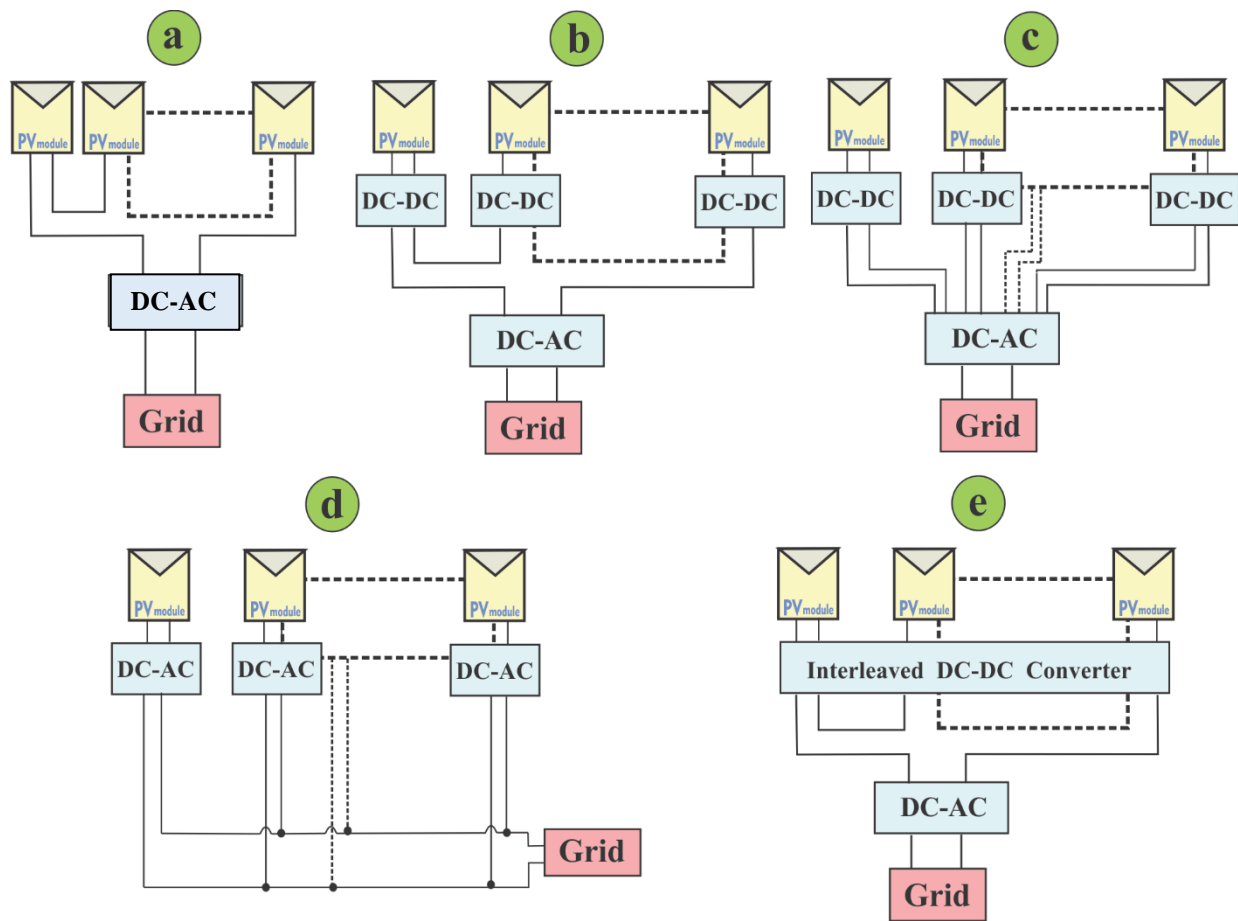


**Fig. 1.29** PV system architectures (a) centralized (b) series-connected MIC (c) parallel-connected MIC (d) micro-inverters and (e) interleaved DC-DC converter

**Table 1.3.** Comparisons of the PV system architectures

Topology	Applicable to PS	Benefits	Shortcomings
“Centralized”	NA	<ul style="list-style-type: none"> <li>• Effective under uniform conditions</li> <li>• Lower cost</li> </ul>	<ul style="list-style-type: none"> <li>• Conventional</li> <li>• Can’t track GP</li> <li>• Less sensitive to “PS” and mismatch power losses</li> </ul>
“Series/parallel (S&P) MIC.”	Yes	<ul style="list-style-type: none"> <li>• S&amp;P MIC suitable for “PS”</li> <li>• Series MIC are appropriate with HV requests</li> <li>• Parallel MIC are appropriate with LV requests</li> <li>• Large scale favored</li> </ul>	<ul style="list-style-type: none"> <li>• Increased cost</li> </ul>
“Micro-inverter”	NA	<ul style="list-style-type: none"> <li>• Suitable for tracking the GP of each module</li> </ul>	<ul style="list-style-type: none"> <li>• Not suitable with “PS”</li> <li>• Uncontrollable DC-link voltage</li> <li>• Higher cost</li> </ul>
“Multi-input DC-DC converter”	Yes	<ul style="list-style-type: none"> <li>• Suitable for PS</li> <li>• Can track GP</li> <li>• DC-link voltage is controlled</li> <li>• Convenient with Conventional MPPT methods</li> </ul>	<ul style="list-style-type: none"> <li>• High cost due to the large number of electronic devices.</li> </ul>

### 1.9.1.3 PV array configuration

Different configurations for photovoltaic modules can alleviate the effects of partial shading. Recent advancements have introduced various photovoltaic array configurations in the literature, including series, parallel, series-parallel (SP), total-cross-tied (TCT), bridge-linked (BL), and honey-comb (HC) arrangements [76, 77]. As shown in Fig. 1.30, Table 1.4 presents the advantages and disadvantages of various photovoltaic array configurations.

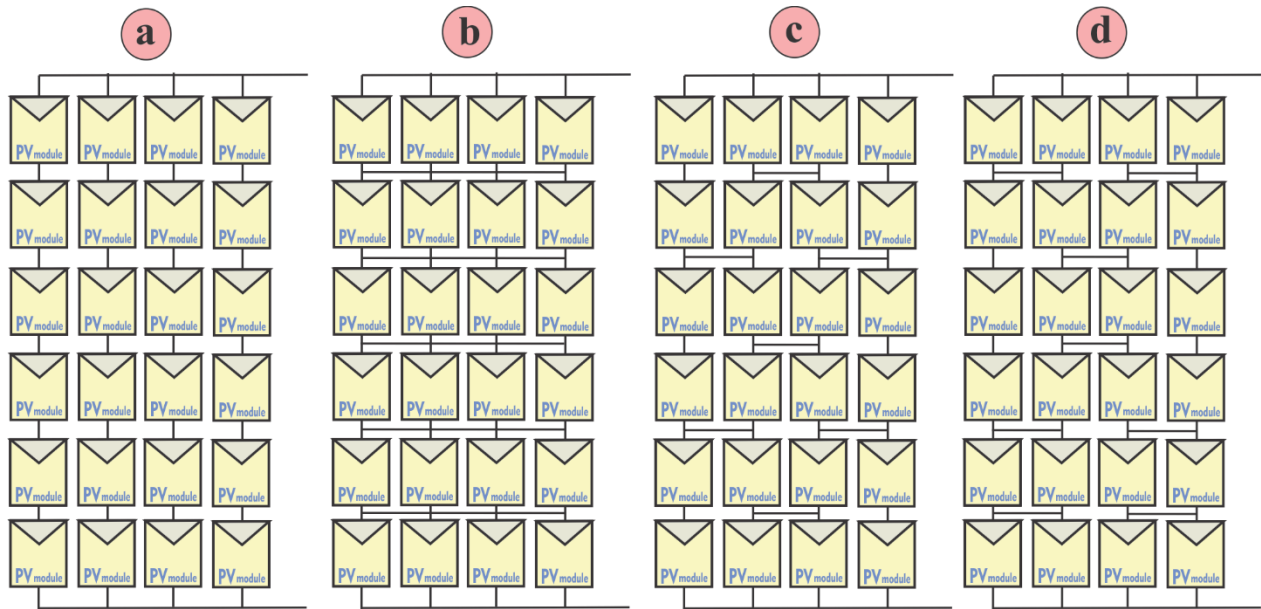


**Fig. 1.30** PV array configurations: (a) SP (b) TCT (c) BL (d) HC



**Table 1.4** Benefits and shortcomings of different PV array configurations

Configuration	Benefits	Shortcomings
<b>SP</b>	<ul style="list-style-type: none"> <li>• Effective under standard circumstances</li> <li>• Optimal cost efficiency</li> <li>• Lower complexity</li> </ul>	<ul style="list-style-type: none"> <li>• SP exhibits greater sensitivity to fluctuating irradiation levels compared to others, with a sharp decrease in power during PS.</li> <li>• Not suitable for PS</li> </ul>
<b>BL</b>	<ul style="list-style-type: none"> <li>• Suitable under PS</li> <li>• BL is 2.5% more efficient than SP</li> <li>• Can supply the grid under “PS”</li> </ul>	<ul style="list-style-type: none"> <li>• Moderate complexity</li> <li>• Moderate efficacy</li> </ul>
<b>TCT</b>	<ul style="list-style-type: none"> <li>• Suitable under “PS”</li> <li>• TCT offers enhanced performance, reduced sensitivity to “PS”, higher efficiency</li> <li>• Can feed the grid under PS</li> </ul>	<ul style="list-style-type: none"> <li>• TCT exhibits maximum connections and is more complicated than other designs.</li> </ul>
<b>HC</b>	<ul style="list-style-type: none"> <li>• Suitable for PS</li> <li>• Moderate MPP improvement</li> <li>• Can supply the grid during “PS”</li> </ul>	<ul style="list-style-type: none"> <li>• Moderate complexity</li> <li>• Medium efficacy</li> </ul>

#### 1.9.1.4 PV array reconfiguration

PV array reconfiguration is a critical strategy employed to enhance the performance and reliability of solar energy systems. This process involves adjusting the physical or electrical configurations of PV modules to optimize power output under varying environmental conditions, such as shading, soiling, or module degradation. The methods for array reconfiguration are primarily categorized into static and dynamic techniques. In the static reconfiguration techniques, the physical position of the PV module's configuration is altered in line with particular configurations to manage the impact of partial shading across the array. Static reconfigurations employ a predetermined interconnection strategy to enhance power output, which can be viewed as a one-time arrangement. The module location remains fixed and does not change dynamically,

as it is established for all shading conditions. Static reconfiguration procedures can conserve many switches and do not necessitate any sensors. Nevertheless, they cannot adaptively determine the ideal interconnection scheme in response to variations in irradiance circumstances, as the interconnection design remains static. The static approaches necessitate proficient individuals to execute physical modifications in the PV modules, and the use of extended connections results in supplementary power losses. The static approaches are mainly restricted to applications in small photovoltaic array configurations. Numerous static reconfiguration strategies and control algorithms have been developed in the literature to alleviate the impact of partial shading, including Sudoku, optimal Sudoku, Futoshiki patterns, magic squares, Zig-Zag arrangements, Competence Square techniques, Dominant Square procedures, Latin squares, odd-even structures, Skyscraper puzzles, Chaotic Baker Map techniques, and the Lo Shu concept [78-81].

In dynamic reconfiguration approaches, the physical positions of the modules in the photovoltaic array remain constant. Still, shadow distribution is accomplished by dynamically altering the electrical interconnections of the photovoltaic modules. Dynamic reconfigurations use switches, sensors, and control techniques to dynamically reconfigure the array by changing the module position in an array to enhance the output power [81]. The literature suggests numerous dynamic reconfiguration techniques for the modules of the photovoltaic array to alleviate the impact of partial shade. Examples include the optimization algorithm utilizing the equalization index, the Dynamic Electrical Scheme, and the Adaptive Array Reconfiguration Strategy. The adaptive approach improves the PV system's overall efficiency and extends individual modules' operational lifespan by ensuring balanced electrical loads [81]. Integrating advanced monitoring techniques has further facilitated dynamic reconfiguration, enabling systems to respond intelligently to fluctuating conditions. Upon detection of PS, the PV array's reconfiguration between fixed and adaptive configurations will be initiated through an adjustable switching matrix, as illustrated in Fig. 1.31. The primary role of the reconfiguration process is to optimize connections to mitigate the “PS” effects and enhance the power output from the photovoltaic array [81, 83].

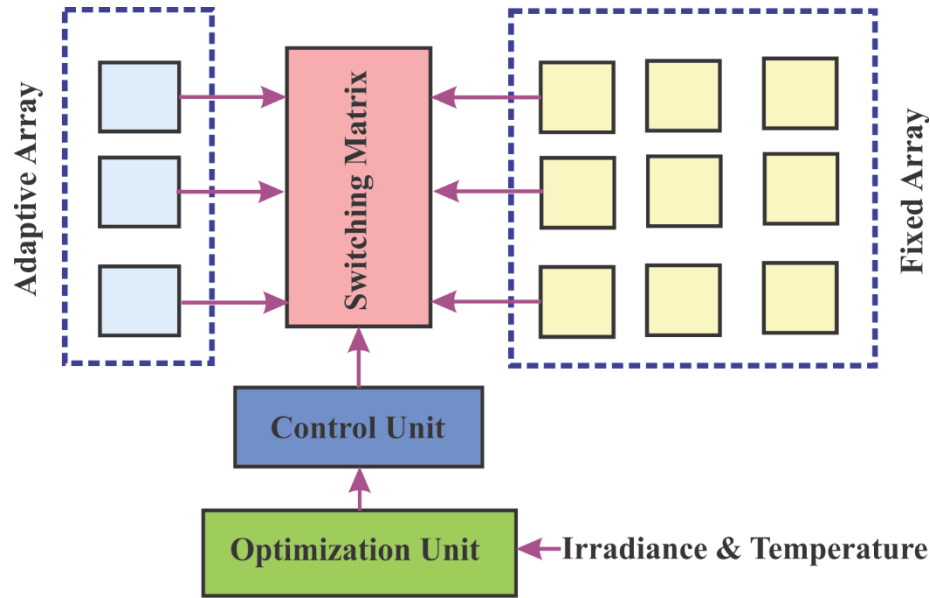


**Fig. 1.31** Adaptive reconfiguration technique process.

Modifying the PV array’s electrical configuration dynamically necessitates numerous switches, sensors, control techniques, and plant area, resulting in heightened costs and complexity of the system. Identifying a suitable electrical switching configuration is a complex and challenging endeavor. Consequently, one potential approach to effectively resolve this issue is the implementation of optimization techniques. Optimization approaches have become efficient solutions for determining the appropriate switching combinations in photovoltaic array reconfigurations. Numerous researchers have utilized metaheuristic algorithms, including the “Genetic algorithm”, “Particle Swarm optimization”, “Artificial Ecosystem-based Optimization”, “Grey Wolf optimizer”, “Grasshopper Optimization algorithm”, “Butterfly optimization algorithm”, “Marine Predators Algorithm”, “Modified Harris Hawks optimizer”, “Coyote Optimization algorithm”, “Firefly Optimization algorithm”, “Atom Search Optimization” and “Dynamic Leader Based Collective Intelligence” (DLCI). [84- 86]. For example, the DLCI technique integrates multiple meta-heuristic algorithms to optimize PV array configurations. DLCI enhances local exploration and global development, effectively avoiding power mismatches caused by local optima. It has shown significant improvements in reducing the number of power peaks under PSCs. These techniques are crucial for enhancing the efficiency and reliability of PV systems, particularly in environments where shading and other mismatches are common. The advantages and disadvantages of the PV array reconfigurations are depicted in [Table 1.5](#).

**Table 1.5** Advantages and disadvantages of the PV array reconfigurations

Topology	Benefits	Shortcomings
<b>Reconfiguration of PV array</b>	<ul style="list-style-type: none"> <li>• Circumvents the “PS” effects</li> <li>• Increase in the PV output power under PSCs up to 45%</li> <li>• Enhanced efficacy</li> <li>• Optimal arrangement for the shaded PV modules</li> </ul>	<ul style="list-style-type: none"> <li>• High complexity due to numerous switching elements.</li> <li>• Increased price</li> <li>• Inappropriate in certain PSCs</li> </ul>

### 1.9.2 MPPT techniques

MPPT is a widely used technique in PV systems to maximize power extraction under all environmental conditions. [Fig. 1.32](#) depicts a PV system integrated with MPPT. This section will be discussed in detail in the next chapter.

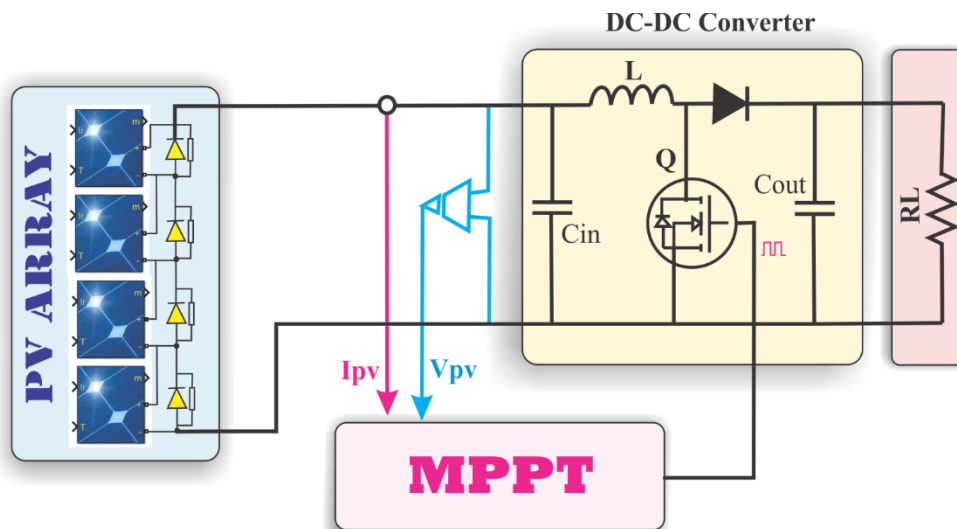


**Fig. 1.32** PV system integrated with MPPT.

## **1.10 Conclusion**

This chapter presents an overview of the photovoltaic system. Additionally, solar cell technology and its working principles, including the effect of temperature and irradiance on PV cell performance, are introduced. Special attention is given to PV array modeling due to the importance of precise modeling in system accuracy. Moreover, electrical power converters are thoroughly discussed due to their crucial importance in photovoltaic energy systems. Finally, the effect of partial shading on PV systems is presented including its mitigation through PV system design topologies, which is considered owing to the inherited features in optimizing the generated power in PV systems.

In the next chapter, we will introduce the different MPPT techniques used for tracking the GMPP under various weather circumstances, including PSCs, with a particular focus on hybrid metaheuristic methods.

## Chapter 2

---

# MAXIMUM POWER POINT TRACKING TECHNIQUES VIA METAHEURISTIC APPROACHES

## Contents

---

2.1	<a href="#">Introduction</a>	57
2.2	<a href="#">MPPT principle</a>	57
2.3	<a href="#">Challenges facing MPPT techniques</a>	57
2.4	<a href="#">Conventional MPPT techniques</a>	59
2.4.1	<a href="#">On-line techniques</a>	59
2.4.1.1	<a href="#">Perturb-and-Observe (P&amp;O) technique</a>	60
2.4.1.2	<a href="#">Incremental Conductance (InCond) technique</a>	60
2.4.2	<a href="#">Off-line techniques</a>	62
2.4.2.1	<a href="#">Fractional Open Circuit Voltage (FOCV) technique</a>	62
2.4.2.2	<a href="#">Fractional Short Circuit Current (FSCC) technique</a>	62
2.5	<a href="#">Maximum power extraction from the photovoltaic system under partial shading conditions</a>	62
2.6	<a href="#">Metaheuristic MPPT Techniques</a>	65
2.6.1	<a href="#">Swarm intelligence-based MPPT techniques</a>	66
2.6.1.1	<a href="#">Particle Swarm Optimization-based MPPT</a>	66
2.6.1.2	<a href="#">Ant Colony Optimization algorithm</a>	68
2.6.1.3	<a href="#">Artificial Bee Colony</a>	70
2.6.2	<a href="#">Evolutionary-based MPPT techniques</a>	72
2.6.2.1	<a href="#">Genetic Algorithm</a>	72
2.6.2.2	<a href="#">Differential Evolution Algorithm</a>	73
2.6.3	<a href="#">Nature inspired-based MPPT techniques</a>	75
2.6.3.1	<a href="#">Cuckoo Search</a>	75
2.6.3.2	<a href="#">Grey Wolf Optimization technique</a>	78
2.6.3.3	<a href="#">Flower Pollination Algorithm</a>	81
2.6.3.4	<a href="#">Firefly Algorithm</a>	82
2.6.3.5	<a href="#">Bat Algorithm</a>	83
2.7	<a href="#">Hybrid-based MPPT techniques</a>	86
2.7.1	<a href="#">Hybrid soft computing – soft computing algorithm</a>	86
2.7.2	<a href="#">Hybrid soft computing - conventional</a>	90
2.7.2.1	<a href="#">Steps of the algorithm</a>	90
2.7.2.1.1	<a href="#">PSO method</a>	90
2.7.2.1.2	<a href="#">PO method</a>	91
2.8	<a href="#">Overview of recent hybrid MPPT techniques in PV systems subjected to PSCs</a>	93
2.9	<a href="#">Conclusion</a>	98

## **2.1 Introduction**

Several maximum power point tracking techniques are available in the current market to ensure that photovoltaic modules operate at their maximum power output, which are divided into two classes, conventional and partial shading-based MPPT techniques [87]. Numerous publications in the literature are proposed for enhancing and optimizing these techniques. Nevertheless, they vary in several aspects, including the number of sensors employed, the tracking accuracy, the steady-state and dynamic efficiencies, the convergence speed, tuning parameters, computational burden, and hardware complexities [88].

This chapter deals with the most recent metaheuristic approaches to harvesting and monitoring the GMPP in PV systems subjected to PS issues. The necessary theory of these techniques is presented, and their features are discussed. This review of shading mitigation techniques through metaheuristic approaches will assist researchers in selecting suitable mitigation techniques for specific PV applications.

## **2.2 MPPT principle**

Maximum Power Point Tracking is an integral part of a photovoltaic system to ensure that solar panels constantly work at their optimal power point, adapting to changing environmental circumstances. MPPT is designed to dynamically monitor the operating point of the modules to ensure the system always extracts the optimum possible power, thereby enhancing the overall efficiency of the PV system. MPPT relies essentially on altering the duty cycle of a DC-DC converter to enhance the performance of photovoltaic systems. The core objective of an MPPT tracker is to find the Maximum Power Point for the current-voltage characteristic of the PV array. At this point, the PV array produces its maximum possible power. Nevertheless, this point shifts with variations in irradiance, temperature, and other constraints, making continuous tracking mandatory.

## **2.3 Challenges facing MPPT techniques**

The dynamic nature of environmental conditions, including irradiance and temperature variations and partial shading of solar panels, are the major challenges faced in monitoring Maximum Power Point Tracking in PV generation systems (PVGS); these factors can significantly affect the efficiency and reliability of the PV system. Additionally, the load variations and oscillations around the MPP, if not considered by the MPPT tracker, might lead to system

instability and important power losses. Furthermore, the complex nature of the algorithms necessary for accurate tracking may result in heightened computing requirements and possible delays in real-time applications. Moreover, the trade-off between tracking precision and reaction time might influence the overall efficacy of MPPT systems, rendering it essential to equilibrate these elements for efficient energy conversion. Furthermore, the integration of MPPT trackers in PV systems subjected to these challenges requires robust and adaptive control strategies to ensure consistent and optimum performance. The challenges facing MPPT techniques are illustrated in [Fig. 2.1](#).

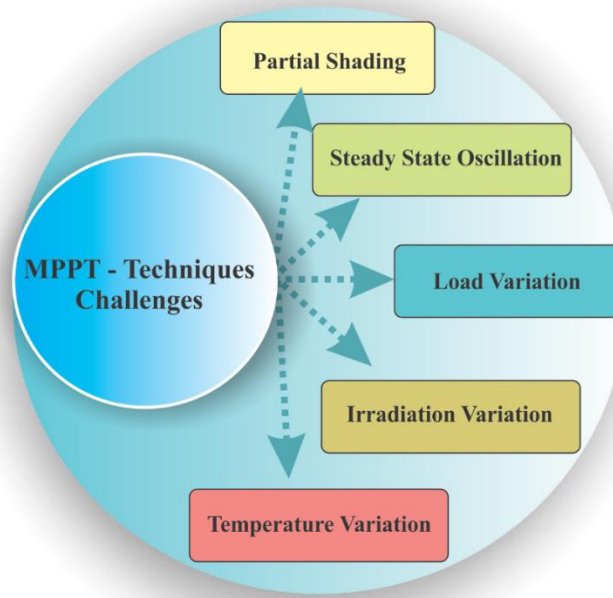


**Fig. 2.1** Challenges Facing MPPT Techniques

The configuration of the PV system is shown in [Fig. 2.2](#). Under uniform circumstances, a singular Maximum Power Point (MPP) is demonstrated in the P–V and I–V characteristics, facilitating the MPP tracking. Conversely, the P– V and I–V curves exhibit several peaks when some photovoltaic modules or cells experience varying solar irradiation levels due to partial shadowing. Consequently, the MPPT algorithm must possess the capability to identify the GMPP from several local power maxima. Numerous MPPT approaches have shown efficacy in monitoring the GMPP and optimizing performance across all operating circumstances. Theoretically, the optimal MPPT approach for a photovoltaic system should have the following capabilities:



1. The capacity to precisely monitor the GMPP under partial shading circumstances.
2. The capacity to adapt to rapidly changing climatic conditions.
3. The system is independent and does not rely on the arrangement of the PV arrays.
4. The system's resilience to climate perturbations and fluctuations in photovoltaic panel parameters.
5. The ease of implementation with minimal computing complexity and reduced system cost.

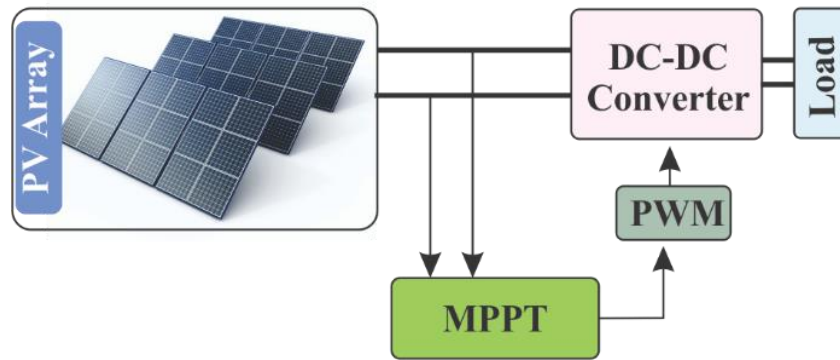


**Fig. 2.2** MPPT control system

## **2.4 Conventional MPPT techniques**

Conventional MPPT techniques are classified broadly into two types:

- (i) Online approaches such as “perturb and observe” (P&O) and “incremental conductance” (InCond).
- (ii) Off-line approaches such as “fractional open circuit voltage” (FOCV) and “fractional short circuit current” (FSCC).

These MPPT techniques are ineffective in accurately monitoring the maximum power point (MPP) during sudden or rapid changes in solar irradiation, as well as under partial shading, which results in fluctuations around the MPP and tracking a local peak (LP) rather than the global peak (GP).

### **2.4.1 On-line techniques**

The term "online" denotes the continuous running of the MPP tracker. The required measurements are sensed without disconnecting the PV system. The online techniques include “perturb and observe” (P&O) and “incremental conductance” (InCond) methods.

### 2.4.1.1 Perturb-and-Observe (P&O) technique

“Perturb and Observe” (P&O) [89] is a frequently used Maximum Power Point Tracking method. This technique involves monitoring the maximum power point by controlling the DC-DC converter's duty cycle and measuring the output photovoltaic power. The output voltage and current ( $V_{pv}$ ,  $I_{pv}$ ) of the PV panel are measured at each sampling time, afterward, the power ( $P_k$ ) is calculated and compared to the previously measured power  $P(k-1)$ . The algorithm follows this process until the Maximum Power Point is reached, at which point the differential ratio of power to voltage is zero ( $\Delta P/\Delta V=0$ ).  $\Delta P$  and  $\Delta V$  are constantly calculated, and the converter's duty ratio sign is altered to attain the MPP. The flow chart of this algorithm is illustrated in Fig. 2.3.

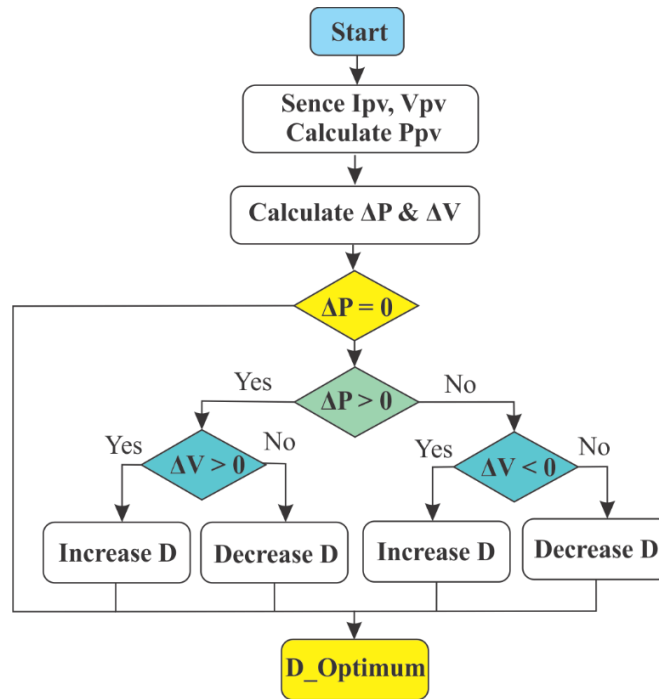


Fig. 2.3 Flow chart of the Perturb & Observe method

### 2.4.1.2 Incremental Conductance (InCond) Technique

The fundamental principle of the “incremental conductance” method [90] is that the slope of the power-voltage curve at the MPP equals zero ( $dP/dV = 0$  or  $dP/dI = 0$  at MPP). The InCond method was developed to address the limitations of the P&O algorithm, including oscillations in steady state caused by duty cycle perturbations. This MPPT approach aims to enhance tracking speed and increase the energy output of the PV system subjected to irradiation changes.

The InCond MPPT method employs equations (2.1) to (2.4) to monitor the MPP.

$$\frac{dP}{dV} = \frac{d(V \cdot I)}{dV} = I + V \frac{dI}{dV} \quad (2.1)$$

Where  $\Delta I/\Delta V$  refers to the incremental conductance whereas,  $I/V$  represents the instantaneous conductance.

$$\begin{cases} \frac{dP}{dV} = 0 & \text{At the MPP} \end{cases} \quad (2.2)$$

$$\begin{cases} \frac{dP}{dV} > 0 & \text{To the left of MPP} \end{cases} \quad (2.3)$$

$$\begin{cases} \frac{dP}{dV} < 0 & \text{To the right of MPP} \end{cases} \quad (2.4)$$

In the InCond. MPPT method the instantaneous conductance, and the incremental conductance are instantly compared where they are equal at MPP. The INC-based algorithm offers advantages over conventional techniques due to its ease of implementation, enhanced tracking speed, and improved efficacy. The flow chart of this algorithm is illustrated in [Fig. 2.4](#).

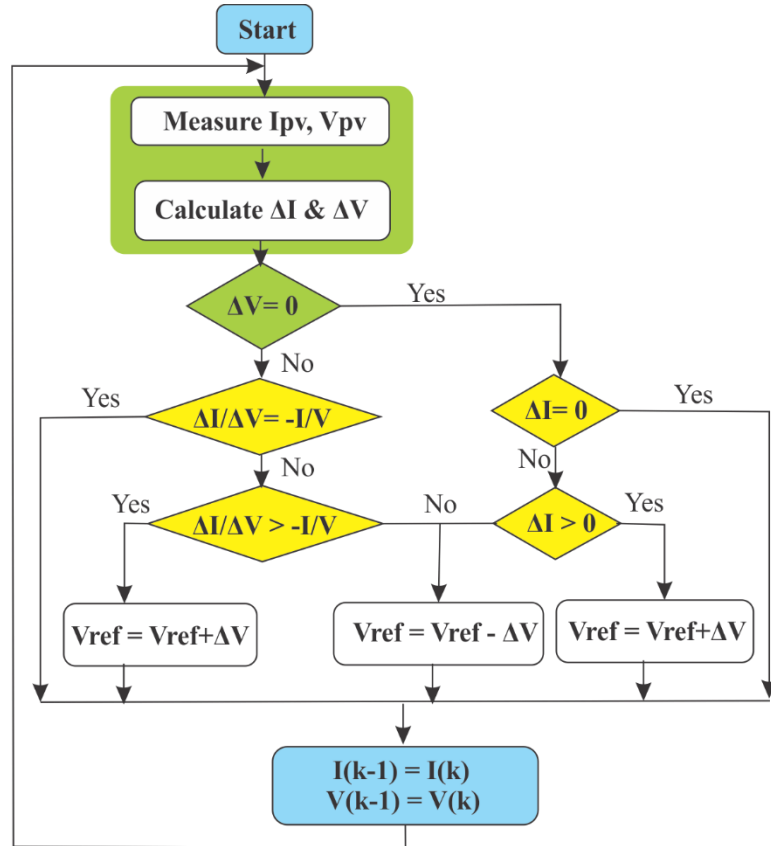


Fig. 2.4 Incremental Conductance Flow chart

### 2.4.2 Off-line techniques

The term “off-line” indicates the process of deactivating the PV system, allowing the tracker to operate according to one of these techniques, which include “fractional open-circuit voltage” (FOCV) and “fractional short-circuit current” (FSCC) techniques.

#### 2.4.2.1 Fractional Open Circuit Voltage (FOCV) technique [91]

This method is referred to as the constant voltage technique. The MPPT monitor using this approach determines the working voltage to be (70–85%) of the open circuit voltage ( $V_{oc}$ ) of the module. The primary limitation of this approach is its reliance on the open circuit voltage value. This necessitates disabling the module output current to measure the open circuit voltage, resulting in considerable power loss in large photovoltaic systems. The open circuit voltage fluctuates with weather conditions, such as ambient temperature and irradiation levels; thus, researchers consistently combine this method with other MPPT methods to ensure the tracker operates effectively under diverse circumstances.

#### 2.4.2.2 Fractional Short Circuit Current (FSCC) technique [92]

This method is referred to as the constant current method. The tracker using this approach picks the operating current at (78–90%) of  $I_{sc}$ , where  $I_{sc}$  denotes the short-circuit current of the module. The primary disadvantage of this approach is its reliance on assessing the value of the short-circuit current. This necessitates disconnecting and short-circuiting the module to get the “short circuit current” value. The disconnection of the photovoltaic module leads to power losses. Given that the “short-circuit current” fluctuates with weather circumstances, such as irradiation variations, researchers consistently combine this approach with additional MPPT methods to ensure the MPPT monitor operates effectively under all situations.

### 2.5 Maximum power extraction from the photovoltaic system under partial shading conditions

When the PV module is linked to a resistive load, the generated output current and voltage are dependent of the module’s operating point. This point is located at the intersection of module and load I-V characteristics as illustrated in [Fig. 2.5](#). The module I-V characteristic exhibits non-linearity, presenting a single maximum power point (MPP) at which the operation is hard to maintain. Furthermore, the I-V and P-V curves of the module are altered by fluctuations in

irradiance, ambient temperature, and partial shading conditions (PSCs), resulting in a new position of the MPP as shown in Fig. 2.6.

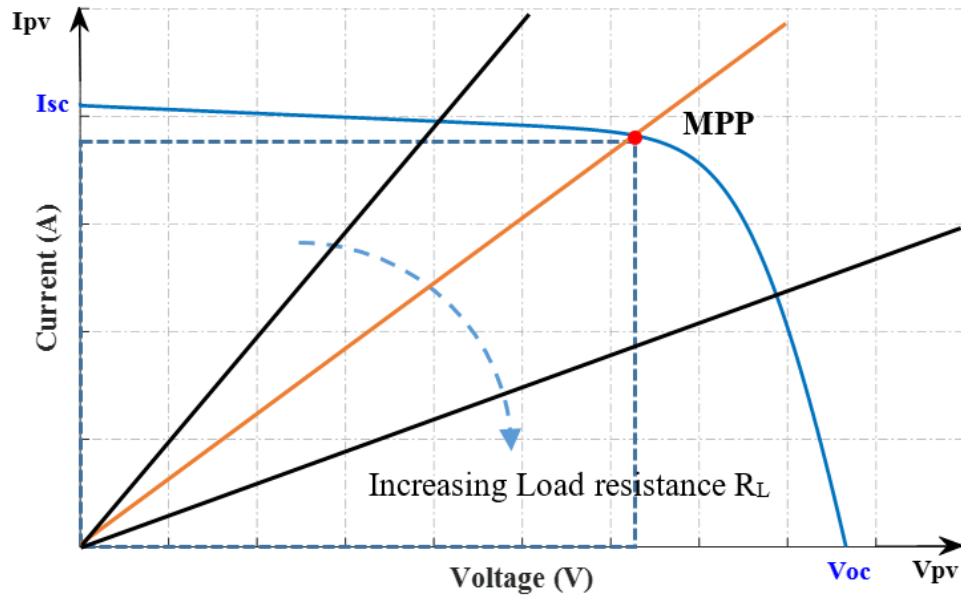


Fig. 2.5 Influence of the load resistance on the operating point

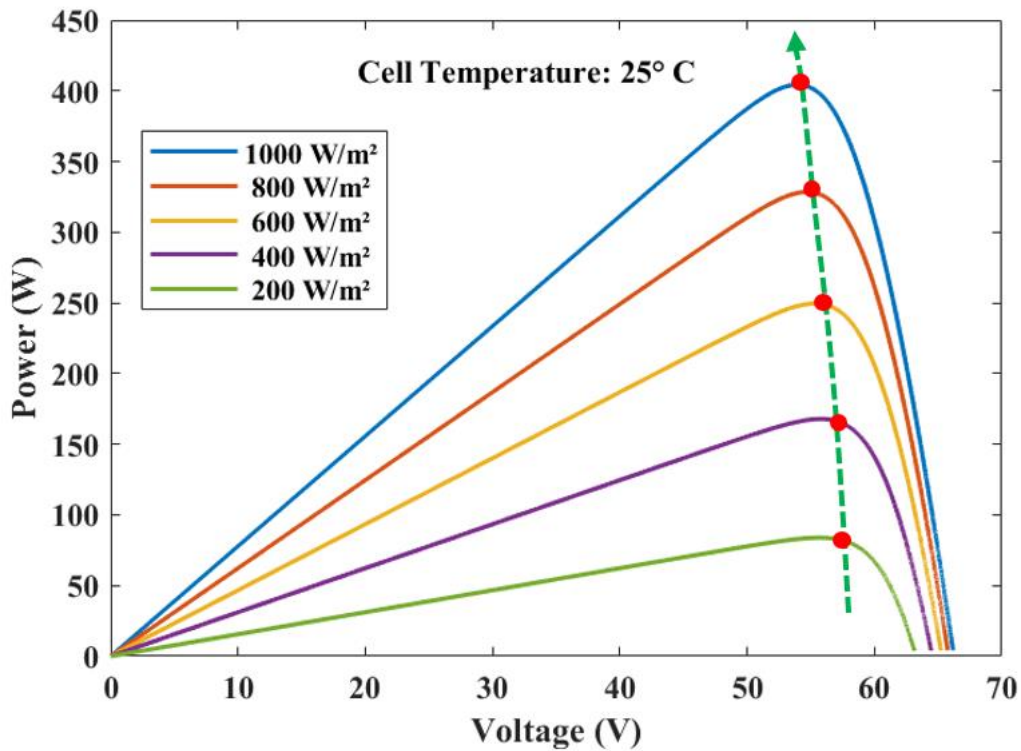


Fig. 2.6 Influence of the irradiance on the MPP.

Partial shading conditions (PSC) adversely affect both the shaded photovoltaic (PV) modules/arrays and the output power produced by the partly shaded photovoltaic (PSPV) system. It diminishes the output power produced by the photovoltaic (PV) system and causes the hot spot issue, potentially resulting in the thermal failure of shaded PV modules. Under PSC, the P-V curve exhibits many peaks, including one global peak (GP) and several local peaks (LPs) as illustrated in Fig. 2.7.

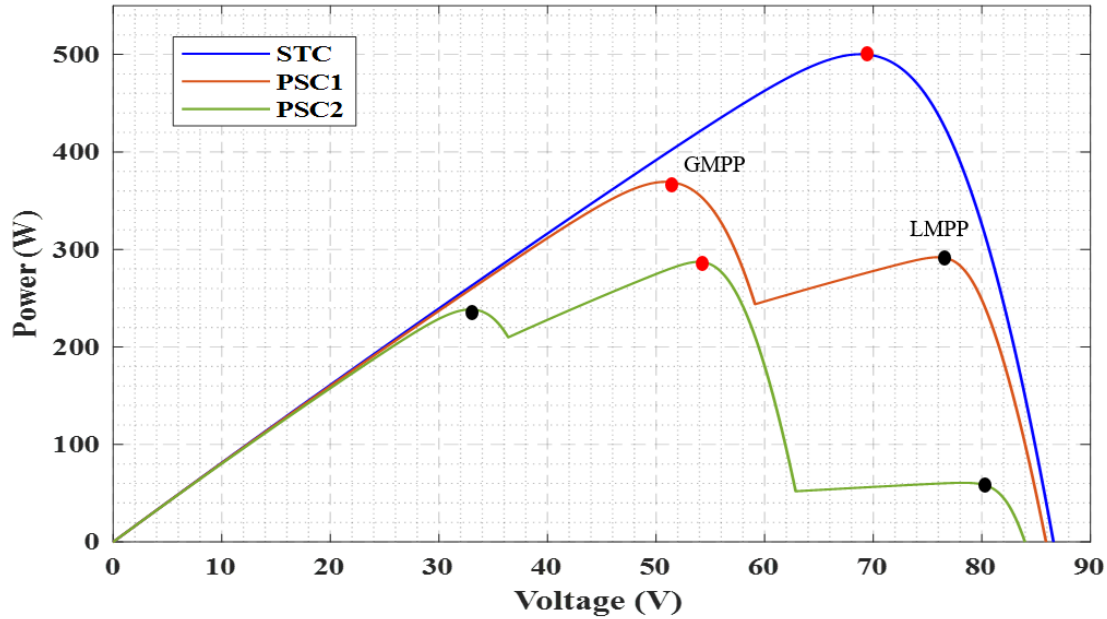


Fig. 2.7 Multi-MPP due to PS effect

The partial shading issue arises when some photovoltaic cells and/or modules are affected by shading. It may arise from nearby buildings, accumulated dust, clouds, or deterioration due to aging. The shaded PV cells/modules are compelled to conduct the high current of the other unshaded PV cells/modules, which makes them consuming power rather than generating it [93]. As the shading area becomes more important, power losses also increase proportionally, resulting in a reduction in PV output power. Therefore, the overall efficiency of the PV system is greatly affected by the shading issue, where power losses may attain 70% of the system's total power. Therefore, monitoring the global maximum power is mandatory for optimal power efficiency [94]. As aforementioned, conventional MPPT methods, especially IncCond and P&O, are effective and reliable in tracking the MPP under standard conditions. Still, they fail to track the GP once shading

or variations in irradiance occur. In contrast, metaheuristic approaches can track and monitor efficiently the GP under PSCs and complex weather circumstances.

## 2.6 Metaheuristic MPPT techniques

Global optimization approaches, including metaheuristics based on computational intelligence (CI) algorithms, are advantageous for addressing real-world nonlinear issues in contrast to basic mathematical methods. [Fig. 2.8](#) presents swarm, differential evolution, and nature-inspired algorithms. The following sections provide a detailed discussion of several metaheuristic algorithms based on CI techniques.

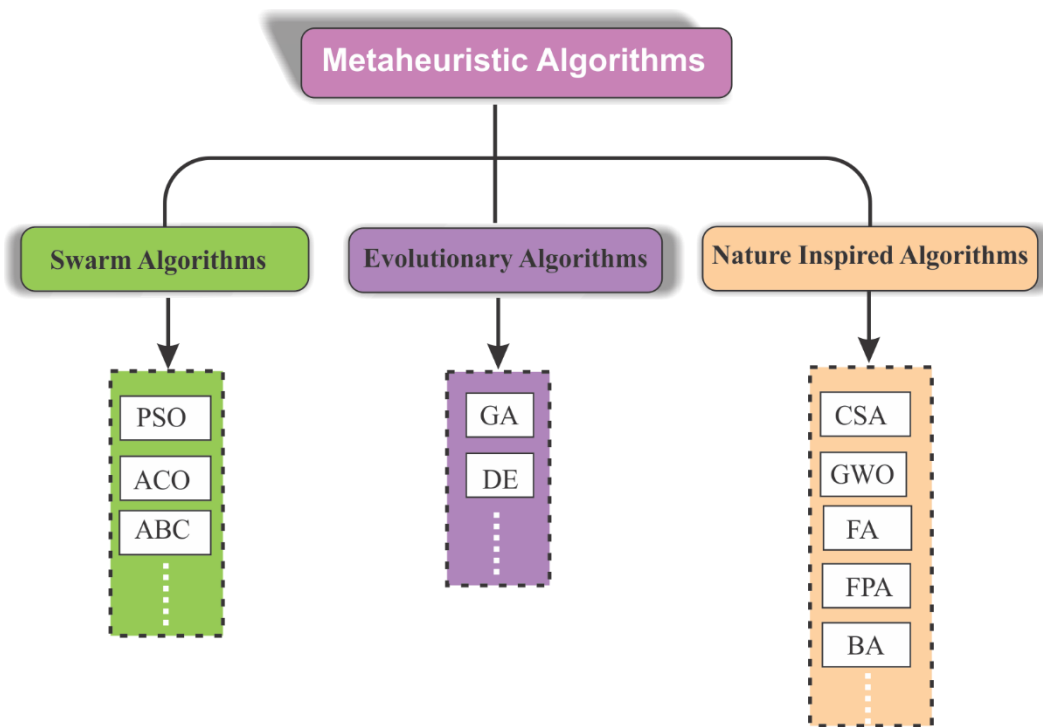


**Fig. 2.8** Classification of MPPT-based Metaheuristic Algorithms

## 2.6.1 Swarm intelligence-based MPPT techniques

### 2.6.1.1 Particle Swarm Optimization-based MPPT

“Particle swarm optimization” (PSO) is a prominent metaheuristic search technique that garners significant interest in engineering applications. PSO was initially proposed in 1995 by Kennedy and Ebrahat, drawing inspiration from the natural behavior of avian flocking [95]. This theory primarily investigates the optimum solution in a certain range known as the solution search space. The PSO adjusts each particle through the possible solution space to identify the optimal solution based on the experiences of both self and adjacent particles throughout the optimization process. Consequently, particles engaged in optimization use their memory to adjust their fitness by emulating the behaviour of successful particles within the swarm. The PSO technique begins with a random set of particles, progresses by seeking optimum solutions from previous iterations, and then assesses particle quality based on the fitness function.

[Fig. 2.9](#) illustrates the flowchart of the PSO-based maximum power point tracking system. An initial set of duty cycles is randomly affected. Subsequently, each one is transmitted to the DC-DC converter. The system's current and voltage are measured to determine the generated photovoltaic power. This power denotes the fitness function of the particle (i). The subsequent step involves recording the comparison between the current fitness value and the power associated with the best particle (pbest) in the past. The new projected power is designated as the optimal fitness value if it exceeds the previous value. Upon assessing all particles, each candidate solution's previous velocity and position are updated. When reaching the stopping condition, the PSO-based tracker provides the optimum duty cycle corresponding to global maximum power [96]. The velocity and position of particles in the PSO algorithm are determined using equations (2.5) and (2.6) [97].

$$v_i^{k+1} = wv_i^k + r_1c_1(pbest_i - d_i^k) + r_2c_2(gbest_i - d_i^k) \quad (2.5)$$

$$d_i^{k+1} = d_i^k + v_i^{k+1} \quad (2.6)$$

Where  $i$  refers to the optimization vector variable, whereas  $k$  represents the number of iterations,  $v$ , and  $d$  denote the velocity and position of the  $i^{th}$  variable across  $k$  iterations,  $w$  represents the inertia weight parameter,  $c_1$  is the cognitive factor for individual candidates,  $c_2$  is the social factor for all candidates, and  $r_1$  and  $r_2$  are randomly selected variables within the interval



[0,1]. The primary objective of these random values is to sustain stochastic behaviour throughout the iterations. The update conditions for the global best ( $G_b$ ) and particle best ( $P_b$ ) are given in equations (2.7) and (2.8).

$$P_{bi} = d_i^k \quad \text{if } F(d_i^k) \geq F(P_{bi}) \quad (2.7)$$

$$G_b = P_{bi} \quad \text{if } F(P_{bi}) \geq F(G_b) \quad (2.8)$$

In practice, the produced power fluctuates because of changes in partial shadowing and irradiation degrees. Consequently, the algorithm must be initiated upon fulfilling Eq. (2.9).

$$\frac{F(d_{i+1}) - F(d_i)}{F(d_i)} > \Delta P \quad (2.9)$$

The parameters influencing PSO performance include cognitive and social coefficients, inertia factor, number of particles, and the maximum number of iterations. The merits of PSO are its global tracking capability, low computing burden, and ease of integration with other algorithms. The shortcomings of PSO include the slow tracking speed of traditional PSO-based MPPT when used in large-scale PV arrays and their sensitivity to control factors.

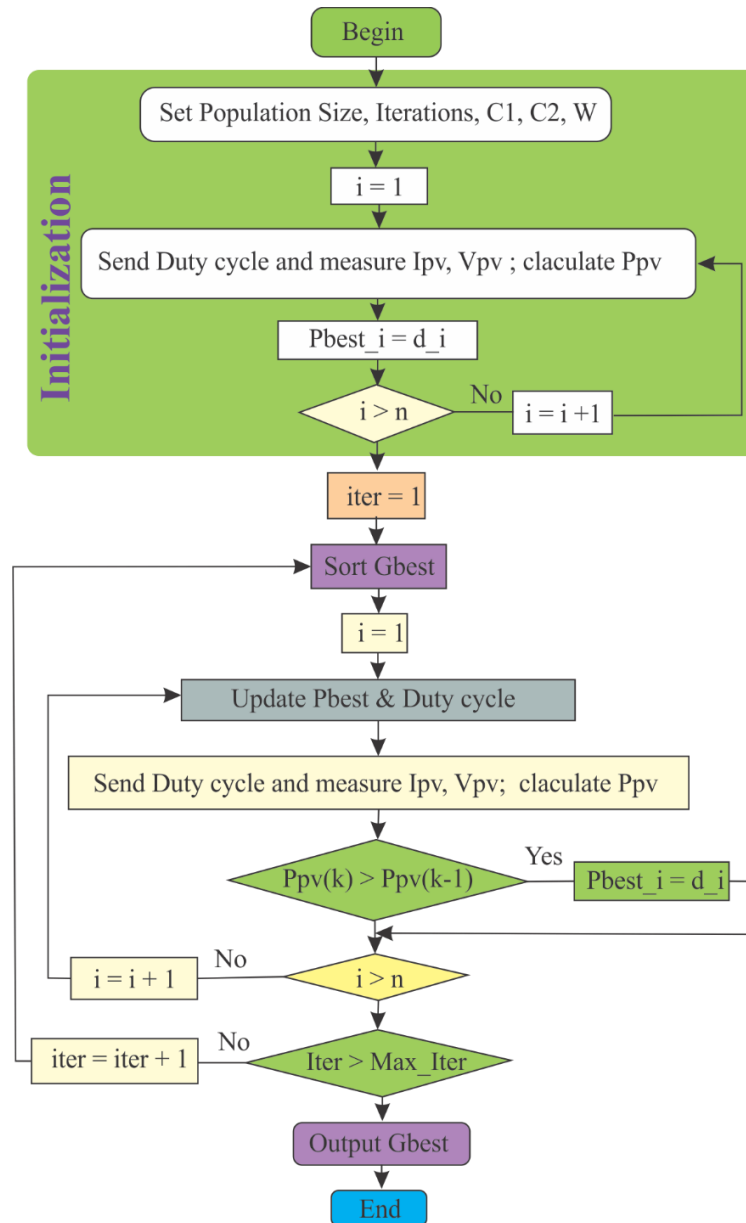
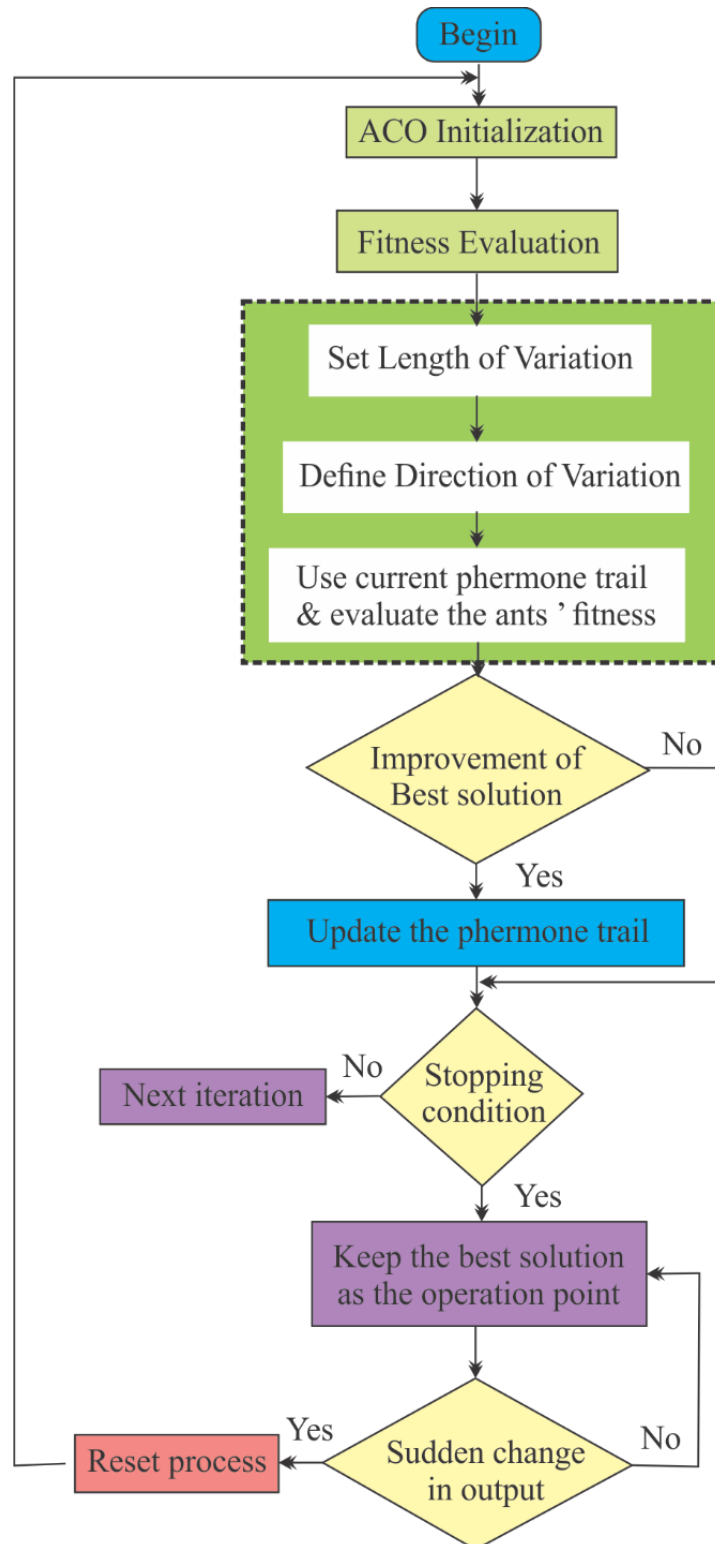


Fig. 2.9 Flowchart of PSO-based Tracker

### 2.6.1.2 Ant Colony Optimization Algorithm

“Ant colony optimization” (ACO) is a metaheuristic technique used for global search to find the optimum solution in stochastic problems. The method was first presented by “Dorigo and Gambardella” in 1997, inspired by the foraging behaviour of ants to choose the optimal way to food. ACO emulates the social comportment of ants in their quest for a food source. [Fig. 2.10](#) provides a concise and systematic overview of ACO. In the ACO-based MPPT tracker, each position corresponds to the voltage value of the photovoltaic array. The objective function



**Fig. 2.10** Flowchart of the ACO Algorithm

represents the output power of the photovoltaic array, while the fitness of each ant is assessed based on its voltage value. ACO has been applied to address challenges in various renewable energy domains [98]. The ACO-based MPPT was evaluated under diverse shading conditions, yielding satisfactory results. The proposed method demonstrated high efficiency and incurred minimal system costs. The system is capable of tracking the global maximum power point utilizing only a current sensor. Moreover, the convergence to the GMPP of the Ant Colony Optimization approach does not depend on the initial conditions.

### **2.6.1.3 Artificial Bee Colony**

An innovative “Artificial Bee Colony” approach (ABC) is formulated to address the limitations of traditional techniques, using a resilient maximum power point tracking scheme with few adjusting parameters and convergence criteria independent of the system's starting circumstances. It is a swarm-based metaheuristic method that efficiently addresses multidimensional and multimodal optimization challenges. The artificial bees are classified into employed, onlooker, and scout bees [99]. The bee that actively forages for food is called an employed bee, whereas a bee that remains in the hive to evaluate and choose food sources is referred to as an onlooker. The scout bee's task is to carry out a random search for new food sources. In the ABC algorithm, the three groups collaborate through coordination and communication to get the ideal solution in minimum time. The duty ratio represents the food location, whereas maximum power denotes the food source. The ABC technique monitors power tracking with high accuracy in partial shading scenarios. The performance of ABC is impacted by several parameters, including the number of trials, the number of candidates in the search space, and the maximum number of iterations. The flowchart of the ABC technique is shown in [Fig. 2.11](#).

The merits of ABC include good accuracy under diverse shading circumstances, fewer parameters to configure compared to “PSO”, “DE”, and “ACO”, minimal complexity, accessible tuning parameters, and independence from starting conditions. The shortcomings of ABC include a slow convergence speed.

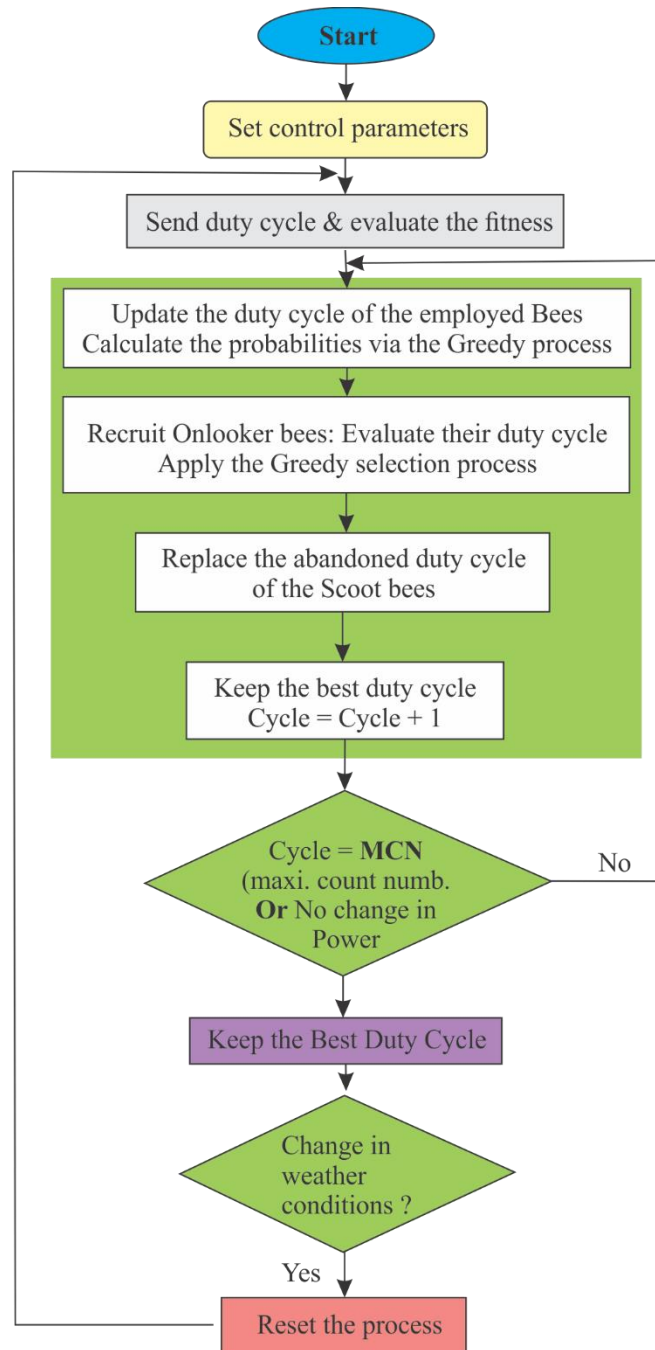


**Fig. 2.11** Flowchart of the Artificial Bee Colony Algorithm

## **2.6.2 Evolutionary-based MPPT techniques**

### **2.6.2.1 Genetic Algorithm**

The “genetic algorithm” (GA) is a metaheuristic optimization technique that derives solutions from the principles of biological evolution. This strategy was proposed by “Holland” in 1975 based on the notion of survival of the fittest. Generally, genetic algorithms represent candidates' solutions, referred to as chromosomes, using fixed-length strings. The evolutionary process facilitates the survival and reproduction of the fittest chromosome over generations. The GA is an iterative technique wherein a population of chromosomes develops and enhances throughout generations influenced by GA operators.

In each generation, parents are chosen from the current population to produce descendants for the subsequent generation. The goal function serves as the primary criterion for enhancing population fitness over time. [Fig. 2.12](#) illustrates the flowchart of the GA algorithm. It illustrates the technique and life cycle of the population, whereas the phases of the genetic algorithm include initialization, selection, crossover, and mutation. Genetic algorithm was adapted to monitor the global maximum power point of the photovoltaic system under PSCs. MPPT control was formulated using the GA technique, and the methodology was validated using two distinct scenarios with partial shading patterns. Nonetheless, the verification aspect is confined to simulated validations, and the method's practicality in a real-world setting has not been shown. The GA method is mostly used in hybrid approaches to enhance the efficacy of existing MPPT techniques. Combining the P&O technique with GA results in a reduction in population size and a decrease in the number of iterations. The hybrid technique exhibited accelerated convergence and enhanced accuracy for the PV system under diverse partial shade patterns compared to a conventional GA approach [[100](#)].

A different kind of hybrid optimization approach involves using genetic algorithms to adjust the settings of a fuzzy logic controller used in maximum power point tracking under partial shading conditions. The efficacy of fuzzy logic control is enhanced when parameters, including rule base and membership functions, are adjusted to their optimal values by genetic algorithm approaches. The GA approach was ultimately used as a mechanism to train the ANN system. In this technique, genetic algorithm is applied to determine the number of neurons in a multilayer perceptron neural control system [[101](#)].

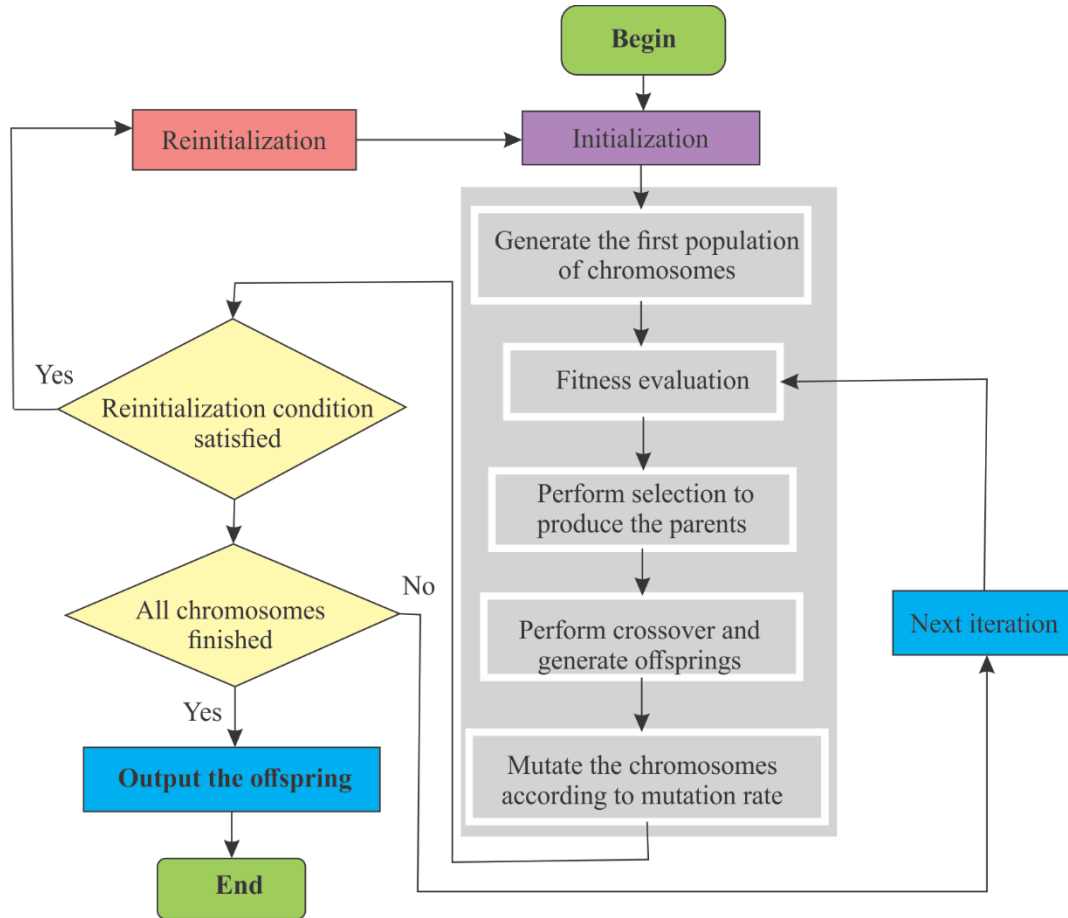


Fig. 2.12 Flowchart of the GA-based MPPT

### 2.6.2.2 Differential Evolution Algorithm

The “differential evolutionary algorithm” incorporates concepts from genetic algorithms, with its initial introduction by “Storn and Price”. Owing to its easy nature, “DE” stands out as a highly effective method in population-based optimization. This algorithm maintains the existing particles that exhibit the best fitness records within the population while substituting the others with new particles. “DE” is appropriate for addressing issues characterized by numerous local maximum peaks [102]. The algorithm comprises four stages: “initialization, mutation, crossover, and selection”. Recently, Renewable energy Systems (RES) used the “DE” method to address the global MPP tracking in the PSC issue.

The duty ratio of the DC-DC converter serves as the target vector in the DE-based MPP tracking method. Nonetheless, the approach relies on a fixed objective function that necessitates the prior determination of the (P–V) curve, rendering the method unsuitable for real-time MPPT

applications [102]. The tracking time was reduced by eliminating the unnecessary measurements from the output of the converter. Fig. 2.13 presents the flowchart of the differential evolution algorithm [103]. The initialization of the algorithm requires the assignment of initial positions to the target vector. The parameters are selected randomly for recombination, thereby enhancing the stochastic characteristics of the DE and ensuring covering the search space.

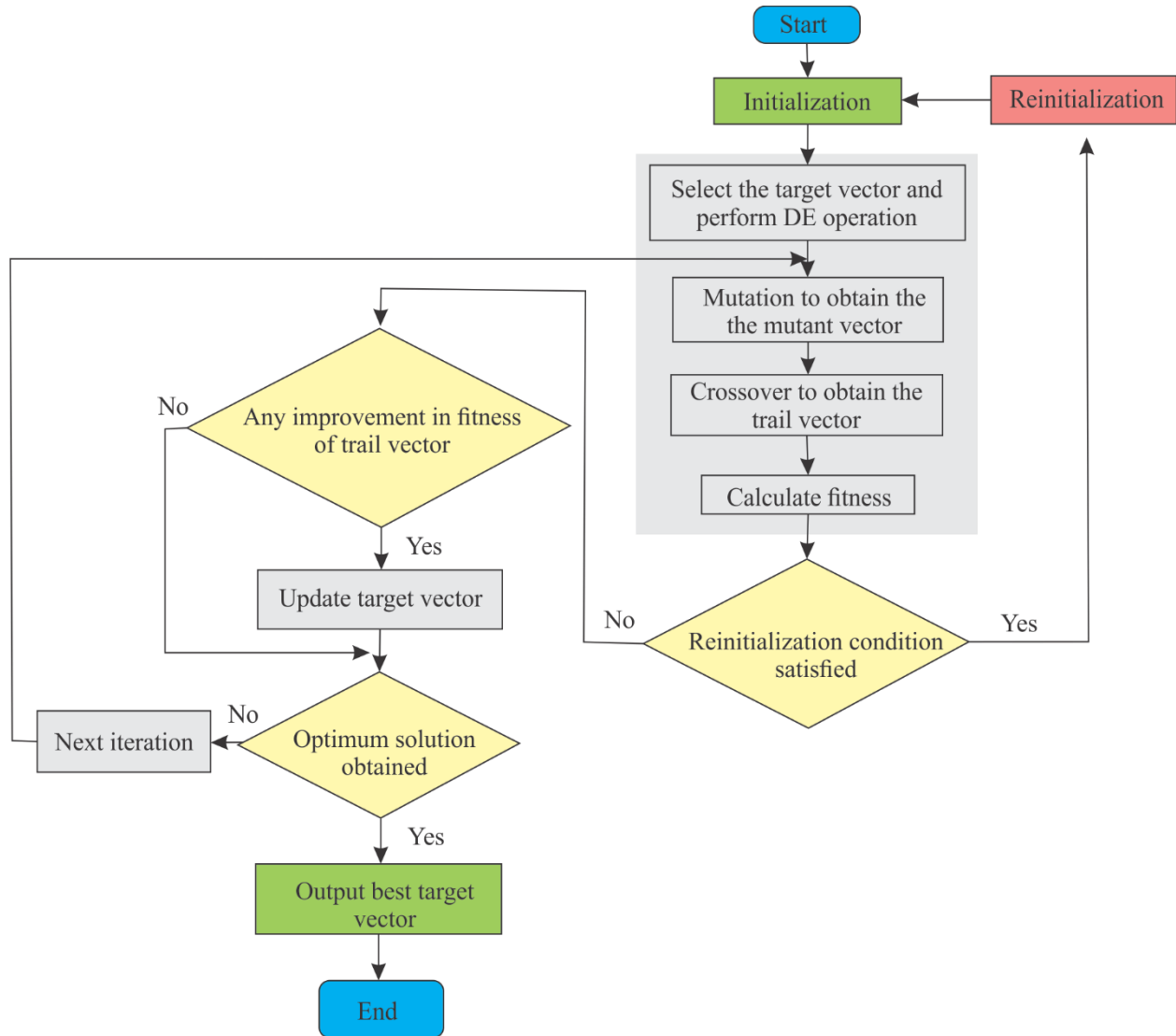


Fig. 2.13 Flowchart of the DE Algorithm



### 2.6.3 Nature inspired-based MPPT techniques

#### 2.6.3.1 Cuckoo Search

The “cuckoo search” (CS) method is derived from the reproductive strategy of certain cuckoo bird species known to deposit their eggs in the nests of other avian species. This parasitic reproductive strategy is the fundamental of the CS optimization technique. A vital component of this approach involves identifying the appropriate host nest. This process parallels food-seeking behaviour, characterized as a random process that can be represented through mathematical functions. A widely utilized model for representing an animal's food-seeking path is the Lévy flight model. The functioning process of the CS approach relies on Lévy flight and constitutes a population-based algorithm. Owing to Lévy flight, the CS approach exhibits superior randomization and accelerated convergence relative to conventional PSO and DE algorithms [104]. [Fig. 2.14](#) illustrates the flowchart for the search process used by the CS-based tracker.

The initial number of duty cycles is assigned randomly. Then, each duty cycle is transmitted to the DC-DC converter. The generated current and voltage are measured to calculate subsequently the resulting photovoltaic power. Which constitutes the fitness value. The duty cycle associated with the optimal fitness function is assigned as the current best nest (dbest). Subsequently, Lévy flight is used to find additional nests and evaluated with the current best fitness value. Afterward, the most unfavorable nest is eliminated and replaced by a new one, thereby simulating the behavior of the host bird in locating and destroying the cuckoo's eggs. The corresponding power for the new nest is measured, and the optimal nest is selected based on current performance metrics. Upon achieving the stopping criterion, the CS-based tracker delivers the optimal duty cycle corresponding to the global optimum power. The Lévy flight model is characterized by a random walk in which step sizes are governed by the Lévy distribution, as defined by the following equation [104].

$$Lévy(\lambda) \approx u = 1^{-\lambda} \quad \text{where;} \quad 1 < \lambda < 3 \quad (2.10)$$

In each iteration, the new position is determined via the Lévy process using Eq. (2.11).

$$x_i^{k+1} = x_i^k + \alpha \oplus Lévy(\lambda) \quad (2.11)$$

In this context,  $i$  represents a candidate solution or an egg,  $k$  denotes the iteration number, the symbol  $\oplus$  signifies entry wise multiplication, and  $\alpha$  refers to the step size that must be

appropriately adjusted in accordance with the constraints of the optimization issue. The parameter  $\alpha$  is typically defined using the first step  $\alpha_0$  and the difference between two samples ( $x_j^t$  and  $x_i^t$ ), as seen by the following equation:

$$\alpha = \alpha_0 + (x_j^k - x_i^k) \quad (2.12)$$

The performance of the CSA is influenced by several parameters, including the initial step size, the percentage of the worst nests  $P_a$ , the Lévy distribution factor, the population dimension, and the number of iterations. The merits of CS include ease of implementation, rapid tracking speed, and simple integration with other swarm-based algorithms. The shortcomings of CS include a tendency to fall into local optima at the boundary when parameters are set inappropriately, resulting in a low convergence rate.

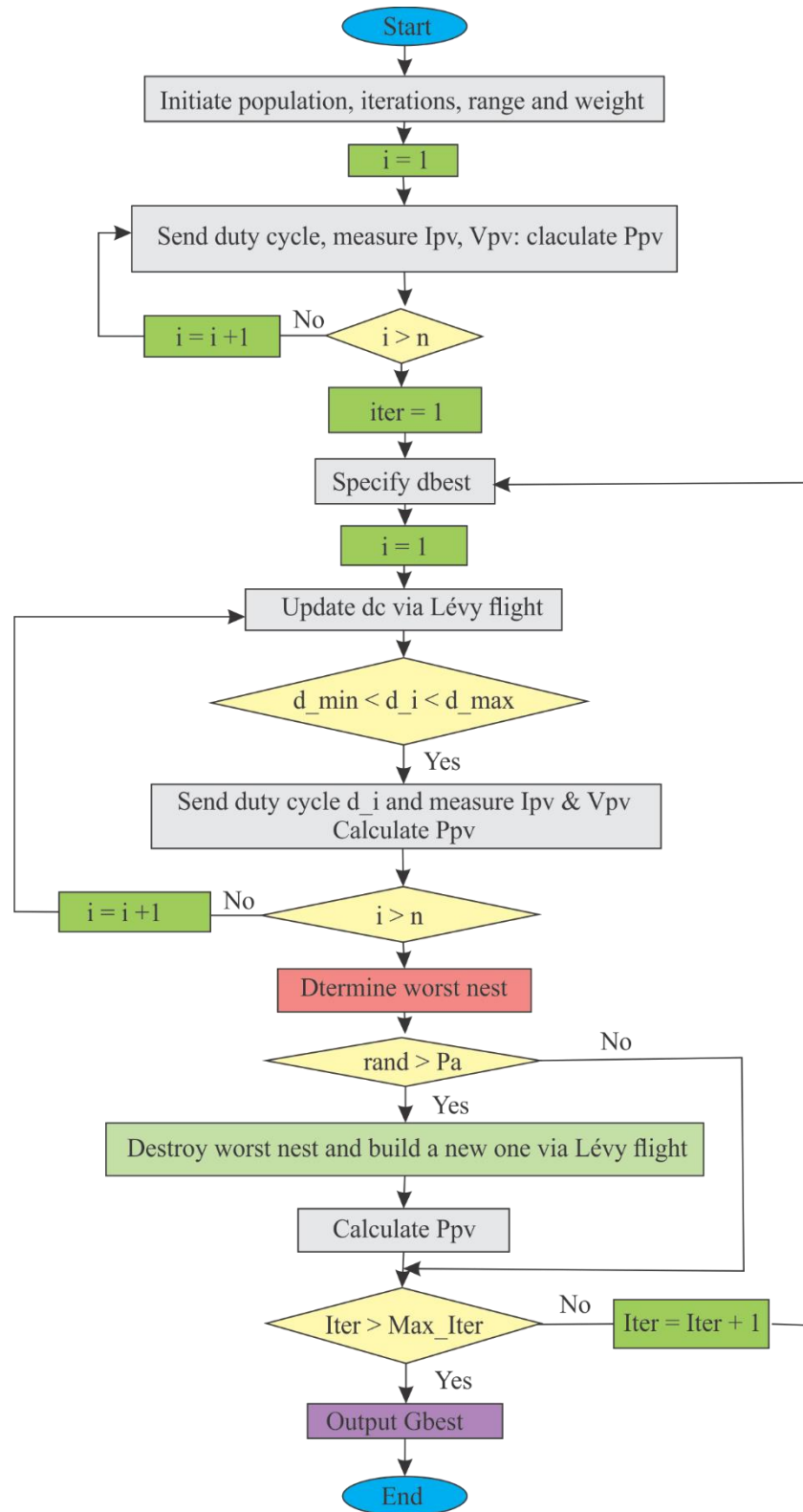


Fig. 2.14 Flowchart of the CS-based MPPT tracker

### 2.6.3.2 Grey Wolf Optimization technique

“Grey wolf optimization” (GWO) represents a population-based optimization approach that draws upon the hierarchical leadership and hunting behaviour of the grey wolf, as introduced in [105]. Grey wolves can be categorized into four distinct types when hunting for prey based on the fitness evaluation of each type. The first type exhibits the highest fitness level, while the fourth type demonstrates the lowest fitness level. The social structure exhibits a stringent hierarchical dominance, consisting of four distinct levels of leadership. Leaders, referred to as alpha ( $\alpha$ ), and subleaders, designated as beta ( $\beta$ ), form what is known as leadership pyramids, as illustrated in Fig. 2.15. In this structure, the dominance of wolves increases from the top to the bottom. Grey wolves exhibit three primary phases in their hunting behavior:

- (a) Seeking, pursuing, and approaching the prey.
- (b) Tracking and surrounding the prey.
- (c) Attacking the prey.

The circling behaviour exhibited by wolves is a crucial component of their hunting strategy and is integral to developing the “GWO” algorithm. The “GWO” method is utilized in MPPT, with the number of collaborating grey wolves corresponding to the converter's duty ratios, while the MPP is represented as the prey being pursued. The following equations [105] mathematically represent the circling comportment of wolves in the design of the GWO algorithm:

$$\vec{D} = |\vec{C} \cdot \vec{x}_{p(t)} - \vec{x}_{(t)}| \quad (2.13)$$

$$\vec{x}_{(t+1)} = \vec{x}_{p(t)} \vec{A} \cdot \vec{D} \quad (2.14)$$

In this context,  $t$  represents the iteration number, while  $x_p$  and  $x$  denote the position vectors of the prey and the grey wolf, respectively. The vectors  $A$  and  $C$  are computed according to Equations (2.15) and (2.16) [105]:

$$\vec{A} = 2 \cdot \vec{a} \cdot \vec{r}_1 - \vec{a} \quad (2.15)$$

$$\vec{C} = 2 \cdot \vec{r}_2 \quad (2.16)$$

Where the parameter  $a$  is linearly decreasing from 2 to 0 through iterations while  $r_1$  and  $r_2$  are random vectors in  $[0, 1]$ . The GWO optimization method is utilized in MPPT, with the number of contributing grey wolves corresponding to the converter's duty cycles, while the MPP is represented as the prey being chased. For each duty cycle, the controller measures  $V_{pv}$  and  $I_{pv}$  via sensors then calculates the output power for the number of grey wolves. [Fig. 2.16](#) illustrates the flowchart of the GWO-based MPPT algorithm [[106](#)].

The parameters influencing performance include the exploration and exploitation parameter, population dimension, and maximum iteration count. The merits of GWO include ease of implementation, minimal parameter configuration, and high tracking accuracy. The shortcomings of GWO include a long convergence time.

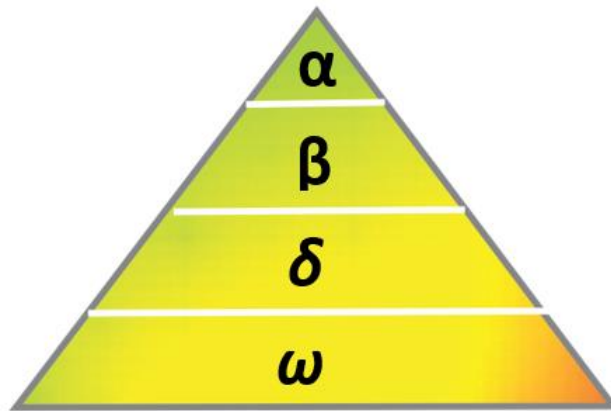


**Fig. 2.15** Leadership pyramids

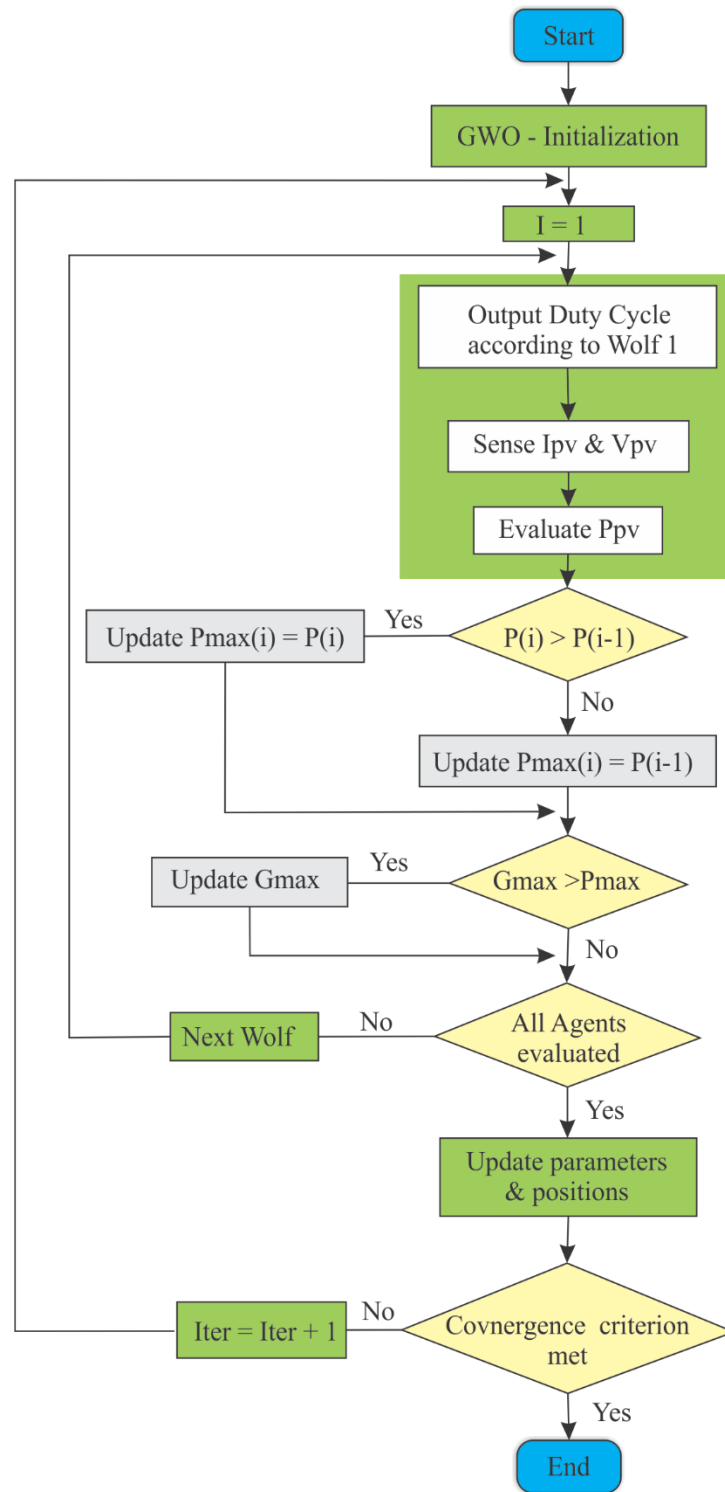


**Fig. 2.16** Flowchart of the GWO Algorithm

### 2.6.3.3 Flower Pollination Algorithm

The “Flower Pollination Algorithm” (FPA) is nature-inspired method derived from the pollination process of flowers. Pollination may occur by self-pollination or cross-pollination. Self-pollination happens when a flower is pollinated internally, while cross-pollination happens when pollen is transferred externally between flowers. It may be propagated by wind, termed abiotic pollination, or by insects, referred to as biotic pollination. The different phases for designing FPA are as follows [107]:

**First step:** Global pollination manifested in biotic and cross-pollination, with pollen-carrying pollinators using Lévy flights.

**Second step:** Local pollination is characterized by biotic and self-pollination mechanisms.

**Third step:** Floral constancy, which is comparable to a reproduction probability of the same species due their similarity.

**Fourth step:** A switch probability  $P \in [0, 1]$ , to regulate the local and global pollination processes.

As mentioned earlier, the procedures must be transformed into appropriate mathematical formulae. During the global pollination phase, pollinators transport flower pollen gametes, enabling the pollen to disperse across considerable distances. Consequently, global pollination (First step) and flower constancy (Third step) may be quantitatively represented as [107]:

$$x_i^{k+1} = x_i^k + \gamma L(\lambda)(g_* - x_i^k) \quad (2.17)$$

$x_i^k$  represents the solution vector at iteration  $k$ , and  $g$  represents the optimal solution (duty cycle).  $\gamma$  represents a scaling factor employed for adjusting the step size.  $L(\lambda)$  stands for the Lévy flights-based step size that reflects the pollination strength. Insects may travel considerable distances with variable step lengths, as described by the Lévy distribution [107]:

$$L \approx \frac{\lambda \Gamma(\lambda) \sin\left(\frac{\pi\lambda}{2}\right)}{\Pi} \frac{1}{S^{1+\lambda}} \quad (S \geq S_0 > 0) \quad (2.18)$$

Where  $\Gamma(\lambda)$  stands for the gamma function.

#### **2.6.3.4 Firefly Algorithm**

The FA is an optimization technique based on population dynamics and exhibits similarities to Particle Swarm Optimization. The FA draws inspiration from luminescent insects and is mathematically formulated in [108]. FA requires fewer parameters for tuning, and the particles in FA approach are more closely around the optimum solution, exhibiting reduced fluctuations.

The flashing light is an essential element of the population-based behaviour of fireflies, used to attract mates and possible prey, as well as serving as a mechanism for protective warning. Consequently, brightness is crucial and used to ascertain the new location of particles inside the search space. For each duty cycle representing a firefly,  $V_{pv}$  and  $I_{pv}$  are measured; subsequently, the output power is calculated. The mechanism of the FA algorithm for Maximum Power Point Tracking is detailed below [109]:

In the first phase, tuning parameters and maximum iteration number are defined. Each duty cycle is considered a position for a given firefly in this approach. The luminosity of each firefly is regarded as the power  $P_{pv}$  produced by the photovoltaic system, according to the location of the firefly. In the second stage, ensure that all fireflies' positions are within the permissible solution space defined  $[d_{min}, d_{max}]$ , referring to the minimum and maximum duty ratios of the DC-DC converter.

In the third stage, the DC-DC converter is run sequentially according to the location of each firefly. For each duty ratio, the associated PV output power  $P_{pv}$  is regarded as the luminosity or light intensity of the relevant firefly. This procedure is performed for all fireflies within the search space.

In the fourth phase, the firefly with the highest luminosity keeps its position while the other fireflies adjust theirs. In the fifth step, conclude the program if the termination requirement is satisfied; otherwise, revert to the third step. The optimization process terminates when the displacement of all fireflies in successive iterations attains a predetermined minimal value.

Upon termination of the program, the DC-DC converter functions at the optimal duty cycle aligned with GMPP. In the last phase (FA: initialization), if the solar irradiation varies, the digital controller detects this change by measuring the alteration in power output [109]. Upon program termination, the DC-DC converter functions at the optimal duty cycle, delivering the global



optimum power. In the last phase, the controller senses any variation in the irradiation to restart the process [109].

The factors influencing the FA performance include initial attractiveness, absorption parameter, random movement parameter, population dimension, and maximum iterations. The advantages of FA include enhanced performance, rapid tracking speed, and insensitivity to starting conditions. The shortcomings of FA include a propensity to converge on local optima when parameters are improperly configured.

### **2.6.3.5 Bat Algorithm**

The “Bat Algorithm” (BA) is a population-based optimization technique implemented by emulating the echolocation features of micro-bats in their food acquisition [110]. Microbats mostly consume insects, which they locate by echolocation. The orientation and strength of the returned signal allow them to identify possible prey in position and direction. Initially, the bat explores the search area, releasing a series of ultrasonic pulses with a certain amplitude and frequency. It gets its feedback signals and analyzes those of the other bats in the swarm via echolocation. If the returned signals exhibit low intensity and high frequency, the prey has probably been identified, prompting the bat to pursue it. As the bat approaches its target, it incrementally increases the frequency of the ultrasonic pulses while reducing their strength.

The bat algorithm sustains a swarm of  $N$  micro-bats, where each particle navigates randomly with a velocity  $v_i$  at position  $x_i$ , exhibiting variable loudness  $A_i$  and pulse emission rate  $r_i \in [0, 1]$ , contingent upon the closeness to their prey. In the optimization process, each bat is randomly given a frequency uniformly selected from the interval  $[f_{min}, f_{max}]$ . The initial velocity  $v_i$  and position  $x_i$  of each bat at time step  $t$  are given as follows:

$$f_i = f_{min} + (f_{max} - f_{min})\beta \quad (2.19)$$

$$v_i^{t+1} = v_i^t + (x_i^t - x_0)f_i \quad (2.20)$$

$$x_i^{t+1} = x_i^t + v_i^{t+1} \quad (2.21)$$

Where  $\beta \in [0, 1]$  is a vector arbitrarily selected from a uniform distribution.  $x^t$  represents the optimal global position attained after evaluating all solutions of the  $N$  bats at each iteration  $t$ . If a random number exceeds the pulse emission  $r_i$ , the exploitation stage is chosen, and the position

is substituted with the solution produced by the local search. Consequently, a new solution is generated locally using a random walk around the present optimal solution:

$$x_{new} = x_0 + \varepsilon A^t \quad (2.22)$$

Where  $\varepsilon$  is a random number drawn from a uniform distribution within the interval  $[-1, 1]$  or a Gaussian distribution, whereas  $A \leq A_i^t$  denotes the mean loudness of all bats at this time. If a random number is less than loudness  $A_i^t$  and the new solution enhances the fitness function, it indicates that the bat is progressing toward the prey. Subsequently, the new solution is accepted, and its intensity and emission rates are updated via equations (2.23) to (2.25) to manage exploration and exploitation processes. In Bat's optimization, the loudness is recommended to diminish from a positive value  $A_i^0$  to  $A_{min} = 0$ , while the pulse rate rises from 0 to  $R_i$ .

$$A_i^{t+1} = \alpha A_i^t \quad (2.23)$$

$$r_i^{t+1} = R_i (1 - e^{-\gamma t}) \quad (2.24)$$

$$|x_i^k - x_j^k| \leq \Delta x \quad i, j = 1, 2, 3 \dots (i \neq j) \quad (2.25)$$

In this context,  $\alpha$  represents a constant within the interval  $[0,1]$ , while  $\gamma$  denotes a positive constant. The bat algorithm is used for monitoring the Global Maximum Power Point via direct duty cycle control of the PWM signal. [Fig. 2.17](#) depicts the flowchart of the bat algorithm-based Maximum Power Point Tracking.

The main factors influencing the performance of the BA include “the movement of virtual bats, velocity, weights, loudness, and pulse emission”. The merits of BA include increased speed, enhanced efficiency, resilience, and reliability compared to traditional and alternative soft computing techniques. The shortcomings of the Bat Algorithm include its rapid initial convergence followed by a deceleration in the convergence rate, the absence of mathematical analysis correlating parameters with convergence rates, and potential limitations in accuracy if the number of function evaluations is insufficient.

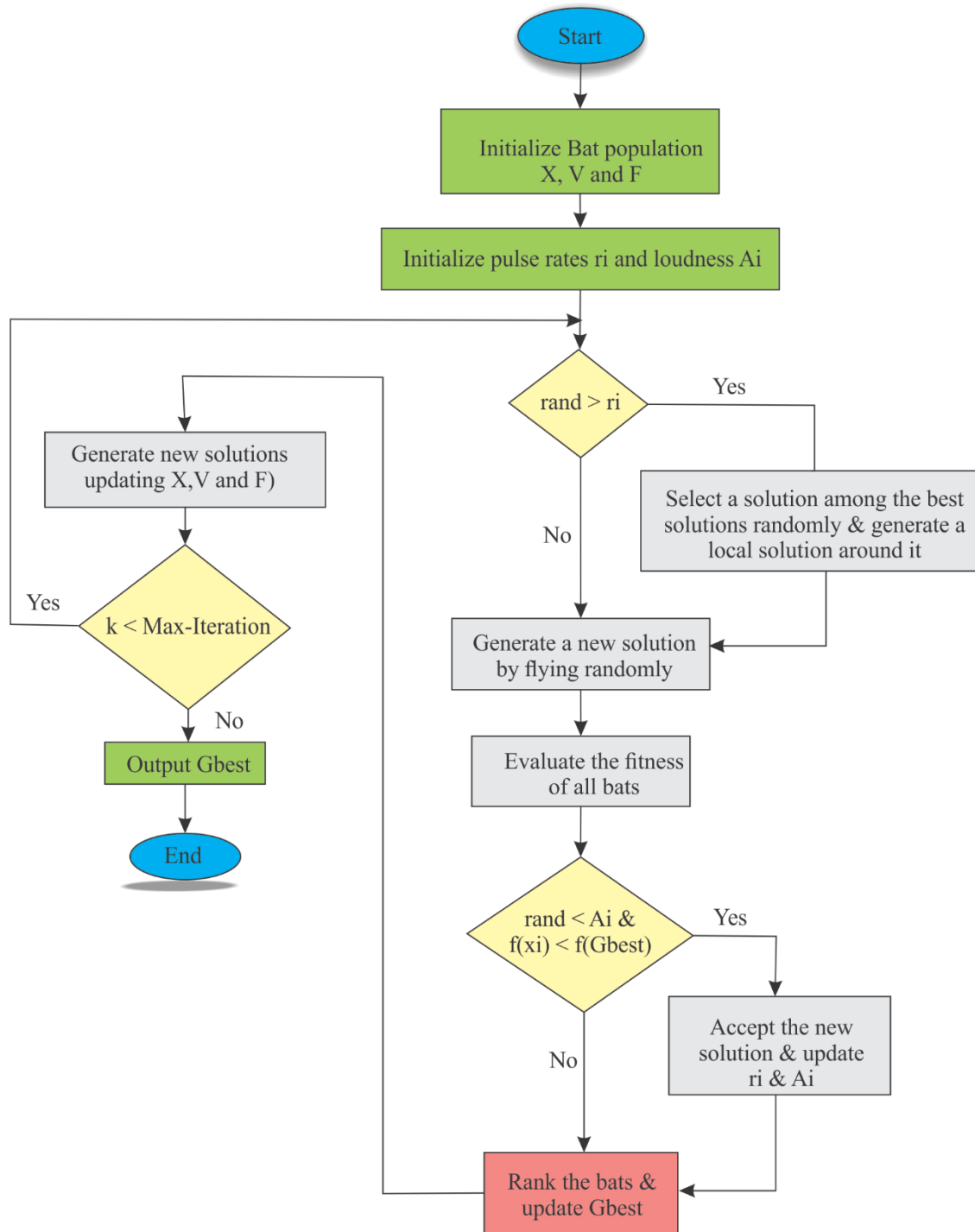


Fig. 2.17 Flowchart of the Bat Algorithm

## **2.7 Hybrid-based MPPT techniques**

Hybrid MPPT approaches involve a combination of conventional and soft computing methods to effectively manage partial shading conditions and accurately track the global peak (GP). This can include various configurations such as “soft computing/conventional”, or “soft computing/soft computing” approaches. Some soft computing maximum power point tracking (MPPT) methods, particularly those utilizing artificial intelligence techniques like “fuzzy logic control” (FLC) [111] and “artificial neural networks” (ANN) [112], exhibit limitations in managing partial shading conditions, which may result in their inability to track the global peak effectively. Consequently, they are optimized and integrated with additional techniques to enhance tracking efficiency and convergence time. The traditional MPPT techniques exhibit limitations in monitoring MPP in PV systems subjected to PS, often remaining fixed at the initial peak, irrespective of whether the context is LP or GP. Consequently, soft computing may be employed to enhance traditional methods and AI approaches, yielding robust and resilient novel algorithms that can efficiently manage the PS effect.

### **2.7.1 Hybrid soft computing-soft computing algorithm**

Various MPPT techniques based on hybridizing two metaheuristic algorithms-based soft computing approaches are found in the literature. Among these techniques, the GWO-PSO algorithm addressed in [113].

The Hybrid “GWO–PSO” is a swarm intelligence-based optimization algorithm developed in 2017 by “Narinder Singh & al”. The fundamental hybridization approach of this algorithm involves integrating the exploration capabilities of the GWO algorithm with the exploitation abilities of the “PSO” algorithm, thereby enhancing the strengths of both variants while reducing their shortcomings. The hybrid “GWO–PSO” algorithm is applied to monitor the MPPT issue. A DC-DC power converter is used to link the output of the PV array with the load. The location of each search agent in the hybrid "GWO–PSO" algorithm is specified as a decision variable, representing the duty ratio of the power converter. The GWO methodology classifies potential solutions into four categories to establish a leadership pyramid: “alpha” denotes the optimal solution, “beta” refers to the second best solution, “delta” indicates the third best solution, and “omega” encompasses the remaining alternatives, as specified in the equations (2.26) to (2.29).

$$\begin{cases} D_\alpha = |C_1 dc_\alpha - w \cdot dc| \\ D_\beta = |C_2 dc_\beta - w \cdot dc| \\ D_\delta = |C_3 dc_\delta - w \cdot dc| \end{cases} \quad (2.26)$$

$$\begin{cases} dc_1 = dc_\alpha - A_1 D_\alpha \\ dc_2 = dc_\beta - A_2 D_\beta \\ dc_3 = dc_\delta - A_3 D_\delta \end{cases} \quad (2.27)$$

$$v_i^{k+1} = w(v_i^k + c_1 r_1 (dc_1 - dc_i^k) + c_2 r_2 (dc_2 - dc_i^k) + c_3 r_3 (dc_3 - dc_i^k)) \quad (2.28)$$

$$dc_i^{k+1} = dc_i^k + v_i^{k+1} \quad (2.29)$$

Where  $dc_i$  represents the duty cycle for each agent,  $v_i$  represents velocity calculated according to the PSO principle whereas,  $A$  and  $C$  are coefficient factors, computed as follows:

$$\vec{A} = 2 \cdot \vec{a} \cdot \vec{r}_1 - \vec{a} \quad (2.30)$$

$$\vec{C} = 2 \cdot \vec{r}_2 \quad (2.31)$$

In this approach, the value of  $a$  is linearly decreasing from 2 to 0 throughout the iterations, with  $r_1$  and  $r_2$  representing random vectors within the interval  $[0, 1]$ .

The hunting procedure is controlled by alpha ( $\alpha$ ), beta ( $\beta$ ), and delta ( $\delta$ ) since they possess superior information about the probable location of the ideal solution. The other search agents, including the omegas, must adjust their placements according to the position of the optimal search agent. Each agent, referred to as the duty cycle, corresponds to fitness function representing the output power of the photovoltaic array. In this approach, the controller measures the PV array's voltage and current for each searching agent and subsequently computes the corresponding generated power. To obtain accurate samples, the time interval between consecutive assessments of the duty ratio ( $T_s$ ) must exceed the settling time of the DC-DC power converter. Additionally, to determine whether a change in climatic circumstances occurs, the following inequality is utilized:

$$\frac{|P_{PV\ new} - P_{PV\ last}|}{P_{PV\ last}} \geq \Delta P \quad (2.32)$$

The hunting procedure of the GWO method is shown in [Fig. 2.18](#), whereas the process of the hybrid GWO-PSO-based MPPT monitor is illustrated in [Fig. 2.19](#).

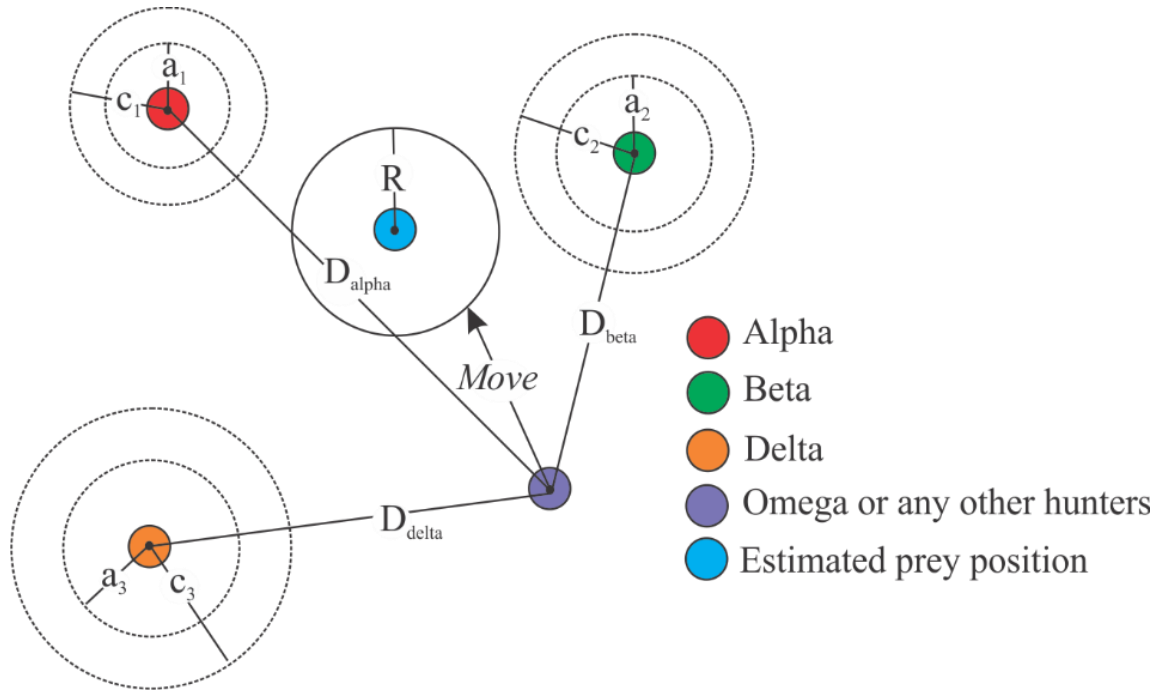


**Fig. 2.18** Hunting procedure of the GWO technique

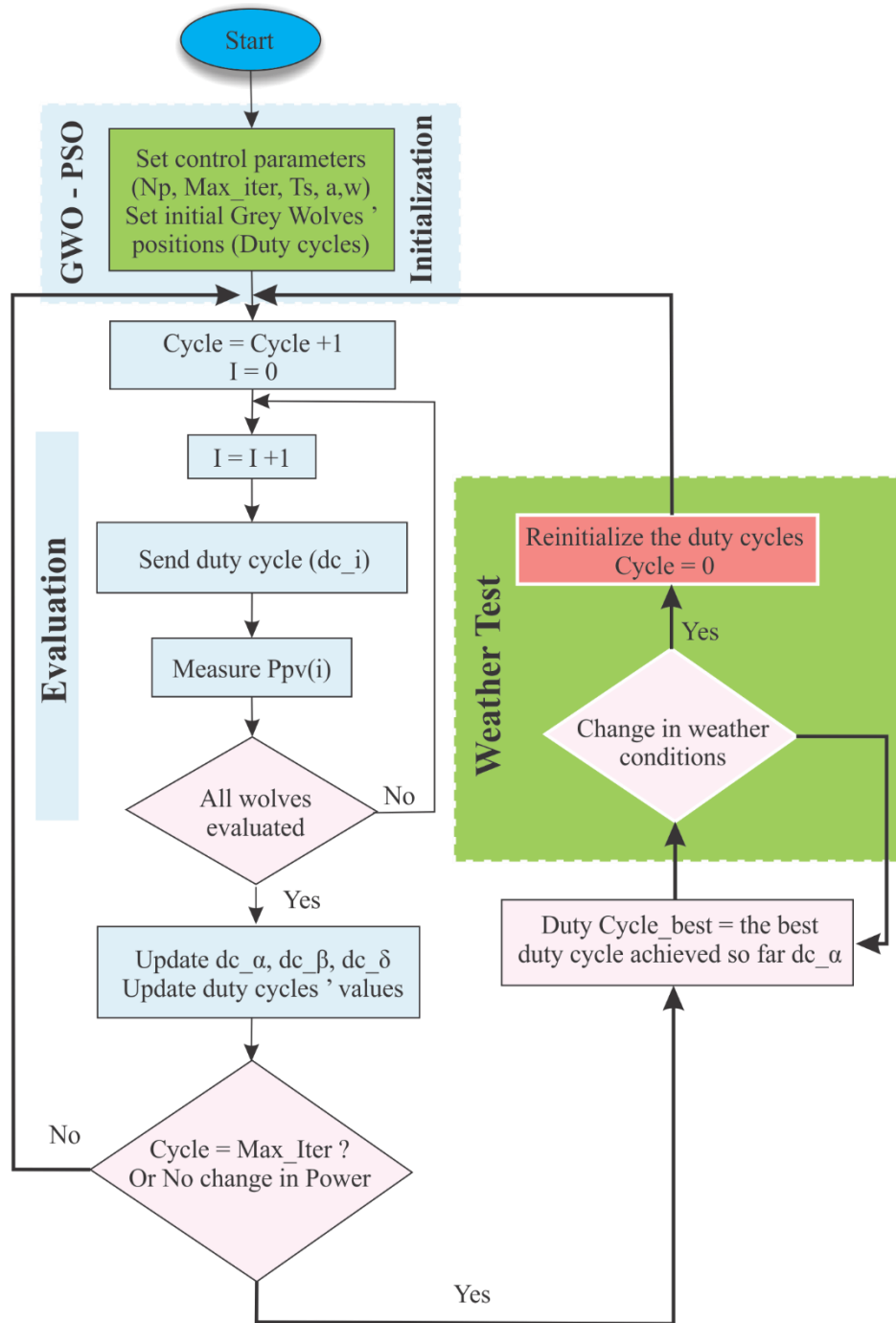


Fig. 2.19 Flowchart of the GWO-PSO Algorithm

### 2.7.2 Hybrid soft computing-conventional

Another type of hybridization is integrating a metaheuristic approach with a conventional method, as discussed in [114].

This approach combines Particle Swarm Optimization for MPPT during the early tracking phases and then applies the standard Perturb and Observe method in the latter stages. The procedure of this technique is as follows:

#### 2.7.2.1 Steps of the Algorithm

This technique employs particle swarm optimization and then transitions to the PO method. Particle Swarm Optimization is a stochastic, evolutionary approach derived from the study of social behaviours in animals, including bird flocking and swarm concepts. It sustains a population of agents referred to as particles. Each particle, representing a possible solution, is affected a randomized position in the possible search space. Each particle communicates the knowledge acquired from its own and its neighbor's flight experiences and adjusts its location accordingly. Thus, each particle advances toward the global optimal point. The following outlines the sequential phases of the hybrid algorithm:

##### 2.7.2.1.1 PSO method [115]

1. Affect the first duty ratios to the solution particles at fixed positions that uniformly span the search space  $[d_{min}, d_{max}]$ , where  $d_{min}$  and  $d_{max}$  denote the power converter's minimum and maximum duty cycle values.
2. Transmit the duty cycles sequentially and compute the corresponding fitness values representing the generated power of the PV array.
3. The highest fitness value identified by particle  $i$  is referred to as its personal best. At each iteration, compare the fitness value of particle  $i$  with particle best ( $P_{besti}$ ). Replace the particle's best position with the current position if the latter has a higher fitness value.
4. The particle with the highest fitness value in the swarm is referred to as the global best ( $G_{best}$ ). There exists a single global best solution to which all particles in the swarm tend to converge. Evaluate the fitness value of particle  $i$  in relation to  $G_{best}$ . If the fitness value of particle  $i$  exceeds  $G_{best}$ , update  $G_{best}$  to the position of particle  $i$ .



5. Calculate the velocity and position of the  $i^{th}$  particle in the  $k^{th}$  iteration employing equations (2.33) and (2.34).

$$v_i^{k+1} = wv_i^k + r_1c_1(pbest_i - d_i^k) + r_2c_2(gbest_i - d_i^k) \quad (2.33)$$

Equation (2.33) indicates that the particle's velocity is influenced by the positions of  $Pbest$  and  $Gbest$ . The updated velocity is adjusted by the factor  $w$  and augmented in the direction of  $Pbest$  and  $Gbest$ . In this methodology,  $c_1$  is a constant known as the cognitive rate, which determines the extent to which the particle is influenced by  $Pbest$ ,  $c_2$  is a constant known as the social rate, which determines the extent to which the particle is impacted by the remainder of the swarm.  $r_1$  and  $r_2$  are variables representing random numbers within the interval [0,1]. The new particle's position is determined using the updated velocity specified in equation (2.34).

$$d_i^{k+1} = d_i^k + v_i^{k+1} \quad (2.34)$$

6. Conclude the program when the distances between  $gbest$  and all other  $Pbests$  fall below 1%; thereafter, transfer the optimal particle,  $d_{optimum}$ , to the PO technique; otherwise, revert to step 2.

#### **2.7.2.1.2 PO method**

1. Initiate the PO stage using  $d_{optimum}$  as the initial value for the duty ratio.
2. Introduce an alteration in the PV array functioning voltage by adjusting the converter duty cycle. If the PV array's power has augmented, adjust the duty cycle accordingly; otherwise, proceed reversely.
3. Continue executing step 2 until GMPP is achieved.
4. Evaluate the PV output power, and if the variation in output power between consecutive samples exceeds 1% of the rated PV output power, restart the search process.

The flowchart of the hybrid PSO-PO algorithm is illustrated in [Fig. 2.20](#).

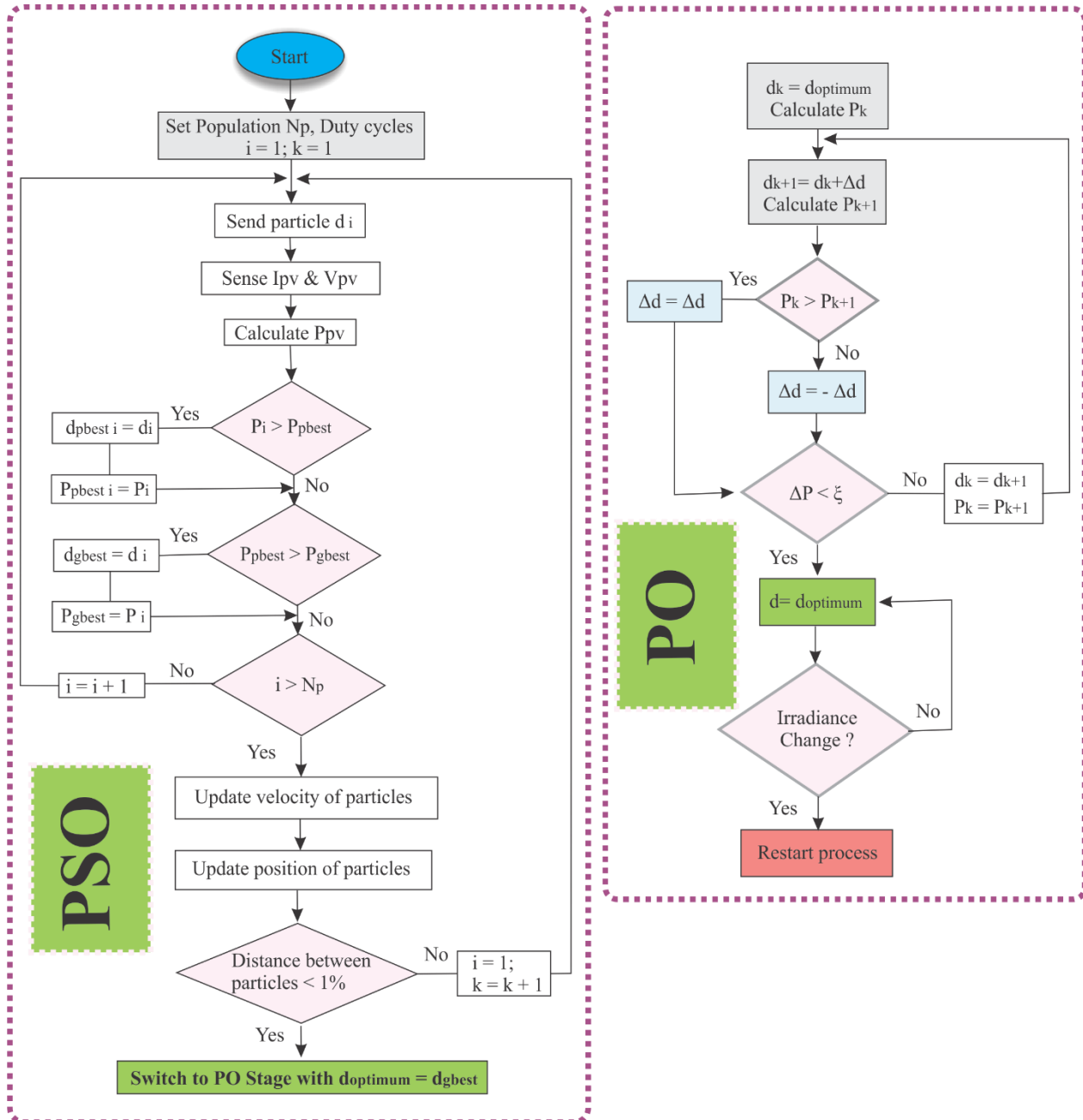


Fig. 2.20 Hybrid PSO-PO Algorithm

## **2.8 Overview of recent hybrid MPPT techniques in PV systems subjected to PSCs**

To enhance the efficiency of typical SI methods and reduce the risk of faulty convergence, various modified versions or hybrid MPPT algorithms have been suggested to address the practical requirements of PV systems, as suggested in [116,117]. The most prevalent features of these algorithms are their high efficiency, robustness, and ability to tackle tracking challenges in uniform and PSCs, as reported in [118]. Recent MPPT controllers use SI to overcome the limitations of traditional methods, as indicated in [119]. In [120], the authors proposed a modified PSO with hybrid adaptive local search (MPSO-HALS) to address the PSO algorithm's shortcomings. Across different scenarios of PSCs, the suggested system exhibits a tracking efficacy exceeding 99% in diverse and intricate PSC circumstances. In [121], an improved PSO-based MPPT method is introduced. This approach overcomes the constraints of conventional PSO algorithms in non-uniform weather conditions. Another variation of the PSO technique is discussed in [122], where a hybrid of Levy flight and particle swarm optimization (LPSO) is put forward. This technique contributed to decreased steady-state oscillation and efficient global power monitoring under severe PSC. In [123], a novel overall distribution (OD) MPPT algorithm, which can rapidly search the area near the global MPP. The authors explored the tiny region around the GMPP to achieve a quick response. Nevertheless, the proposed model ignores the PV array's precise details, which could compromise the overall power monitoring efficiency under challenging environmental circumstances. The study discussed in [124] provides a machine learning-based controller for PV systems under PSC. Bayesian fusion prevents the controller from being trapped at the local minima of the shaded P-V characteristic. The suggested controller demonstrated faster response time and higher efficiency than current intelligent approaches. Nevertheless, some oscillations are observed at steady-state. Moreover, complex PS scenarios are not tackled, which will limit its efficiency when applied to large PV systems and severe weather conditions. Fuzzy adaptive PSO for MPPT was addressed in [125]; however, modifying the PSO parameters required a computation-intensive controller task. Furthermore, the suggested approach must be verified under complex weather circumstances and fast changes in irradiance to verify its robustness and suitability to confirm the findings. The hybridization of two SI algorithms, PSO and GWO, is reported in [126]. While the technique effectively tracks the GMPP, significant downsides include processing complexity, restrictions in extreme cases, and implementation issues in practical PV systems. In [127], the Particle-Swarm Fireworks Algorithm (PS-FW) algorithm is presented as a hybrid technique for

GMPPT. Exploration and exploitation are balanced through the PSO's velocity and the FWA's mutation and explosion spark operators. The findings of the proposed hybrid technique outperform its singular algorithm versions. Despite the system's high efficacy, the suggested approach demonstrates high initial oscillations; moreover, the algorithm was not verified under rapid changes in weather conditions and complex PSCs. Additionally, tests are addressed under small PV systems, which will induce some challenges when large PV systems are considered. The hybrid Differential Evolution and PSO algorithm (DEPSO) is introduced in [128]; the proposed technique features rapid tracking under PSCs. The work introduced in [129] presents a new adaptive PSO (NA-PSO) approach to improve power tracking for PV systems in dynamic shading scenarios. While the NA-PSO strategy significantly enhances system performance, it may still require further testing and validation under various operational circumstances to ensure its robustness and effectiveness in real-world applications. In [130], a new GMPPT technique is proposed with the integration of the Salp Swarm Optimization (SSO), Differential Evolution (DE), and P&O algorithms. A modified SSA-based MPPT is presented in [131], incorporating an adaptive control parameter named ASSA. The hybrid technique alternates between the ASSA and P&O algorithms to enhance power tracking. ASSA is only used to identify the optimum power location, while inside this region, the tracking procedure is carried out using a variable step size P&O algorithm. In [132], the hybrid GWO-P&O MPPT algorithm is proposed. GWO is initially used offline to move the operating point closer to the MPP, and then the P&O algorithm takes over to locate the GMPP. The suggested hybrid method outperforms GWO when employed alone. The combination of GWO and Modified Fast Terminal Sliding Mode Controller (MFTSMC) is presented in [133]. The experimental outcomes show that the proposed system overcomes conventional designs. Nevertheless, the GWO-MFTSMC algorithm must be fine-tuned in terms of operational and control parameters to obtain optimum performance. In [134], the authors introduced an improved version of the GWO. This approach replicates the hunting strategies used by grey wolves. The primary benefits of this technique are enhanced tracking efficiency and the removal of both transient and steady-state oscillations, as reported in [135]. In [136], the GWO is combined with an ANFIS to generate a hybrid MPPT controller. However, GA-based MPPT controllers demand significant computational complexity and proper parameter tuning, resulting in premature convergence under some complex PSC scenarios. In [137], a novel MPPT design based on the Seagull optimization algorithm (SOA) is introduced. Compared to the PSO technique, the SOA

methodology results in quicker convergence and minor oscillations around the Global Peak (GP). However, in this study, only the 4S configuration is used to evaluate the suggested MPPT algorithm, which raises issues when large PV systems are addressed. In [138], a combination of cuckoo search and a PID controller is suggested to monitor the power tracking of a PV system under PSCs. The concept behind this hybridization is to use the advantages of these two strategies while eliminating their disadvantages when employed alone. Nevertheless, the efficacy of the suggested control technique is examined only for three shading scenarios. Moreover, this study did not investigate complex shading profiles and quick changes in irradiance to verify the reliability and resilience of the proposed system. The hybrid CS and Artificial Bee Colony (ABC) algorithms for MPPT are introduced in [139]. This method integrates the levy flight mechanism's local and global random search in the cuckoo algorithm. It also introduces adaptive weight factors and gravitational mechanisms between neighboring particles to track the MPP effectively. Nevertheless, the generalizability of the results may be restricted by the system validation using small PV systems. Additionally, this work did not investigate the robustness of the proposed hybrid algorithm in extreme environmental conditions, which are critical factors to consider when evaluating the reliability and stability of MPPT algorithms in solar PV applications. In [140], the CS is presented. This strategy is based on the reproductive behaviour of cuckoo birds, which involves laying their eggs in the nests of other bird species. The levy flight mechanism is used in the search process to find the optimal solution. This method exhibits faster convergence compared to PSO and DE and is less reliant on initial conditions. A comparative performance analysis of PV modules using CS and PSO techniques is reported in [141]. In [142], a hybrid CS and Golden Section Search Algorithm (CS-GSS) is introduced. The search process is initiated with CS to avoid being stuck in a local maximum. Subsequently, the tracking procedure transitions to the GSS algorithm to locate the GMPP precisely. According to the authors, the proposed system offers a tracking time reduction of over 25% compared to other techniques. A novel MPPT technique based on solar irradiance estimation is presented in [143]. The complex multiple MPP issue is converted to a single MPP problem, where an intelligent neural network-based predictor integrating a cost-effective solar irradiance estimator is put forward. To achieve the GMPP task, the predictor uses the PV current and voltage to determine the precise optimum power region of the PV system. However, the system requires a considerable amount of data for training and a good knowledge of the PV modules' characteristics. In [144], a robust integral back-stepping (RIB)-based MPPT

control is suggested. This method primarily relies on two loops. In the first stage, an ANFIS network creates a real-time reference peak power voltage. Subsequently, the duty ratio of the power converter is continually adjusted to force the PV system to function at this set point. Nevertheless, the suggested approach should be verified under complex scenarios of partial shadings to consider the reliability and relevance of the findings. A novel MPPT framework based on the modified shuffled frog leaping algorithm (MSFLA) is proposed in [145]. This system performs well under changing weather conditions and outperforms conventional approaches. Nevertheless, the proposed approach should be verified under CPSCs and rapid changes in weather circumstances. Moreover, tests are not conducted under large and medium PV system situations, which may affect the reliability of the proposed system. In [146], the authors proposed a novel hybrid algorithm that combines two SI techniques: the marine predator algorithm (MPA) and the mayfly optimization algorithm (MFA). The developed bio-inspired algorithm outperforms comparable algorithms in terms of efficiency and oscillation reduction. Another bio-inspired technique for MPPT is addressed in [147], which utilizes Salp Swarm Optimization (SSO). This method utilizes the inherent ability of salps to optimize the generated power efficiently. Under specific severe MPPT scenarios, SSO has demonstrated considerable redundancy and efficiency. Nevertheless, complex scenarios of partial shadings need to be addressed in this research, which may restrict the generalizability of the findings. In [148], the authors presented the hybrid SSO and P&O (SSO-PO) for MPPT, where the SSO is initially used to locate the MPP, and subsequently, PO takes over for faster convergence. The Grasshopper Optimization Algorithm (GOA) is presented in [149]. The MPPT approach based on GOA emulates the foraging behaviour of grasshoppers. This algorithm is effective in power extraction and fluctuations reduction for tracking MPP under PSCs. However, it demonstrates a long convergence time. A modified deterministic Jaya (DM-Jaya)-based MPPT algorithm is developed in [150] based on the modified Jaya generic algorithm. The proposed approach was only verified under three shading profiles, which may lead to difficulties and premature convergence under severe environmental conditions. Extensive tests are required to validate the robustness of this algorithm. The Bat search algorithm (BA) is suggested in [151]. The bat-based MPPT optimization approach is based on wild bats' echolocation activity while searching for prey [152]. BA increases the possibility of escaping the LMPP and shortens the tracking time. According to [153], hybrid approaches, such as Bat-P&O, Bat-Beta, and Bat-INC, improve system efficiency even during transient periods. One optimization method that takes inspiration from ants'

foraging behaviour is the Ant Colony Optimization (ACO) algorithm reported in [154]. In [155], an improved P&O algorithm for MPPT through a colony of foraging ants is introduced. An experimental implementation of the ACO-based MPPT optimizer is conducted in [156]. The ACO strategy relies on considering the shortest determined way to a goal, depicted as a path from colony to food supply. The concept of an ABC is presented in [157]. The ABC algorithm's main features are its independence from the system's starting conditions and its convergence to the GMPP with fewer tuning parameters, as mentioned in [158]. Nevertheless, this intricate approach exhibits a slower tracking speed than comparable MPPT systems. Moreover, the algorithm may settle at a LMPP rather than a GMPP under severe weather conditions. The gravitational search algorithm combined with the P&O method (GSA-PO) for MPPT is addressed in [159]. The search for GMPP is initiated with the GSA, and then the PO algorithm takes over the tracking process. Nevertheless, it demonstrates a long convergence time. A Fusion Firefly Algorithm with Simplified Propagation is presented in [160]. The proposed hybrid FFA algorithm offers high accuracy and efficiency and overcomes the conventional FA algorithms. As a conclusion of this section, a comprehensive review of the most essential and recent MPPT techniques was presented and critically analyzed. Various factors and parameters should be considered while selecting a specific technique, such as application, efficiency, cost of implementation, convergence speed, resilience in handling PSCs, as well as stability of the system during sudden variations in weather conditions.



## **2.9 Conclusion**

A thorough examination of significant shading mitigation approaches documented in the literature is explicitly presented, highlighting the effectiveness of metaheuristic-based MPPT techniques in addressing partial shading issues. This chapter concisely describes contemporary MPPT algorithms, specifically addressing MPPT optimization strategies primarily aimed at partial shadowing circumstances in photovoltaic systems. This evaluation covers other contemporary metaheuristic as well as hybrid approaches to enhance the performance of PVGS affected by PS issues. The advantages and disadvantages of several optimization strategies are examined to choose an appropriate MPPT tracker under partial shadowing conditions. Given the significance of MPPT in partial shading conditions, it can be concluded that considerable research potential exists to identify an appropriate MPPT that can enhance the output efficiency of PGS. This chapter serves as a valuable resource for scholars and researchers engaged in photovoltaic systems, focusing on generating efficient, clean, and sustainable energy. The next chapter will be dedicated to the presented research work, which combines two metaheuristic-based MPPT trackers to effectively monitor the generated power in PV systems subjected to partial shading issues.



## Chapter 3

---

# PROPOSED HYBRID MPPT ALGORITHM FOR PV SYSTEMS SUBJECTED TO PARTIAL SHADING CONDITIONS

## Contents

---

3.1 <a href="#">Introduction</a> .....	100
3.2 <a href="#">Simulation of the PV array characteristics under partial shading</a> .....	100
3.3 <a href="#">Overview of used MPPT techniques</a> .....	103
3.3.1 <a href="#">PSO-based MPPT algorithm</a> .....	103
3.3.2 <a href="#">Cuckoo Search via Levy Flights</a> .....	104
3.3.2.1 <a href="#">Levy Flights</a> .....	105
3.4 <a href="#">Proposed hybrid PSO-CS-based MPPT technique (SHA)</a> .....	106
3.4.1 <a href="#">SHA-based MPPT details</a> .....	107
3.4.2 <a href="#">Convergence and initialization criteria</a> .....	108
3.5 <a href="#">Description of the proposed PV system</a> .....	109
3.6 <a href="#">Results and discussion</a> .....	111
3.6.1 <a href="#">Tracking performance under standard test conditions</a> .....	112
3.6.2 <a href="#">Tracking performance under rapid change in irradiance</a> .....	115
3.6.3 <a href="#">Performance comparison with other MPPT techniques</a> .....	117
3.6.4 <a href="#">Tracking performance for a parallel configuration</a> .....	121
3.6.5 <a href="#">Tracking performance for the second set of shading profiles</a> .....	122
3.6.6 <a href="#">Statistical analysis</a> .....	124
3.6.7 <a href="#">Comparative study</a> .....	125
3.7 <a href="#">Conclusion</a> .....	129

### **3.1 Introduction**

This chapter addresses a hybridization of two SI algorithms, namely CS and PSO in a single hybrid algorithm named Smart Hybrid Algorithm (SHA), to enhance the performance of PV systems and harvest the optimum power under various weather conditions. The necessary theory as well as working principle of our approach is presented and discussed through multiple performance tests to confirm the robustness and suitability of our optimizer in monitoring the global maximum power in PV systems subjected to PS circumstances.

### **3.2 Simulation of the PV array characteristics under partial shading**

A PV array comprises a set of series/parallel PV panels. A series connection raises the system's voltage, whereas a parallel connection raises the current. This combination allows for obtaining the desired ratings of power. Mismatch losses are more common in PV cells in serial connections when their electrical characteristics differ or when subjected to PS, acknowledged as the primary source of energy losses in PV power systems. Under PSC, the panel exposed to shading absorbs the power provided by other modules; it acts as a charge instead of a generator, resulting in the "hot spot" effect. To overcome this issue, we connect bypass diodes at the terminals of each panel. At standard conditions, they are reversely biased and forwardly biased whenever partial shading occurs. Under conditions of uniform irradiance, the power-voltage (P-V) characteristics display a unique MPP. However, because of the bypass diodes, it will show many LMPPs and one GMPP during PSC, while the current-voltage (I-V) characteristics will demonstrate many steps. [Fig. 3.1](#) depicts an example of the impact of PS on the output characteristics of the PV panel. This figure shows one GMPP in the middle and three other local maxima. The number of these maxima is directly affected by PS's different scenarios.

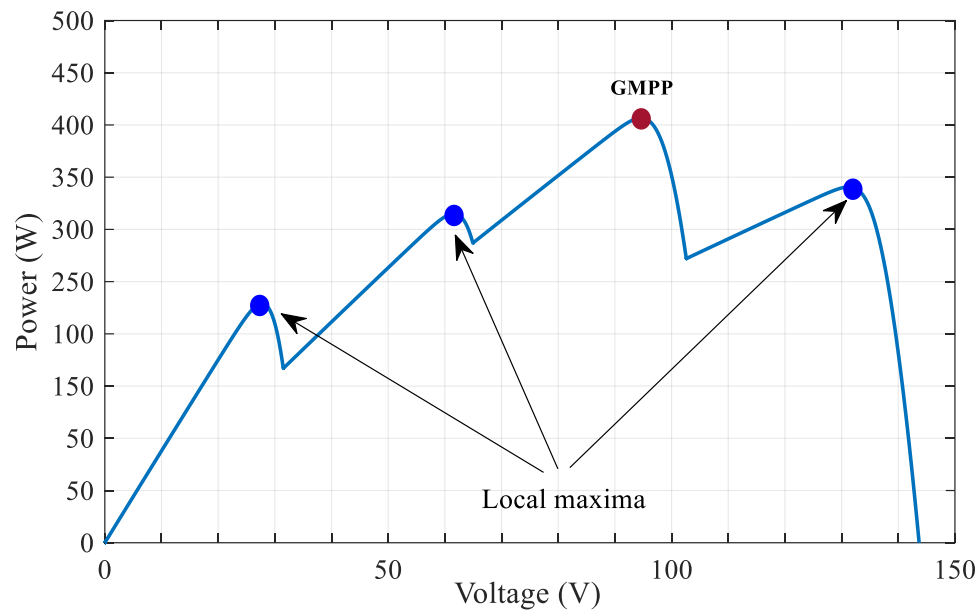


**Fig. 3.1** P-V characteristic under partial shading conditions.

The proposed hybrid algorithm is subjected to different PS scenarios, as depicted in [Table.3.1](#) and [Table.3.2](#). According to the type of shading pattern, the GMPP may occur in either the low or high voltage range; this comportment makes applying the traditional MPPT algorithms a hazardous task. The purpose of altering shadow patterns is to vary the location of the GMPP from left to right to test how well our optimizer performs in various PSC scenarios and to demonstrate its suitability in tracking the GMPP. [Fig. 3.2](#) illustrates the P-V characteristics for the first set of partial shading profiles under study for both series and parallel PV array configurations. Meanwhile, [Fig. 3.3](#) represents the corresponding P-V curves for the second set of PS scenarios.

**Table 3.1** First set of detailed profiles of PS used in this study.

Patterns	Configuration	Irradiance on each PV module ( $\text{W/m}^2$ )	Peak power value (W)			
			Peak1	Peak2	Peak3	Peak4
STC	4S	1000-1000-1000-1000	996	-	-	-
Profile 1	4S	400-600-1000-500	229,1	315	406,7	445,9
Profile 2	4S	1000-300-1000-400	484,7	336,5	341,2	-
Profile 3	4S	500-800-1000-1000	484,7	637,9	565,7	-
Profile 4	4S2P	G1: 400-600-1000-500 G2: 300-500-700-600	390.7	618.6	806.9	783.6

**Table 3.2** Second set of detailed profiles of PS used in this study.

Patterns	Configuration	Irradiance on each PV module ( $\text{W/m}^2$ )	Peak power value (W)
Profile 5	8S	1000 200 800 300 400 700 300 900	202.6 - 427.6 - 609.6 - 741.9 567 - 591.6 - 467.8
Profile 6	10S	1000 900 600 200 400 400 300 300 600 700	189.5 - 415.3 - 535.8 - 788.4 775.8 - 763.5 - 586.8
Profile 7	12S	1000 800 600 400 700 300 100 300 300 600 400 700	176.4 - 366.1 - 699.2 - 946.3 889.5 - 924.8 - 359.7

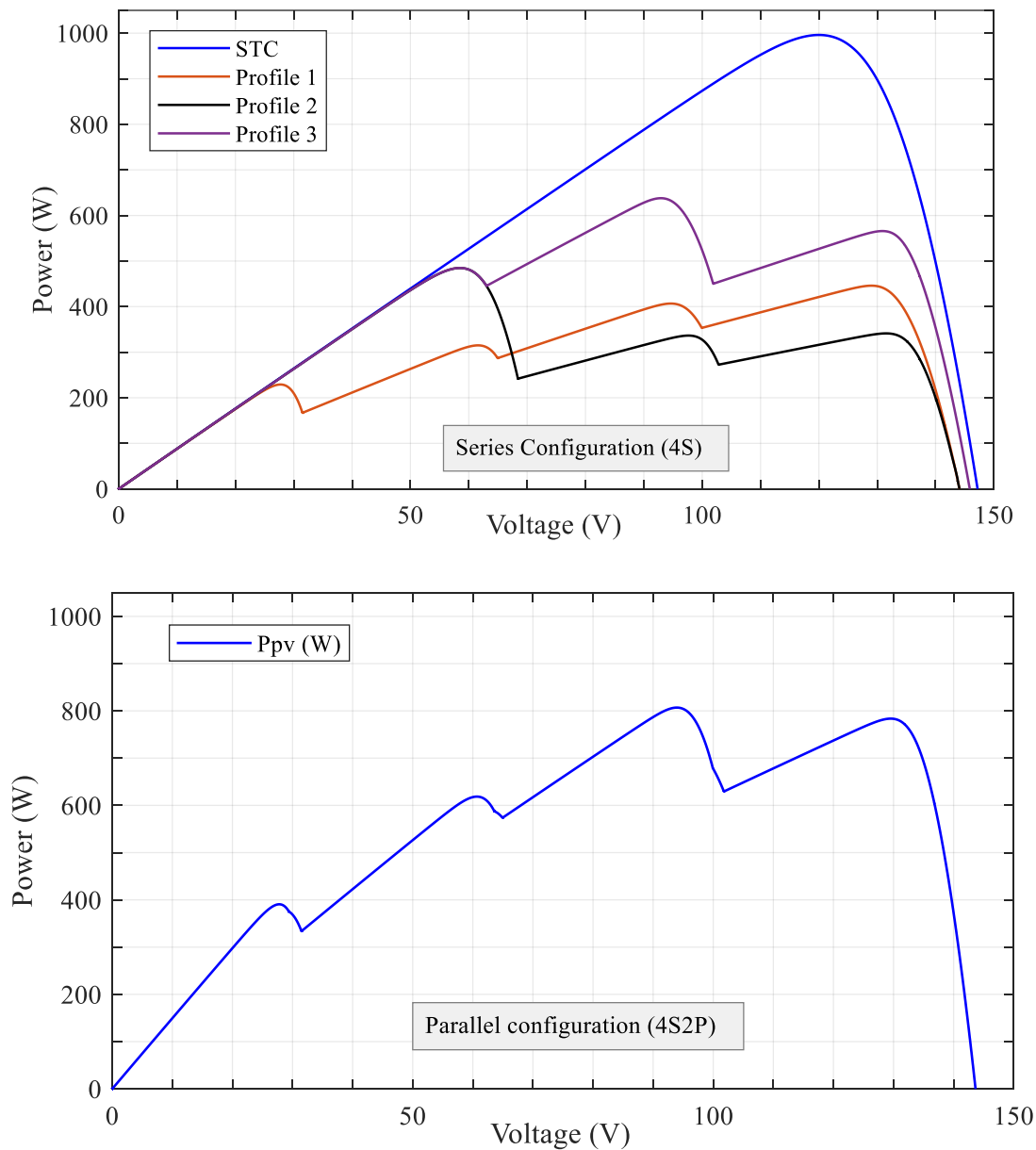


**Fig. 3.2** P-V characteristics for the first set of PS profiles under 4S and 4S2P configurations.

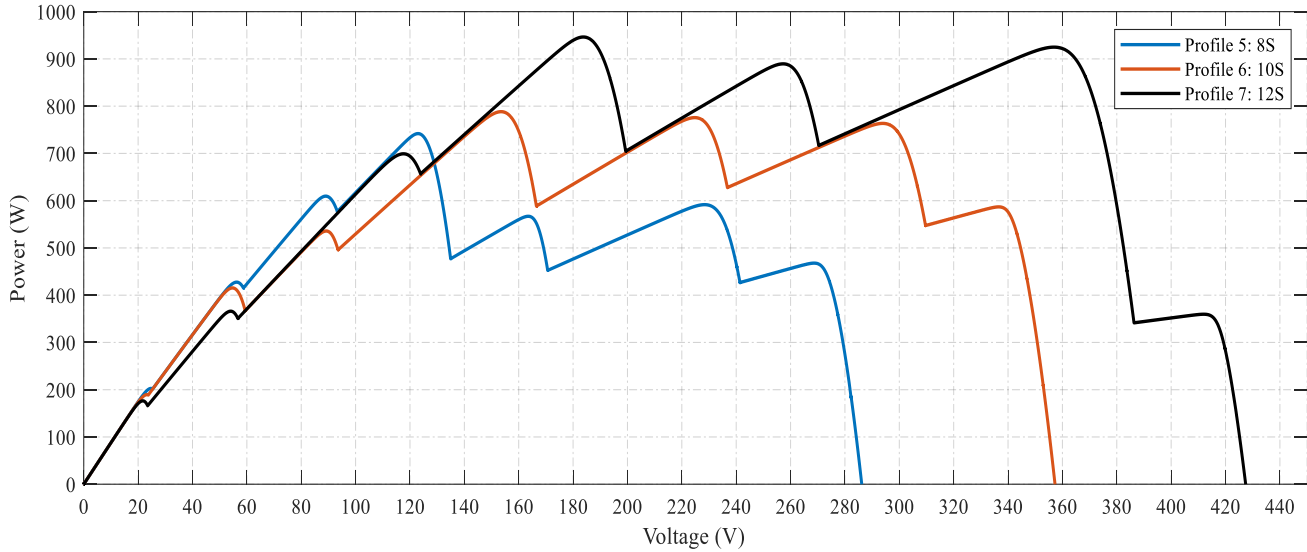


**Fig. 3.3** P-V characteristics for the second set of PS profiles under 8S, 10S, and 12S configurations

### 3.3 Overview of used MPPT techniques

A comprehensive literature search reveals that the hybrid PSO-CS (SHA) algorithm has not been presented in any other technical publication. Furthermore, the suggested approach has never been used for MPPT. As a result, this effort is performed to cover this research deficiency. The proposed SHA is convenient for complex nonlinear optimization issues. It uses the PSO algorithm's exploitation process and the CS algorithm's exploratory mechanism. The suggested approach involves advantages such as rapid convergence to the GMPP and low power fluctuations during the search process. The SHA can track the GMPP under complex partial shadowing circumstances with outstanding, steady-state, and dynamic efficiencies.

#### 3.3.1 PSO-based MPPT algorithm

PSO is a population-based strategy. It is used effectively to address many engineering optimization issues. The population in this approach is composed of a swarm of particles. Particles continually adapt their search trajectories by varying velocities depending on their individual and collective search histories. Each particle represents a probable candidate solution. As a result, it updates its location and communicates the information obtained from its own flying experience and that of its neighbors. Each particle advances to the optimal global location in this manner. The location and velocity of each particle in the swarm are modified as given in equations (3.1) and (3.2). The PV system's duty cycle and output power are the particle's position and the objective function, respectively.

$$v_i^{k+1} = w_i v_i^k + r_1 c_1 (pbest_i - d_i^k) + r_2 c_2 (gbest_i - d_i^k) \quad (3.1)$$

$$d_i^{k+1} = d_i^k + v_i^{k+1} \quad (3.2)$$

From equation (3.1), we can deduce that the velocity of the particle changes depending on *pbest* and *gbest*. The velocity is multiplied by  $w_i$  corresponding to the inertia weight and considers the *pbest* and *gbest* entities. The constants  $c_1$  and  $c_2$  are variables that describe how *pbest* and *gbest* affect the particle;  $r_1$  and  $r_2$  are arbitrary numbers from the range [0,1]. Finally, equation (3.2) is applied to get the new position for the particle. It should be mentioned that this technique is suitable for tracking the GMPP; however, due to the random nature of this approach, the algorithm may become trapped in a local maximum in some complex partial shading scenarios, causing a significant loss of energy, unless the tuning parameters are changed. Furthermore, this approach exhibits steady-state oscillations and a higher computing time, which prolongs the convergence time.

### 3.3.2 Cuckoo Search via Levy Flights

CS is a metaheuristic search method inspired by cuckoo breeding behaviour, as described in [161]. It has been recently proposed among the best optimization algorithms [162]. In addition to reproductive behaviour, cuckoos are considered to move following a Lévy flying pattern in the “CS” algorithm. The Lévy flight consists of a direct path accompanied by abrupt rotations in random ways. The CS's properties enable extensive search space exploration compared to other evolutionary computing techniques. According to [163], Lévy flights can increase the effectiveness of resource searches in an unpredictable environment. Because of the Lévy distribution, the steps are made up of numerous short steps and, sometimes, long-distance jumps, as shown in Fig. 3.4. These long steps may significantly boost the search efficiency of CS as compared to other metaheuristic algorithms in some contexts, particularly for multimodal, nonlinear issues. CS is substantially more concise than other optimization techniques due to several attributes. We can highlight the following points:

- CS is an algorithm based on populations like “GA” and “PSO”, but it involves elitism in the selection process.
- Tuning parameters in CS are less than other optimization algorithms such as “GA” and “PSO”.
- Contrary to PSO, sample initialization does not influence CS's performance.

- Cuckoo algorithm global search is typically based on Lévy flights instead of conventional random walks. Since the mean and variance of Lévy flights are infinite, "CS" can explore the search space more precisely compared to algorithms that employ normal Gaussian processes. Occasionally, the steps get larger, resulting in a quicker convergence. This benefit makes the cuckoo search very effective.
- As an ultimate feature that should be mentioned, CS is highly suitable for handling PS owing to its inherent propensity to strive for the best optimum.

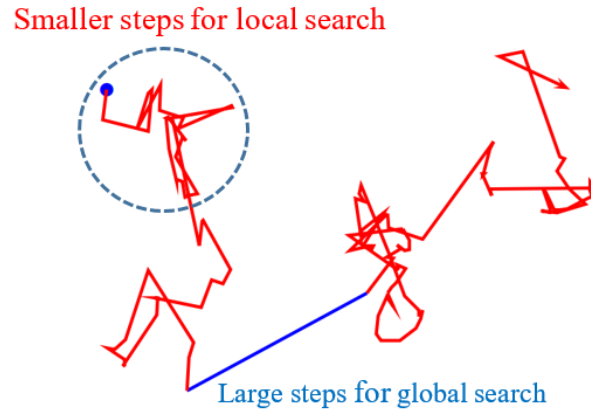


**Fig. 3.4** Lévy's flights in consecutive 50 steps.

### 3.3.2.1 Lévy Flights

The lévy flight search pattern is one of the most essential aspects of the “CS” when looking for a new generation of nests. This process is used in the search algorithm for optimization problems. Eq. (3.3) gives the new nests' position via The Lévy flight search process.

$$x_i^{k+1} = x_i^k + \alpha \oplus \text{Lévy}(\lambda) \quad (3.3)$$

In eq. (3.3),  $\alpha$  is the Lévy multiplying coefficient,  $\oplus$  denotes the entry-wise multiplication, and  $\lambda$  is the Lévy flight parameter. Eq. (3.4) defines the Lévy distribution.

$$L(s, \gamma, \mu) = \begin{cases} \sqrt{\frac{\gamma}{2\pi}} \exp\left[-\frac{\gamma}{2(s-\mu)}\right] \frac{1}{(s-\mu)^{3/2}} & 0 < \mu < s < 0 \text{ (for steps } \mu > 0 \text{)} \\ 0 & \text{otherwise} \end{cases} \quad (3.4)$$

Where  $\gamma$  is a scale parameter. The step length is calculated as follows:

$$s = \frac{u}{|v|^{1/\beta}} \quad (3.5)$$

Where  $\beta=1.5$  and  $u$  and  $v$  are normal distributions as defined in equation (3.6).

$$u \sim N(0, \sigma_u^2) \text{ and } v \sim N(0, \sigma_v^2) \quad (3.6)$$

The variables  $\sigma_u$  and  $\sigma_v$  are expressed in equation (3.7).

$$\sigma_u = \left\{ \frac{\Gamma(1 + \beta) \sin(\pi\beta/2)}{\Gamma[(1 + \beta)/2] \beta 2^{(1+\beta)/2}} \right\}^{1/\beta} \text{ and } \sigma_v = 1 \quad (3.7)$$

Despite its numerous benefits, incorrect tuning parameter selection may influence the “CS” approach, resulting in decreased efficiency and steady-state oscillations. To address the outlined issues, we presented the SHA. The main advantage of the suggested technique is the deep cooperation between PSO at the exploitation level and CS at the exploration stage. Moreover, an elitism process is considered to discard the worst-performing particles and achieve performance in terms of convergence time, low power perturbations, outstanding steady state, and dynamic efficiencies. This approach can track the GMPP under severe environmental circumstances such as CPSCs and rapid irradiance changes.

### **3.4 Proposed hybrid PSO-CS-based MPPT technique (SHA)**

The proposed approach combines the PSO and CS. Both algorithms work closely to ensure a high balance between exploitation and exploration. The Lévy flight search pattern is embedded into the SHA to boost its performance instead of the random searching technique at the exploration phase of the search process. Another feature that characterizes the proposed SHA is the integration of a reset function that detects any variation in weather circumstances to restart the search process for the new GMPP; our method operates independently of the number of iterations, ensuring consistent results regardless of the complex nature of the shading patterns. This sets it apart from many iterative algorithms, which can reach their maximum number of iterations without converging on the real GMPP. As a result, these algorithms may experience premature convergence in complex scenarios; however, the SHA is always on standby position to seek the real GMPP. It should be noticed that the Lévy flights are a more effective way to explore the search space since their step length tends to become considerably more significant as the process is running due to the power-law distribution. The proposed algorithm is embedded into the MPPT function to optimize the PV system’s output power. In our approach, the output of the MPPT function is fed to the power



converter as a duty cycle; this latter is permanently adjusted to maximize the objective function expressed as follows:

$$f(V_{pv}, I_{pv}) = \max_d (V_{pv} * I_{pv}) = \max_d (P_{pv}) \quad (3.8)$$

Where  $d$  is the duty cycle that controls the converter with a lower limit of 0 and an upper limit of 1.  $V_{pv}$  and  $I_{pv}$  are the measured voltage and current, respectively, and  $P_{pv}$  is the output power of the PV array.

### 3.4.1 SHA-based MPPT details:

The SHA is designed following this sequence of steps:

1. Set the population size  $n$ , inertia weight  $\omega$ , and acceleration coefficients ( $c_1$ ,  $c_2$ ),  $\beta$ ,  $\alpha$ , and  $P_a$
2. Specify the particle limits.
3. Set up the first generation of candidates to cover the search space.
4. For each candidate, evaluate the fitness function  $P_{pv}$ .
5. Find the best positions of particles  $p_{best}$  then determine the global best position  $g_{best}$  based on Eqs. (3.1) and (3.2).
6. Set the new value of the inertia weight  $\omega$  according to this equation:

$$\omega = \left( 1.1 - \frac{p_{best}}{g_{best}} \right) \quad (3.9)$$

7. Use Eq. (3.10) to replace worst performing particles within a probability  $P_a$

$$d_i^{k+1} = d_i^k + \alpha \oplus \text{Lévy}(\lambda)(g_{best} - d_i^k) \quad (3.10)$$

It is essential to emphasize that the proposed optimizer is based on an elitism-based process since it discards the worst-performing particles and replaces them with new solutions using equation (3.10); this process ensures rapid convergence and better exploration of the search space.

### 3.4.2 Convergence and initialization criteria

Two criteria are considered in the tracking process: once the SHA approaches the real GMPP, the distance between the searching particles becomes very small. The desired threshold is as given in (3.11):

$$|d_{new} - d_{prv}| < \Delta d \quad (3.11)$$

Keep the obtained global best solution  $d_{Optimum}$  and stay in a standby position until a new change is detected; in this case, restart the process based on Eq. (3.12).

$$|Irradiation_{new} - Irradiation_{prv}| < \Delta irradi \quad (3.12)$$

The flowchart of the proposed SHA is illustrated in Fig. 3.5.

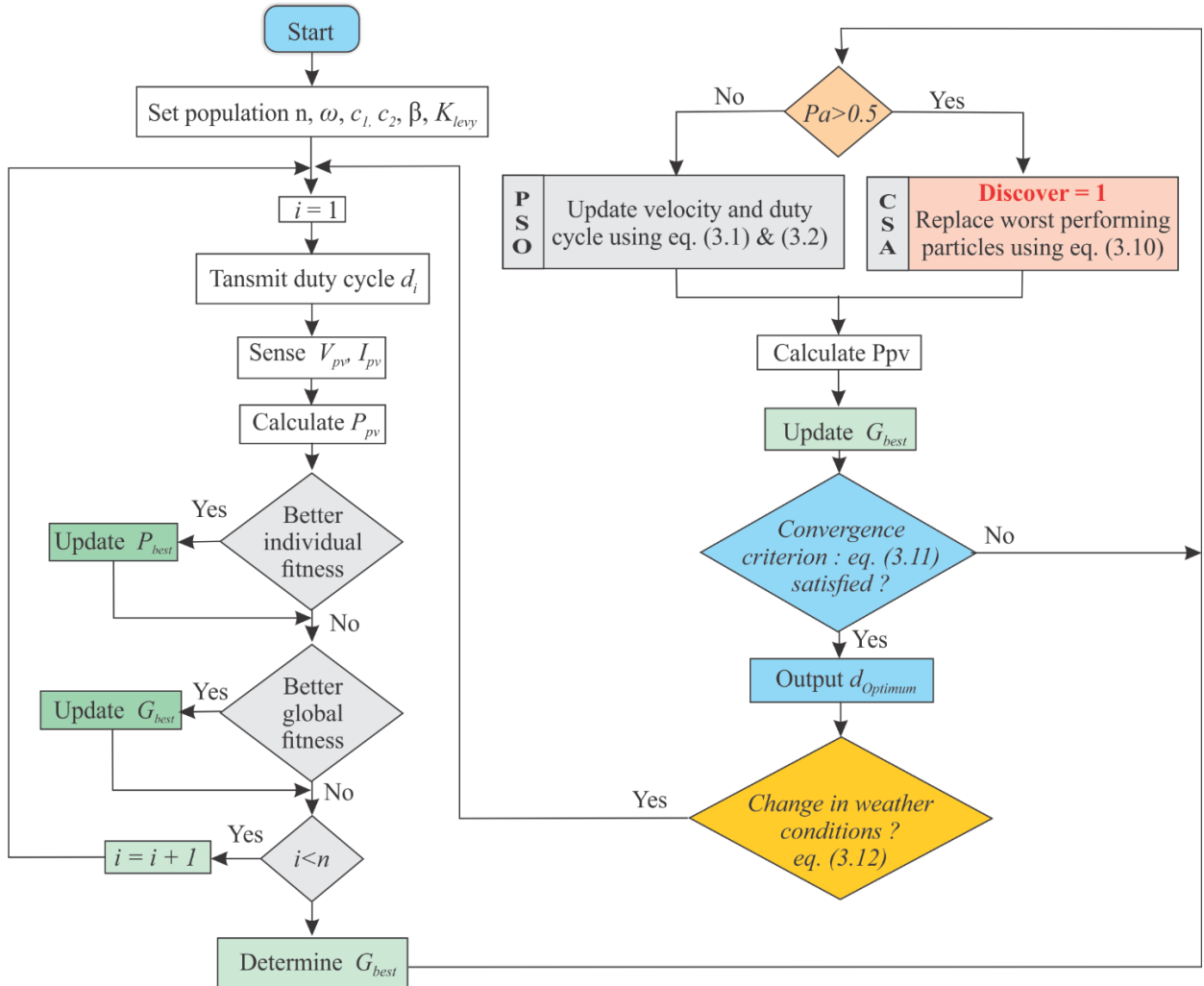
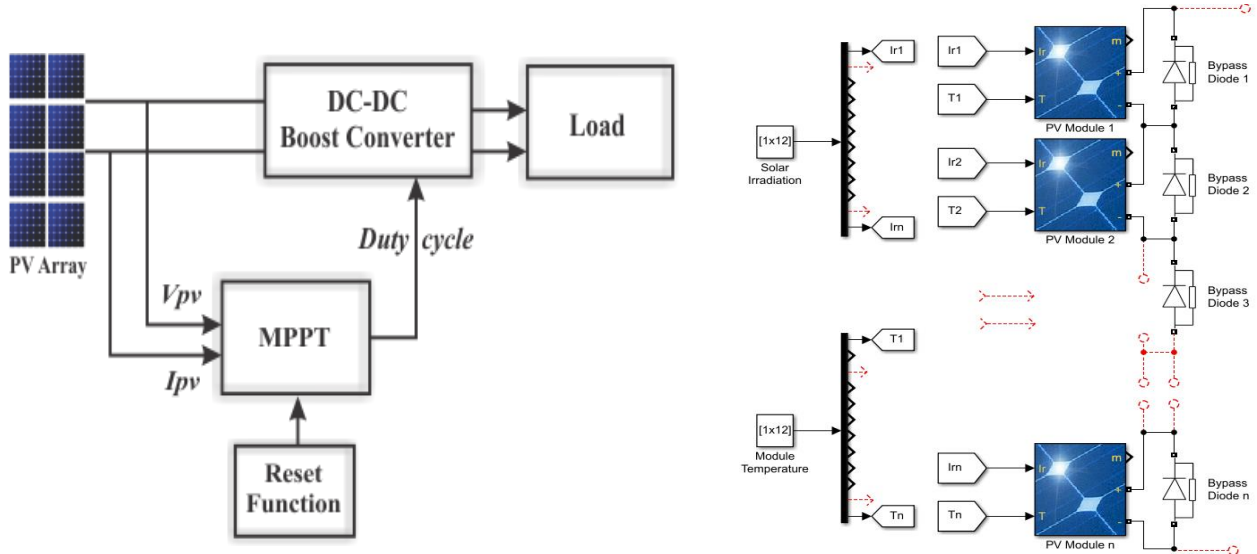


Fig.3.5 Flowchart of SHA-based MPPT

### 3.5 Description of the proposed PV system

The proposed SHA is tested in a MATLAB/Simulink environment to determine its efficiency in tracking the optimum required global power. To verify the robustness and suitability of the proposed SHA-based MPPT approach to track the GMPP, in-depth simulation tests are conducted under both homogenous and nonhomogeneous weather conditions. Eight shading profiles and one rapid change of irradiance are considered under 4S, 8S, 10S, 12S, and 4S2P PV configuration modes. [Fig.3.6](#) depicts the diagram of the MPPT PV system along with the studied series PV array configuration. As mentioned, the PV array consists of PV panels connected in series along with bypass diodes to prevent the hot spot phenomenon. For optimal output efficiency, a boost converter is implemented to regulate and match the output of the PV array. The DC-DC boost converter's design parameters are precisely calculated to lessen the output voltage and current fluctuations and to satisfy the continuous conduction mode. The converter's values are as follows:  $f_s = 20 \text{ kHz}$ ,  $C_{in} = 10 \mu\text{F}$ ,  $C_{out} = 467 \mu\text{F}$ ,  $L = 1.1478 \text{ mH}$ ,  $R_L = 53 \Omega$ . It is important to consider the settling time of the DC-DC converter by correctly adjusting the time between two successive samples of the duty cycle. Simulation tests are carried out under a sampling time of 0.2 ms. The used PV module's specifications are depicted in [Table 3.3](#), whereas [Table 3.4](#) depicts the detailed algorithm parameters.



**Fig. 3.6** Proposed MPPT PV system along with PV array series configurations (n=4, 8,10 and 12)

**Table 3.3** TP250 MBZ PV module parameters at STC.

Characteristics	Value
$P_{max}$ (W): Maximum power	249
$V_{oc}$ (V): Open-circuit voltage	36.8
$V_{mp}$ (V): Voltage at MPP	30
$I_{mp}$ (A): Current at MPP	8.3
$I_{sc}$ (A): Short circuit current	8.83
Current temperature coef. (%/deg.C)	0.063805
Voltage temperature coef. (%/deg.C)	-0.33
N°. of cells	60

**Table 3.4** Detailed algorithm parameters

Algorithm	Parameters	Value
PSO	$\omega$	Decreasing eq. (13)
	$c_1$	1.00
	$c_2$	1.40
	$P_a$	0.50
CS	“Lévy coef.”	0.80
	$\beta$	1.50
PO	$\Delta d_{(PO)}$	0.001
SHA	$\Delta irradi$	0.05
	Duty Cycle	[0-1]
	$N_p$	04

The PV current, voltage, and reset function are the system inputs; the resulting output is fed to the PWM, which is then supplied to the MOSFET power switch. The PWM is permanently adjusted through the MPPT function output to ensure the optimum duty cycle is delivered for optimal power performance. A thorough simulation analysis is performed under STC, partial shade conditions, and rapid irradiance change. Several patterns with different levels of partial shading are tested to verify the reliability of the proposed optimizer. For this study, the cell temperature remains constant at 25 °C under all circumstances. The different PS scenarios studied in this thesis are depicted in [Table.3.1](#) and [Table.3.2](#). The following metrics are considered in evaluating the

robustness of the proposed SHA: convergence time, static efficiency, and dynamic efficiency for each scenario in tracking the GMPP. The tracking efficiency is defined as:

$$\eta_{Static} = \frac{P_{MPPT}}{P_{max}} \times 100 (\%) \quad (3.13)$$

$P_{MPPT}$  and  $P_{max}$  are, respectively, the MPPT steady-state power and the maximum delivered power by the photovoltaic panel. The dynamic performance considers the transient behaviour and the steady state conditions. It is calculated as given in eq. (3.14).

$$\eta_{Dynamic} = \frac{\int_{t_1}^{t_2} p(t) dt}{\int_{t_1}^{t_2} P_{MPPT} dt} \times 100\% \quad (3.14)$$

Where  $p(t)$  and  $P_{MPPT}(t)$  are the measured power and the maximum power on the P-V curve at time  $t$ , respectively. Depending on the shading pattern, the GMPP might happen at low or high voltage ranges. The shading patterns are purposefully set such that the GMPP position changes from the left to the right of the PV curve to test the robustness of the SHA in determining the global optimum power. Our simulation results show that no matter where the GMPP is placed, the suggested approach can acquire the GMPP under all test scenarios. Furthermore, the proposed hybrid algorithm is benchmarked against the PSO, CS, and PO techniques, and a performance comparison is established against various well-known MPPT techniques. To evaluate the performance of the proposed method, we initially started the tests with the 4S configuration. The first performance evaluation of the SHA algorithm is the test under STC, where the four modules receive a uniform irradiance of  $1000 \text{ W/m}^2$  while the temperature is set constant at  $25^\circ\text{C}$ . Under this case, the P-V curve demonstrates only one peak. Secondly, the system is tested against a rapid change of irradiance. At this stage, the SHA is successively exposed to the three studied shading profiles (SP1, SP2, and SP3).

### 3.6 Results and discussion

This section presents and discusses the results obtained from the proposed hybrid MPPT controller. Our optimizer is subjected to numerous validation tests under STC, PSCs, and rapid irradiance change in conjunction with two PV array configurations series and series-parallel configurations. Moreover, a performance comparison is carried out against well-known similar MPPT techniques.

### **3.6.1 Tracking performance under standard test conditions**

As aforementioned, each panel receives an irradiance of  $1000 \text{ W/m}^2$  in this case, while the temperature is fixed constant at  $25^\circ\text{C}$ . As shown in [Fig. 3.2](#), [Fig. 3.7](#) illustrates the search process for the global optimum under STC. This scenario's P-V characteristic demonstrates a unique peak at 996 W. Under this profile, the SHA optimizer starts searching for this global optimum by dispensing the first particles over the search space; then, all particles start cooperating by transmitting their own best and global values. Our algorithm successfully tracks the optimum value where all particles could converge to the required GMPP with a final global best value of  $G_{best} = 0.47$ .

As mentioned, the SHA features an elitism process in tracking the GMPP. This feature is illustrated in [Fig. 3.8](#). The selection process provides accuracy and fast-tracking of the global optimum solution. This figure shows that worst cases or less performing particles represented here with (\*) are destroyed or eliminated and replaced with more performing particles represented with (o) using eq. 3.10. The selection process continues in this manner until the desired GMPP is obtained.

The dynamic performance of the SHA under STC is illustrated in [Fig. 3.9](#). The SHA converges to this global MPP at 992.90 W within 1.05 s with 99.69 % static efficiency. Some power fluctuations are observed at the beginning of the search process due to intermittent search between PSO and CS; however, these fluctuations are less critical since their duration is small.

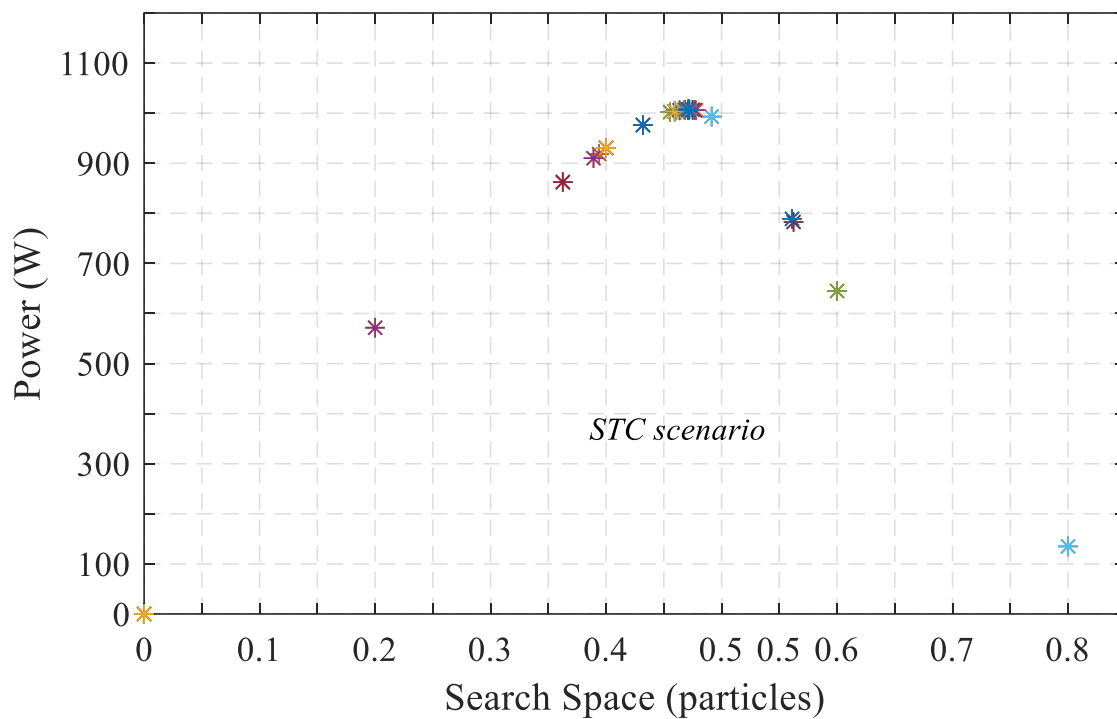


**Fig. 3.7** Search process ( $P_{est}$  and  $G_{best}$ ) for the SHA under STC ( $G=1000 \text{ W/m}^2$ ,  $T= 25^\circ\text{C}$ )

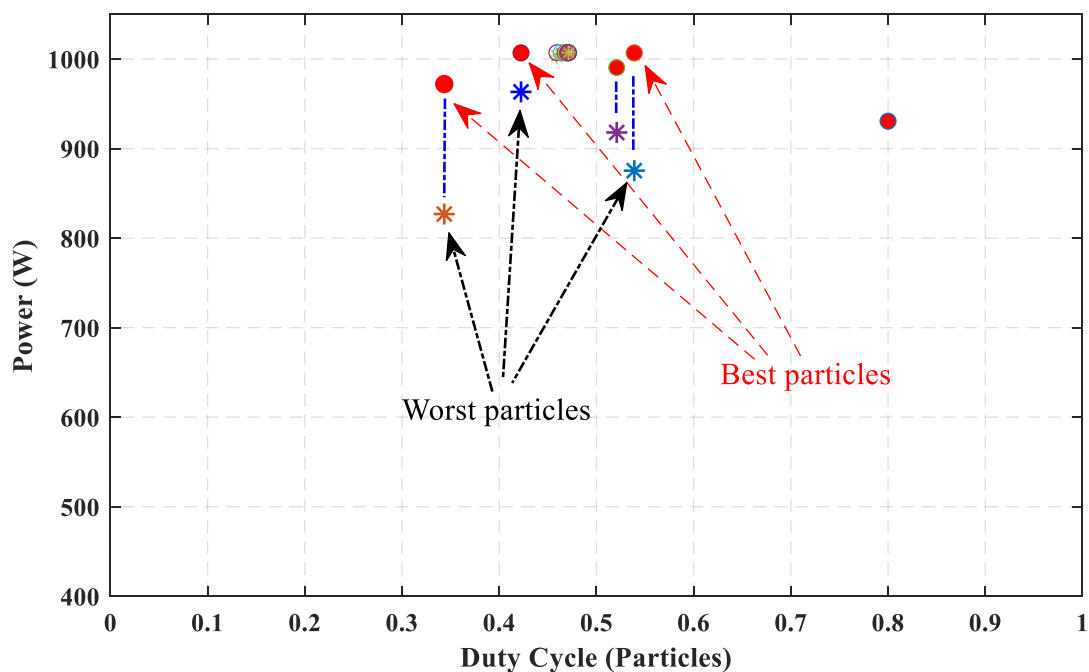


**Fig. 3.8** Selection process for SHA under STC.

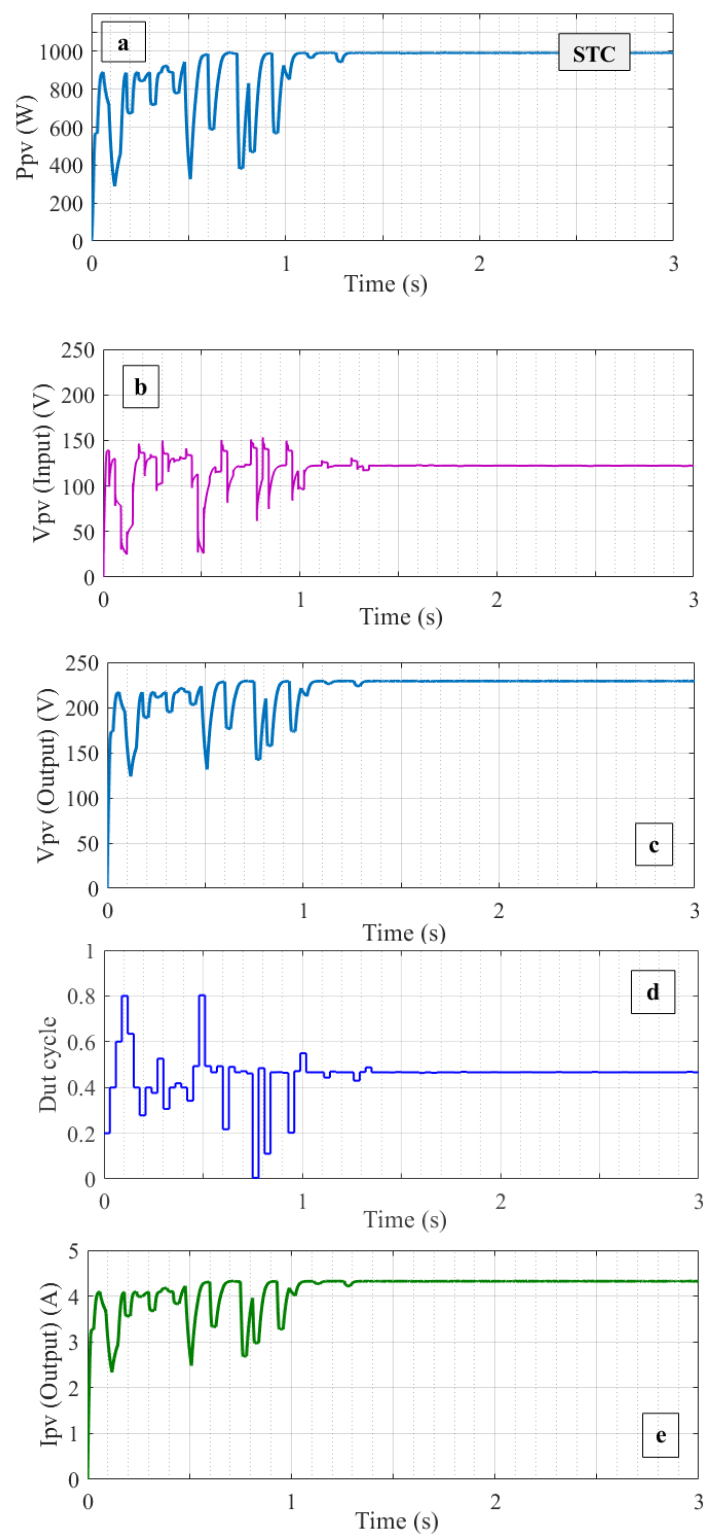


Fig. 3.9 SHA performance under STC. ( $G=1000 \text{ W/m}^2$ ,  $T= 25^\circ\text{C}$ )



### 3.6.2 Tracking performance under rapid change in irradiance

In this case, the system is subject to a rapid change of irradiance every three seconds. As shown in the dynamic response in [Fig. 3.10](#). The proposed algorithm successfully tracks the real power as the shading profiles change from SP1 to SP3. This change in shading is instantly detected by the reset function, which restarts the search process for the new global maximum. In the first three seconds, the system is subjected to SP1 in this case; the P-V curve illustrates four maxima (229.1 W, 314.9 W, 406.7 W, and 445.90 W) where the GMPP is found on the right side. SHA successfully located this global maximum after 0.85 s with 100 % steady-state efficiency and low power fluctuations. We intentionally changed the shading profile at time  $t = 3$  s so that the GMPP moves from right to left of the P-V curve to verify the system's performance under this significant change in position. This case presents three power peaks (484.70 W, 336.5 W, and 341.2 W). Although the GMPP changed position from extreme right to extreme left, our system could converge to this new global power after 0.98 s with 99.67 % steady state efficiency, demonstrating very high robustness. This performance is due to the deep cooperation between PSO and CS, where the roles are exchanged between exploitation at the PSO level and exploration at the CS level, where low-performing particles are destroyed and replaced with new updated ones using equation 3.10. At  $t = 6$  s, SHA is faced to the third shading profile, where the GMPP is located in the middle of the P-V characteristic. Under this profile, the P-V characteristic presents three power peaks (484.7 W, 637.9 W, and 565.7 W). The system locates the GMPP after 1.10 s and demonstrates 99.37% steady-state efficiency.

[Fig. 3.10](#) illustrates the search process for the global optimum of the proposed optimizer under a rapid change in irradiance. In this situation, the SHA is tested against three successive scenarios, starting from SP1 and continuing to SP3. The movement of particles in the search space seeking the optimum solution is displayed in [Fig. 3.11](#). Initially, all particles cooperate by transmitting their knowledge ( $G_{best}$ ,  $P_{best}$ ) to find the first global optimum corresponding to SP1, and they succeed in reaching this GMPP located at 445.9 W with all particles converging to the  $G_{best}$  of 0.162. Then, a change in irradiance occurs after three seconds, corresponding to SP2; at this stage, the system restarts itself, and the particles are spread again over the search space to harvest the second optimum. All particles could also converge to the second GMPP at 484.7 W, with a  $G_{best}$  of 0.626. Finally, at  $t = 6$  s, the irradiance is changed to SP3. The SHA detects this

change and restarts the system to search for the new optimum. Our optimizer successfully tracks the new optimum where all particles could converge to the third GMPP located at 637.9 W with a global best value of  $G_{best}= 0.491$ .

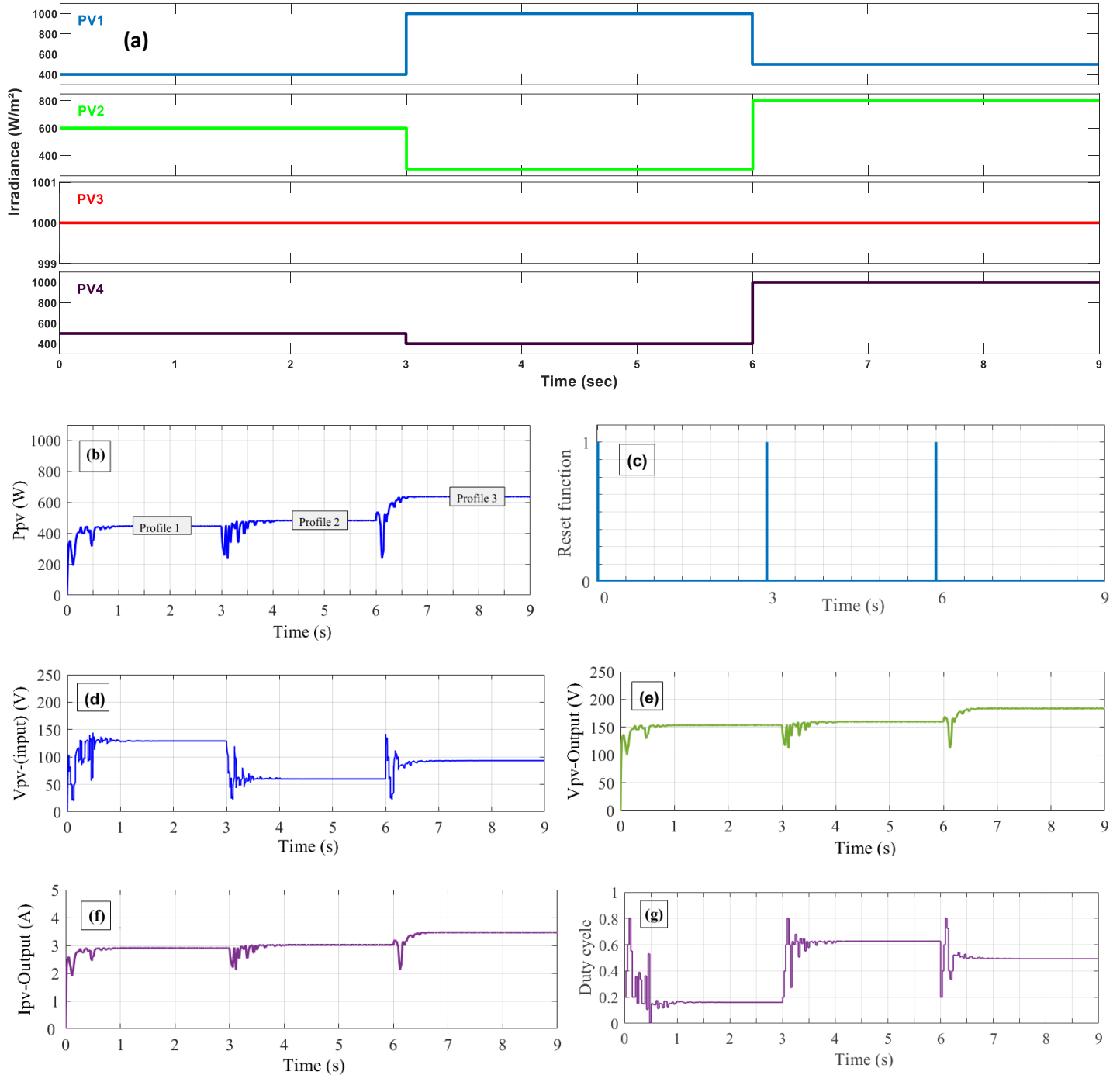


**Fig. 3.10** SHA performance under rapid change in irradiance. (a) Irradiance profiles (b) Tracked power (c) Reset function (d) input voltage (V) (e) Output voltage (V) (f) Output current (A) (g) duty cycle

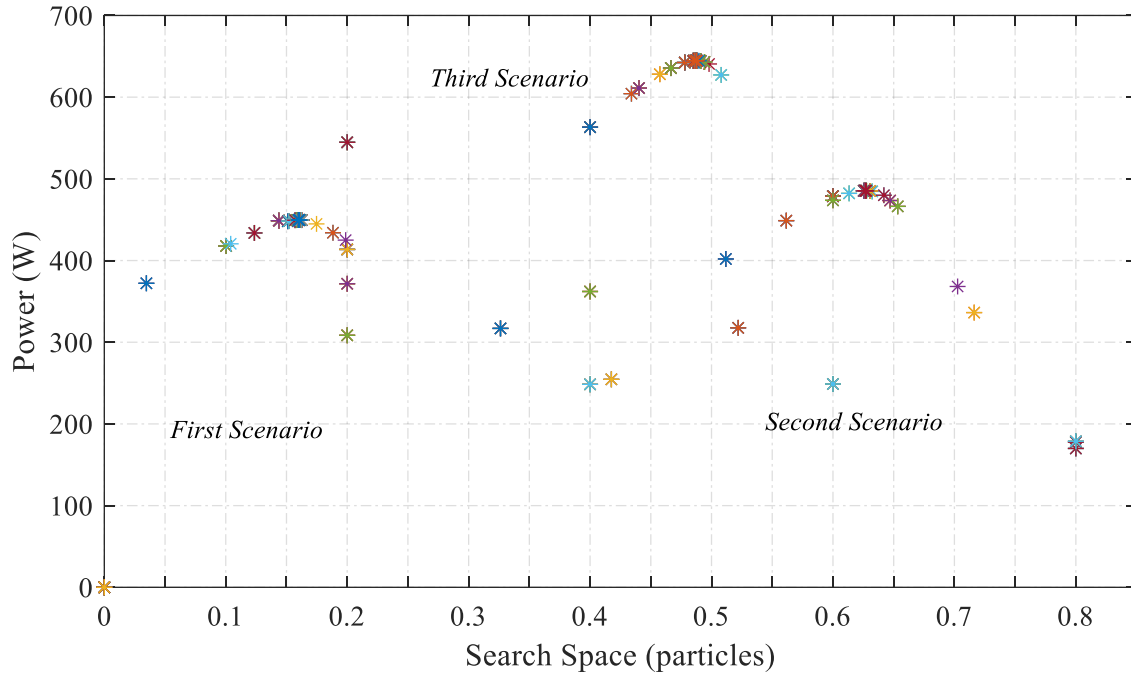


**Fig. 3.11** Search process ( $P_{est}$  and  $G_{best}$ ) for SHA under rapid change in irradiance.

### 3.6.3 Performance comparison with other MPPT techniques

[Fig. 3.12](#) displays the performance of the proposed approach with other swarm intelligence MPPT techniques. The SHA is benchmarked against PSO, CS, and the conventional PO algorithm under SP1.

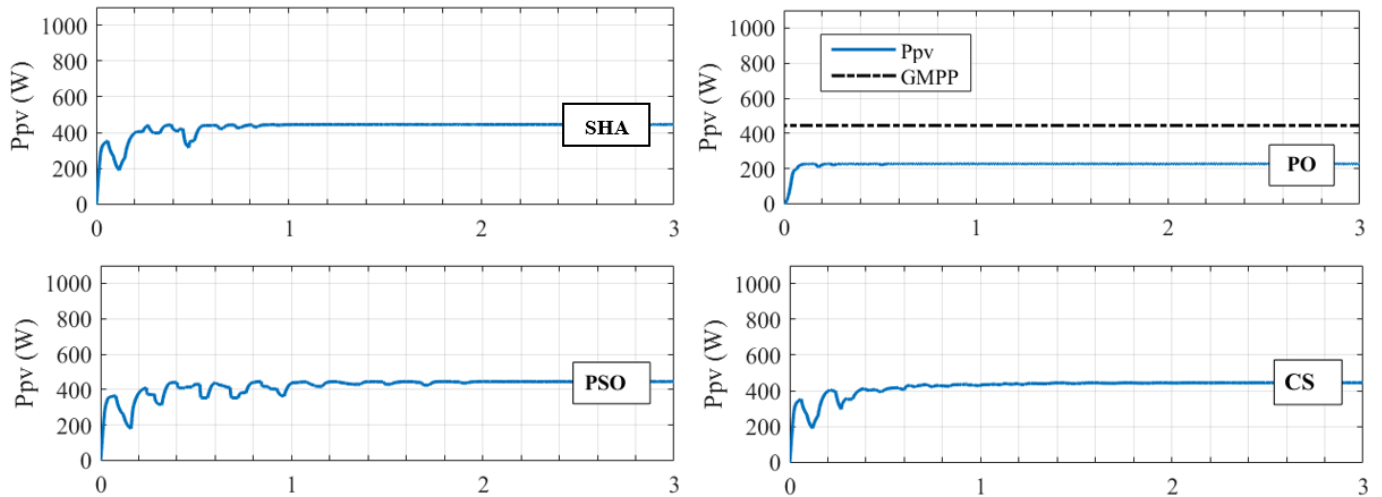


**Fig. 3.12** Performance comparison of SHA with other techniques under shading profile 1

Under this shading profile, all the algorithms can locate the GMPP successfully except the PO algorithm, which is trapped at a local maximum. The tracking performance shown in this figure illustrates the merits of the cooperation between PSO and CS in the search process to achieve the best compromise in terms of exploitation and exploration, hence achieving outstanding results in terms of convergence time and real power tracking with high performance in both steady state and dynamic efficiencies and low power fluctuations. This case illustrates that the PSO algorithm could track the GMPP after 2 s. Still, with a lower dynamic efficiency of 94.32 % due to power fluctuations at the exploitation level in the local search, whereas the CS could converge with a lower time of 1.56 s and a relatively better dynamic efficiency of 95.36 % in contrast, the result of this combination was the achievement obtained by the SHA, producing better power tracking performance under both dynamic and steady-state situations, it took only 0.85 s for the SHA to locate the GMPP at 100 % steady state efficiency and 96.19% dynamic efficiency. [Table 3.5.](#) illustrates a performance comparison of the SHA with other techniques, whereas the dynamic response under shading profiles 2 and 3 is shown in [Fig. 3.13](#) and [Fig.3.14](#).

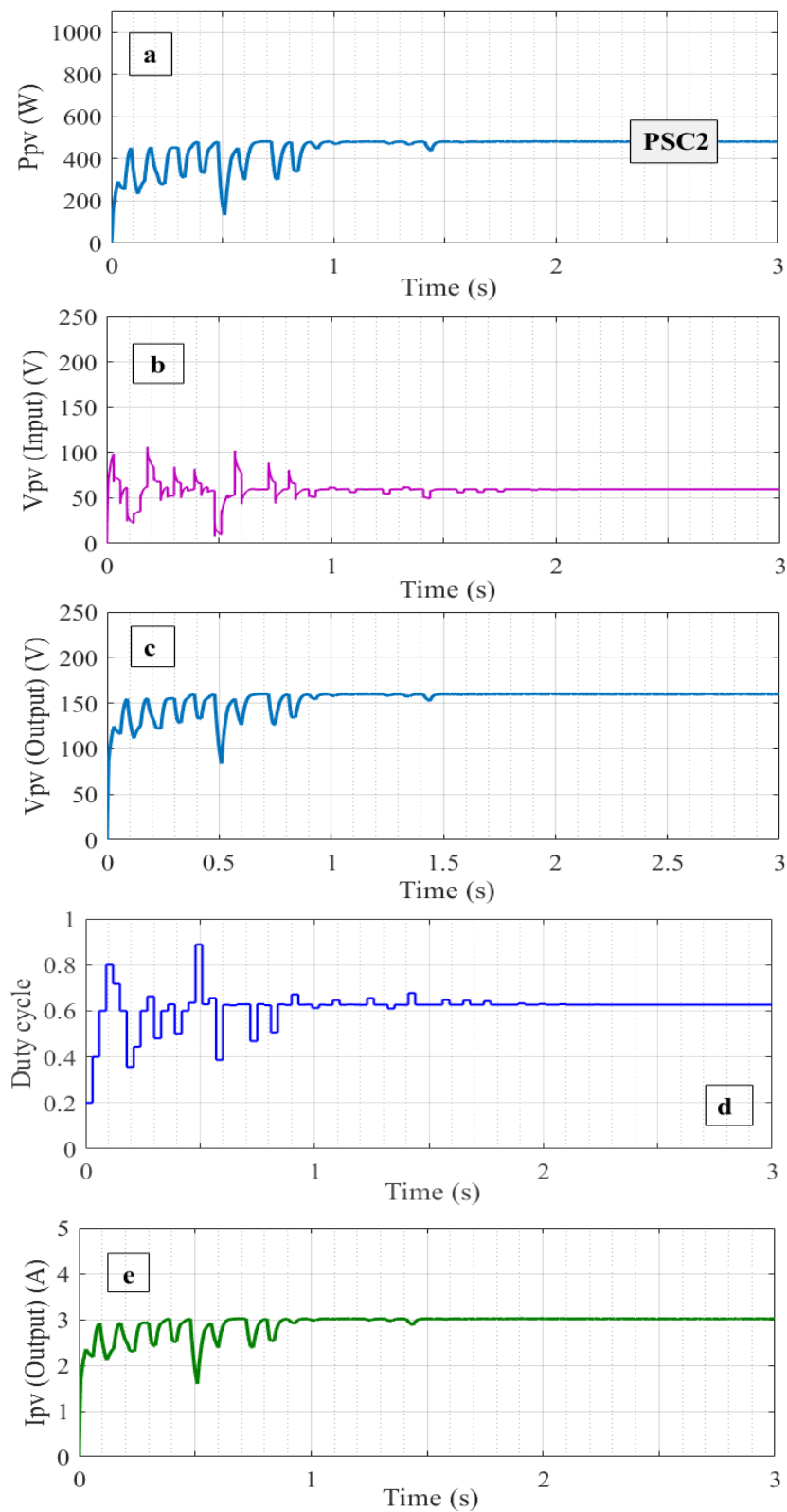


**Fig. 3.13** SHA performance under shading profile 2.

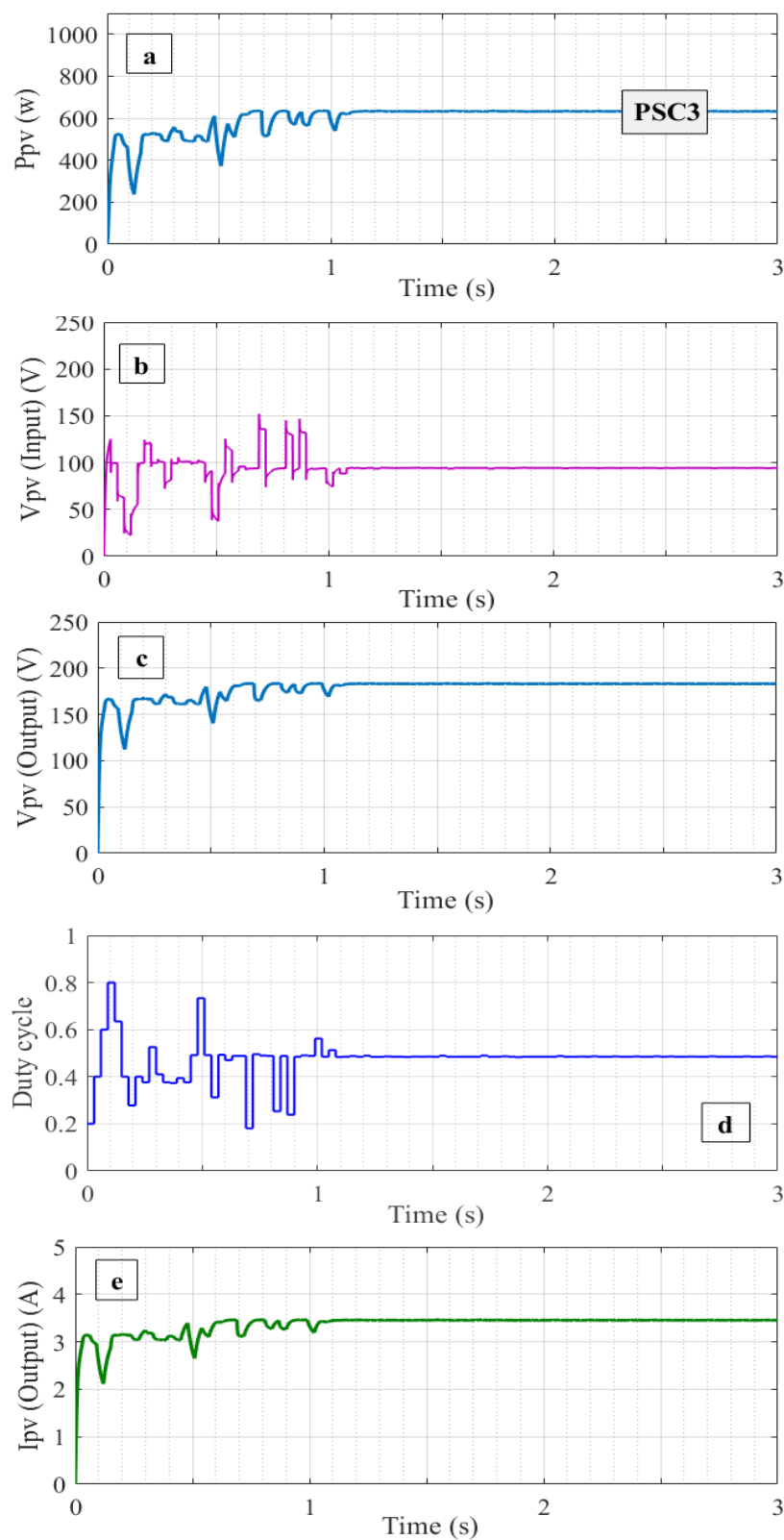


**Fig. 3.14** SHA performance under shading profile 3.

### 3.6.4 Tracking performance for a parallel configuration

The 4S2P configuration is considered to test the proposed SHA's robustness and suitability for tracking the GMPP under different scenarios. The two PV panel groups are subjected to this set of irradiances (G1: 400 600 1000 500; G2: 300 500 700 600) W/m<sup>2</sup>, whereas the temperature is fixed constant at 25°C. The dynamic response of the system is shown in [Fig. 3.15](#). Under this case, the P-V curve illustrates four power peaks (390.7 - 618.6 - 806.9 -783.6) W as shown in [Fig. 3.2](#). Moreover, there is a slight difference between the global peak located in the third position of the P-V curve and the fourth peak. Despite this slight difference, our optimizer was able to quickly locate the GMPP within 1.05 s and attain an efficiency of 99.39 % at steady-state, demonstrating low power fluctuations and outperforming both PSO and CS. In contrast, the PO algorithm was trapped in a local maximum. The detailed results are depicted in [Table. 3.5](#).

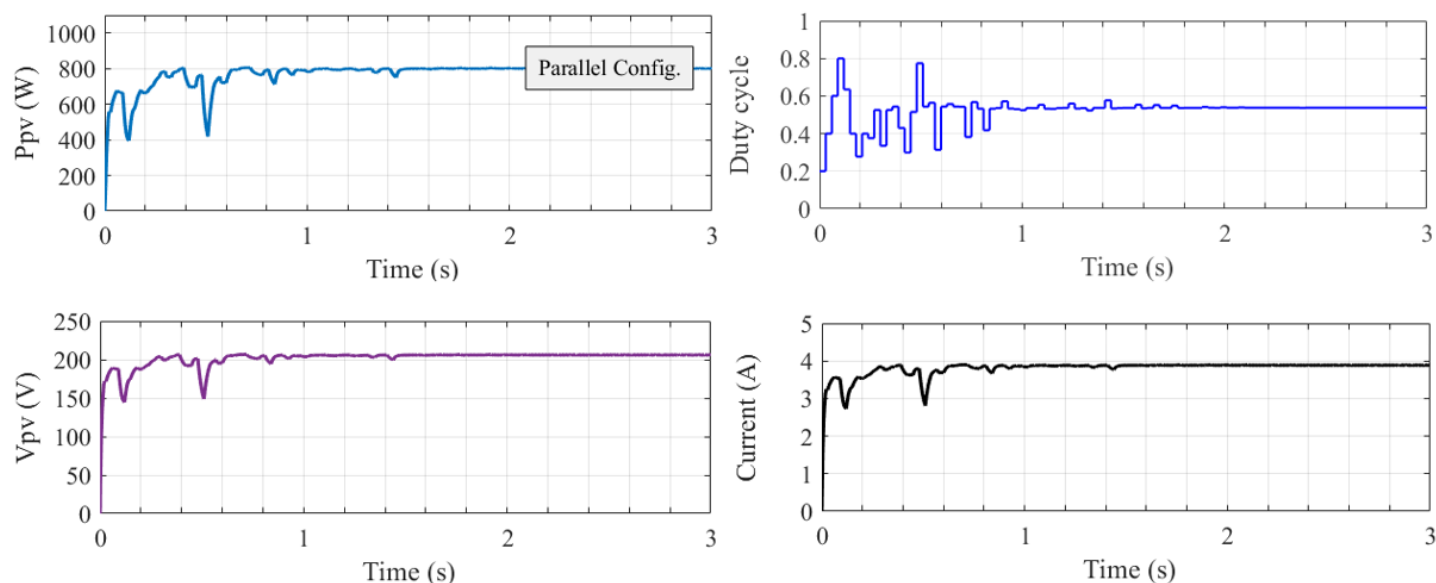


**Fig. 3.15** Performance of SHA under shading profile 4 (4S2P)

**Table 3.5** Performance comparison of the SHA with other methods for the first set of shading profiles

SHADING PROFILES	PV CONFIGURATION	MPPT TECHNIQUE	P <sub>MAX</sub> (W)	TRACKED POWER (W)	CONVERGENCE TIME (S)	STATIC EFFICIENCY (%)	DYNAMIC EFFICIENCY (%)
STC	4S	SHA	996.00	992.90	1.05	99.69	91.50
		PSO		995.70	2.05	99.96	91.66
		CS		950.30	1.56	95.41	91.76
		PO		987.20	0.16	99.11	93.42
Profile 1	4S	SHA	445.90	445.90	0.85	100.00	96.19
		PSO		445.90	1.94	100.00	94.32
		CS		445.60	1.39	99.93	95.06
		PO		228.00	0.14	51.13	50.19
Profile 2	4S	SHA	484.70	483.10	0.98	99.67	93.05
		PSO		483.30	2.36	99.71	88.30
		CS		483.20	1.24	99.69	96.21
		PO		478.30	0.13	98.67	92.76
Profile 3	4S	SHA	637.90	633.90	1.10	99.37	93.94
		PSO		628.10	2.86	98.46	85.16
		CS		637.20	1.24	99.89	96.13
		PO		478.10	0.14	74.94	72.87
Profile 4	4S2P	SHA	806.9	802.00	1.05	99.39	95.37
		PSO		801.70	2.60	99.35	92.48
		CS		801.30	0.70	99.30	95.99
		PO		606.60	0.10	75.17	72.95

### 3.6.5 Tracking performance for the second set of shading profiles

To test the performance and robustness of our system in a more complex configuration of PV modules, we have extended the number of PV modules successively to 8, 10, and 12 using the series configuration as illustrated in [Fig. 3.6](#). The different scenarios are as depicted in [Table. 3.2](#). The corresponding P-V curves are illustrated in [Fig. 3.3](#). The obtained dynamic responses for the different scenarios are shown in [Fig. 3.16](#), [Fig. 3.17](#) and [Fig. 3.18](#).

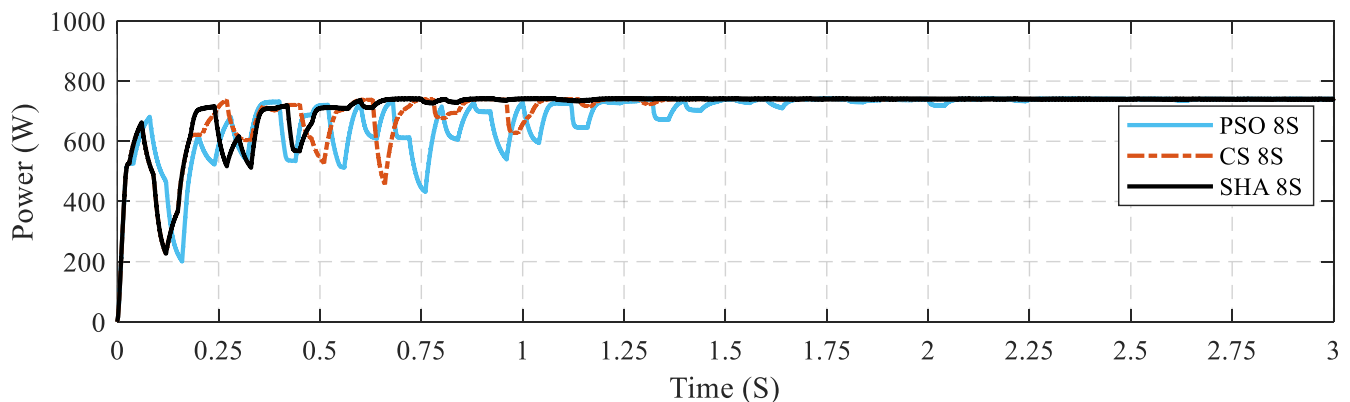


**Fig. 3.16** Performance of SHA, PSO and CS under 8S configuration



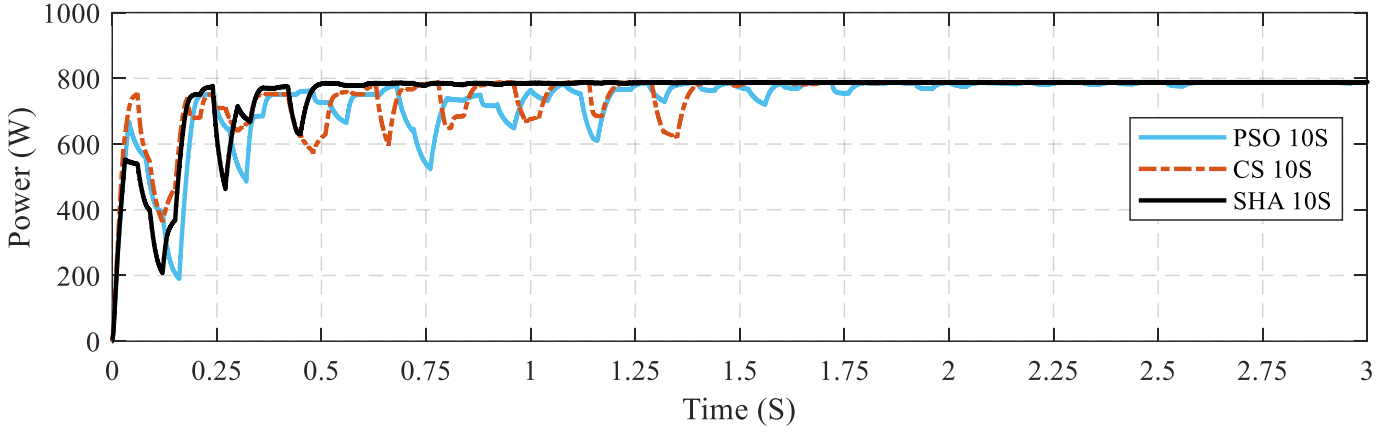


**Fig. 3.17** Performance of SHA, PSO and CS under 10S configuration

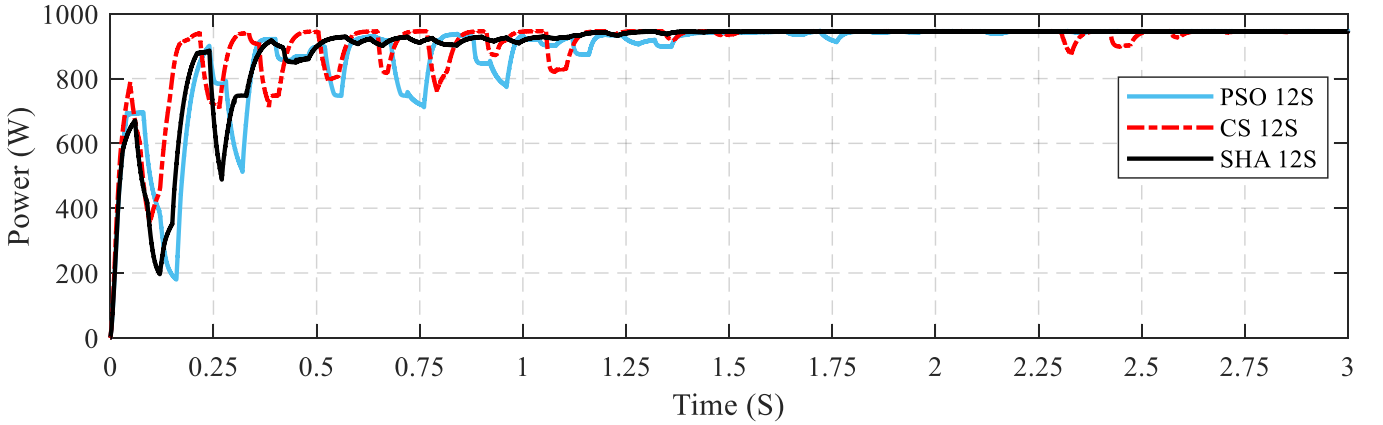


**Fig. 3.18** Performance of SHA, PSO and CS under 12S configuration

[Fig. 3.16](#) illustrates the power tracking process under shading pattern 5 using the 8S configuration. Under this case, the output P-V characteristic demonstrates seven peaks where the GMPP is at 741.9 W, as shown in [Fig. 3.3](#). Despite the complexity of this scenario, our optimizer could converge to the right GMPP within 0.67 s only performing 99.92 % static efficiency moreover, it experiences lower transient and steady-state fluctuations compared to PSO and CS. In counterparts, both PSO and CS could converge to the GMPP within 2.08 s and 1.36 s, successfully demonstrating lower dynamic efficiency compared to the proposed approach. [Fig. 3.17](#) illustrates the dynamic response for the 10S configuration. In this situation, the GMPP is at 788.4 W; additionally, the P-V characteristic exhibits two other local maxima that are very close to the global peak, which are located at 775.8 W and 763.5 W. Despite this complex scenario, our optimizer could converge to the GMPP within 0.5 s, accomplishing 100% static efficiency. In contrast, PSO

and CS came far behind the proposed approach regarding tracking time and power fluctuations. The SHA is finally tested against profile 7, constituting a more complex scenario to confirm its suitability and robustness in monitoring global maximum power tracking. The dynamic response for this profile is illustrated in [Fig. 3.18](#), which corresponds to the 12S configuration. Under this situation, the GMPP is at 946.3 W, and the output P-V demonstrates another adjacent local peak at 924.8 W; despite the slight difference between these two peaks, our optimizer could converge to the right GMPP within 1.16 s, performing 99.99% static efficiency. From these findings, we can conclude that the proposed SHA outperforms both PSO and CS regarding convergence time and power efficiency under all the addressed studied tests. The average convergence time is 0.78 s, whereas the average static efficiency is 99.97%. The detailed simulation results are depicted in [Table 3.6](#).

**Table. 3.6** Performance comparison of the SHA with other methods for the second set of shading profiles

SHADING PROFILES	PV CONFIGURATION	MPPT TECHNIQUE	P <sub>MAX</sub> (W)	TRACKED POWER (W)	CONVERGENCE TIME (S)	STATIC EFFICIENCY (%)	DYNAMIC EFFICIENCY (%)
Profile 5	8S	SHA	741.90	741.30	0.67	99.92	95.78
		PSO		741.10	2.08	99.89	92.45
		CS		740.60	1.36	99.82	94.87
Profile 6	10S	SHA	788.40	788.40	0.50	100.00	95.90
		PSO		788.20	2.58	99.97	92.98
		CS		788.30	1.50	99.98	94.75
Profile 7	12S	SHA	946.30	946.20	1.16	99.99	95.50
		PSO		946.00	1.82	99.96	93.16
		CS		943.90	2.62	99.74	95.45

### 3.6.6 Statistical analysis

It should be noted that SI optimizers are typically based on a random search process and do not ensure that the exact GMPP is tracked in each of their iterations. Therefore, a performance statistical analysis is required to verify the correctness of the proposed approach in tracking the correct GMPP under the different shading scenarios. A 100-trial test for the five shading profiles studied is carried out, where three criteria are considered in these tests: average MPPT power, standard deviation, and variance. The obtained results are represented in [Table. 3.7](#).

**Table 3.7** Statistical analysis of SHA against PSO and CS

SHADING PROFILES	MPPT TECHNIQUE	AVERAGE $P_{MPPT}$ (W)	STD	VAR
STC	SHA	992.85	0.05	0.0025
	PSO	995.50	0.20	0.0400
	CS	952.50	2.20	4.8400
Profile 1	SHA	445.85	0.05	0.0025
	PSO	445.65	0.25	0.0625
	CS	445.45	0.15	0.0225
Profile 2	SHA	483.20	0.10	0.0100
	PSO	483.45	0.15	0.0225
	CS	483.10	0.10	0.0100
Profile 3	SHA	634.50	0.60	0.3600
	PSO	629.05	0.95	0.9025
	CS	636.60	0.60	0.3600
Profile 4	SHA	802.10	0.10	0.0100
	PSO	800.85	0.85	0.7225
	CS	801.15	0.15	0.0225

The obtained results illustrated in [Table. 3.7](#) demonstrate the robustness of SHA and stability during the trial tests, where it shows the highest performance in terms of dispersion and scattering, which is confirmed by having the lowest values of standard deviation and variance under all cases. We can conclude that the SHA can handle GMPP successfully under diverse shading profiles. While SHA offers significant advantages in addressing the MPPT issue, the complexity of the hybrid method may lead to potential drawbacks such as computational complexity, limitations in extremely complex scenarios, and implementation challenges, especially when considering its adoption in practical PV systems.

### 3.6.7 Comparative study

To examine the proposed optimizer's performance compared to alternative MPPT techniques found in the literature, a performance evaluation of average convergence time and average steady-state efficiency is established; these averages are the obtained mean values during the different test scenarios. [Table. 3.8](#) depicts the performances of these MPPT techniques, while [Fig. 3.19](#) illustrates the graphical representation of the obtained results.

**Table 3.8** Performance comparison of the SHA with other SI-based MPPT techniques for the first set of shading profiles.

REFERENCE	MPPT TECHNIQUE	AVERAGE CONVERGENCE TIME (S)	AVERAGE STEADY-STATE EFFICIENCY (%)
Proposed technique	SHA	1.00	99.79
[126]	GWO-PSO	2.08	99.56
[127]	PS-FW	5.52	96.87
[129]	NA-PSO	4.00	98.90
[134]	An Improved Gray Wolf Optimizer	2.45	99.63
[137]	Seagull	1.14	97.86
[149]	GOA	3.05	99.66
[150]	DM-Jaya	1.20	99.87
[152]	An Improved Bat Algorithm	3.60	99.85
[153]	Bat-PO	5.60	99.80
[160]	Fusion FA	2.50	89.60
[164]	GOA-INC	2.38	99.85

Table 3.8, Fig. 3.19, and Fig. 3.20 illustrate the outperformance of the proposed SHA over many SI-based MPPT techniques in terms of convergence time and steady-state efficiency. The average convergence time of the proposed method under the first set of shading profiles is 1.00 s, whereas the average steady-state efficiency is 99.79 %. Moreover, the performance of our optimizer under the second series of tests is greatly enhanced, with a convergence time of 0.78 s and 99.97% steady state efficiency. This performance is due to the merit of fusing the two SI algorithms, namely PSO and CS, where the search process is highly improved at both the exploitation and exploration stages, where the least-performing elements are discarded and replaced by the best-performing ones using the exploration virtue of the CS algorithm. This performance makes the suggested optimizer highly recommended for tracking the GMPP under homogenous and nonhomogeneous weather conditions and rapid changes in irradiance.

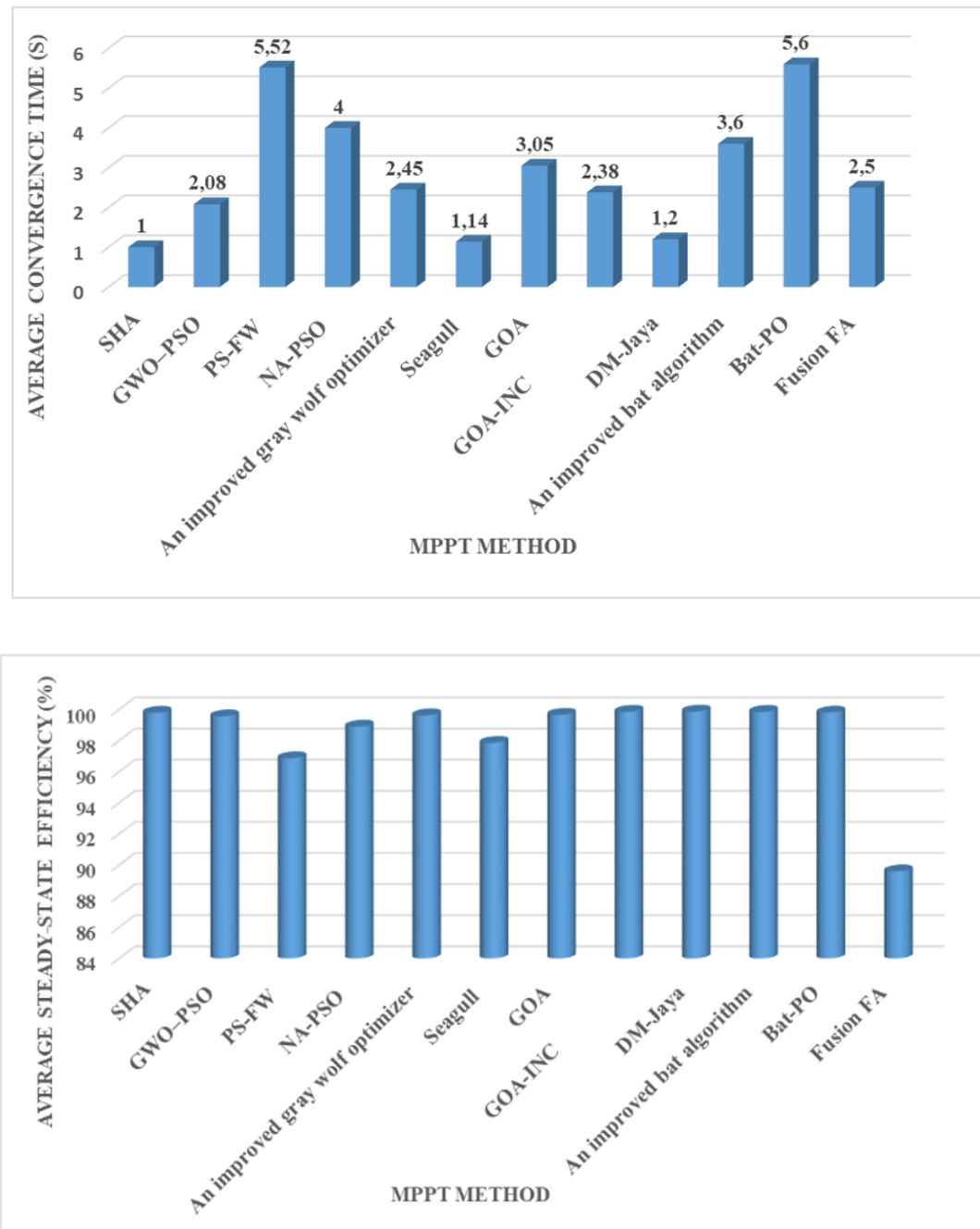


**Fig. 3.19** Graphical representation of average convergence time and average static efficiency for the first set of shading profiles

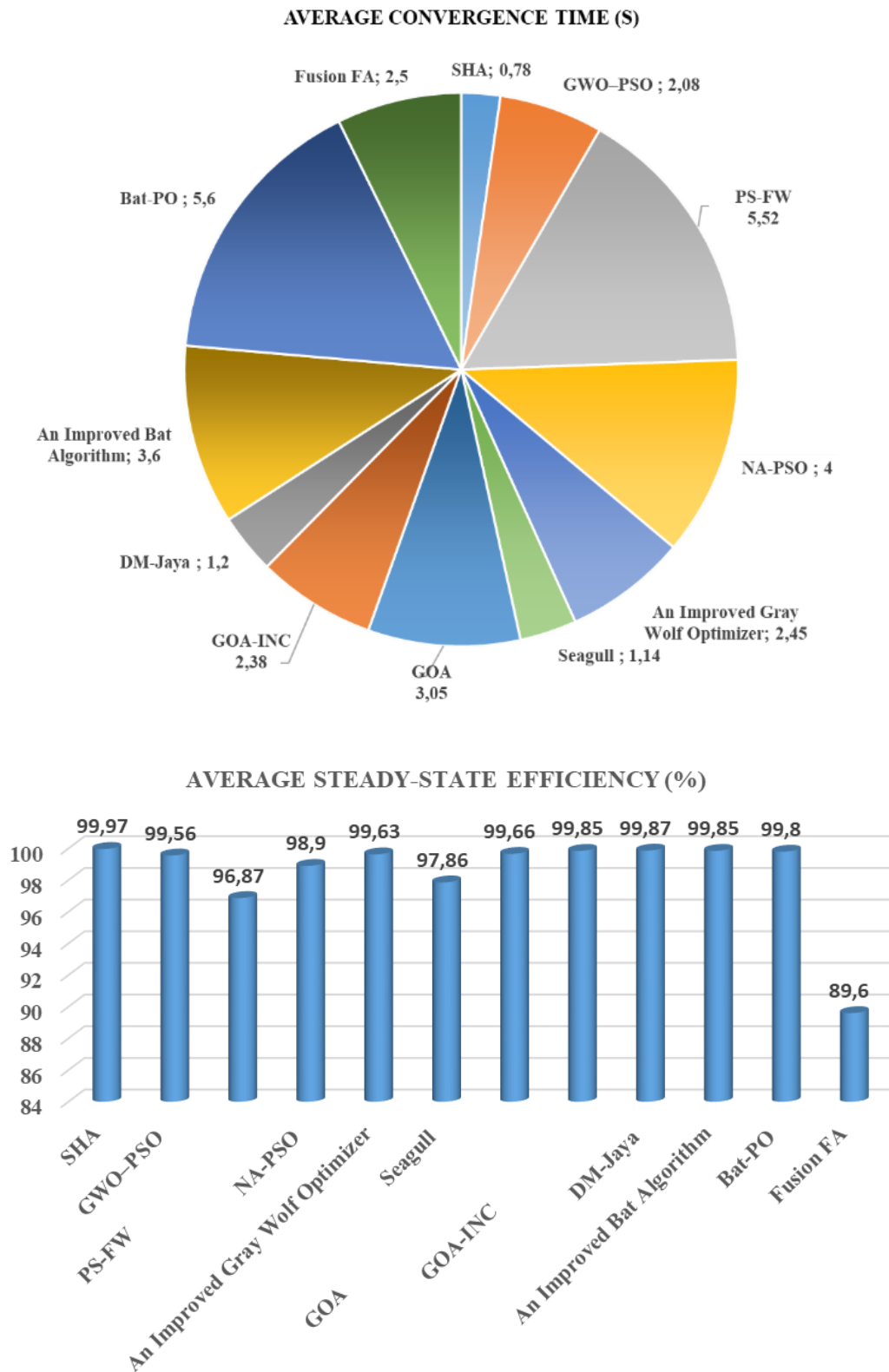


**Fig. 3.20** Graphical representation of average convergence time and average static efficiency for the second set of shading profiles

### **3.7 Conclusion**

In this chapter, a Novel Hybrid Algorithm called Smart Hybrid Algorithm (SHA) for GMPPT in PV systems subjected to PSCs is introduced. It combines two SI algorithms, namely PSO and CS. This hybridization extends their performances while reducing their disadvantages when used separately. The developed optimizer avoids the common disadvantages of conventional MPPT techniques and provides a simple and robust MPPT monitor to handle PS in PV systems effectively. Several tests were conducted thoroughly under STC, PSCs, and rapid irradiance change to examine the robustness and performance of the proposed approach in tracking the GMPP, using eight shading profiles in conjunction with two PV array configurations, 4S, 8S, 10S, 12S, and 4S2P. The proposed hybrid algorithm is benchmarked against PSO, CS, and PO algorithms. A performance comparison is carried out against well-known SI-based MPPT algorithms. The findings demonstrate its outperformance regarding convergence speed, power fluctuations during the search process, and steady-state and dynamic efficiencies. According to the results, the average steady-state efficiency exceeds 99.79%, whereas the average convergence time is less than one second. It also offers a convergence time reduction of at least 14% compared to other techniques. The suggested algorithm can track the GMPP under all test scenarios, regardless of the GMPP position. Our algorithm features a reset function embedded within the system to restart the search process at any change in weather conditions. The proposed approach comes with high performance due to the deep cooperation between PSO and CS, where the roles are exchanged between exploitation at the PSO level and exploration at the CS level. SHA is an Elitism-based MPPT algorithm since a performance evaluation of participating particles is done during the search process, where only the best-performing elements are kept. In contrast, the worst ones are destroyed and replaced with new particles. Based on the simulation findings, the suggested method is highly recommended for monitoring GMPP under all weather conditions. Because of the multiple benefits of this hybrid algorithm, this study will likely get significant attention from the PV community, academics and industry professionals.

### **General conclusion**

The generated energy from photovoltaic systems is considered one of the most efficient and well-desired renewable energy sources for small and large-scale power generation, because of its wide range of applications and long-term economic advantages. However, the PV array voltage and current characteristics are highly nonlinear and are severely affected by changing weather circumstances. Moreover, when the irradiation is not equally distributed, local and global maxima are introduced in the I-V and P-V curves. This issue prevents conventional MPPT techniques from obtaining the correct GMPP since these algorithms primarily focus on local search and thus cannot ensure the optimal global solution, leading to considerable power losses. Consequently, optimizing an algorithm that continually tracks the maximum power produced by PV arrays and extracts the GMPP from the PV system in real-time is vital. When environmental conditions change, the PV system's GMPP also changes to a new position, which imposes a new challenge; hence, tracking the MPP is inevitable.

To address this issue, the current study offers a novel approach to optimize the power generated from PV systems affected by PS circumstances. In this regard, this thesis emphasized improving the efficiency of PV systems subjected to partial shading effect through hybridizing two metaheuristic algorithms. These latter approaches are highly intelligent and self-learning algorithms with multiple interacting agents for finding the best solutions to complex optimization problems, simulating intelligent processes and comportment observed from nature. The main objective of this hybridization is to enhance the features of the involved Swarm Intelligence (SI) algorithms while reducing their shortcomings when used separately.

Particle Swarm Optimization (PSO) and Cuckoo Search Algorithm (CSA) are powerful optimization techniques that address various engineering optimization problems with several peaks. They prove many benefits in extracting the GMPP under PSCs. However, when used separately, they may demonstrate some difficulties, such as converging to a local optimum rather than the global maximum, especially under certain complicated PS scenarios, or when their tuning parameters are not adjusted precisely to follow the weather variations.

To overcome these limitations, this task is achieved thanks to the hybridization of these two well-known metaheuristic algorithms resulting in single and robust hybrid algorithm named Smart Hybrid Algorithm (SHA). The proposed algorithm is embedded into the MPPT function to



optimize the PV system's output power. Thus, the approach put forward in this work offers a number of significant improvements over the conventional techniques as well as many SI techniques found in the literature. Both algorithms work closely to ensure a high balance between exploitation and exploration. The Lévy flight search pattern is embedded into the SHA to boost its performance instead of the random searching technique at the exploration phase of the search process. Thus, this collaboration enables harvesting the GMPP delivered by the PV system under uniform and complex PSCs and alleviates each algorithm's drawbacks when used individually.

A comprehensive evaluation is carried out to justify our algorithm's viability. Several tests were conducted thoroughly under STC, PSCs, and rapid irradiance change to examine the robustness and performance of the proposed approach in tracking the GMPP, using eight shading profiles in conjunction with two PV array configurations, 4S, 8S, 10S, 12S, and 4S2P. The proposed SHA is benchmarked against PSO, CS, and PO algorithms. A performance comparison is carried out against several well-known SI-based MPPT algorithms. The findings demonstrate its outperformance regarding convergence speed, power fluctuations during the search process, and steady-state and dynamic efficiencies. According to the results, the average steady-state efficiency exceeds 99.79%, whereas the average convergence time is less than one second. It also offers a convergence time reduction of at least 14% compared to other techniques. The suggested algorithm can track the GMPP under all test scenarios, regardless of the GMPP position. Besides the points mentioned above, the proposed approach comes with these focal merits:

The main contribution of the proposed approach is hybridizing two swarm intelligence-based MPPT techniques to extend their performances while reducing their disadvantages when used separately.

- The proposed method for tracking the GMPP has yet to be described in any earlier technical publication on power optimization of PV systems under PSCs.

- The developed MPPT technique avoids the common disadvantages of conventional MPPT techniques and provides a simple and robust MPPT tracker to handle partial shading in PV systems effectively.

- Our optimizer features a reset function that detects any variation in weather circumstances to restart the search process for the new GMPP

- The SHA is independent of the number of iterations, as is considered in many iterative algorithms. These latter algorithms may reach the maximum number of iterations without converging to the real GMPP, resulting in premature convergence under some complex circumstances; however, the SHA is always in a standby position seeking the real GMPP.

- SHA is an Elitism-based MPPT algorithm since a performance evaluation of participating particles is done during the search process, where only the best-performing elements are kept. In contrast, the worst ones are destroyed and replaced with new particles.

- The SHA does not require prior knowledge of PV module characteristics.

Based on the simulation findings, the suggested method is highly recommended for monitoring GMPP under all weather conditions. Because of the multiple benefits of this hybrid algorithm, this study will likely get significant attention from the PV community, academics, and industry professionals.

### **Scope for future work**

We believe that the main contributions of our work can be extended to further research related to the outcomes of this thesis. Several avenues for improvement or extensions can be addressed to continue enhancing this work.

In our next contribution, we intend to add the GWO technique as a third method, conduct the necessary analysis, inject our optimizer into a grid-connected PV system, and perform experimental validation of the simulation results to authenticate its effectiveness in real-world partial shading scenarios.

### Bibliography

- [1] T.-Z. Ang, M. Salem, M. Kamarol, H. S. Das, M. A. Nazari and N. Prabakaran, « A comprehensive study of renewable energy sources: Classifications, challenges and suggestions », *Energy Strategy Reviews*, vol. 43, p. 100939, sept. 2022, doi: [10.1016/j.esr.2022.100939](https://doi.org/10.1016/j.esr.2022.100939).
- [2] J. Wang and W. Azam, « Natural resource scarcity, fossil fuel energy consumption and total greenhouse gas emissions in top emitting countries », *Geoscience Frontiers*, vol. 15, n° 2, p. 101757, march 2024, doi: [10.1016/j.gsf.2023.101757](https://doi.org/10.1016/j.gsf.2023.101757).
- [3] F. Barbir, T. N. Veziroğlu and H. J. Plass, « Environmental damage due to fossil fuels use », *International Journal of Hydrogen Energy*, vol. 15, n° 10, p. 739-749, 1990, doi: [10.1016/0360-3199\(90\)90005-J](https://doi.org/10.1016/0360-3199(90)90005-J).
- [4] P. A. Østergaard, N. Duic, Y. Noorollahi and S. Kalogirou, « Advances in renewable energy for sustainable development », *Renewable Energy*, vol. 219, p. 119377, dec. 2023, doi: [10.1016/j.renene.2023.119377](https://doi.org/10.1016/j.renene.2023.119377).
- [5] Z. Gareiou, E. Drimili and E. Zervas, « Public acceptance of renewable energy sources », in *Low Carbon Energy Technologies in Sustainable Energy Systems*, Elsevier, 2021, p. 309-327. doi: [10.1016/B978-0-12-822897-5.00012-2](https://doi.org/10.1016/B978-0-12-822897-5.00012-2).
- [6] F. Bashir and S. Gull, « The Role of Renewable Energy in Mitigating Climate Change », *SSRN Journal*, 2024, doi: [10.2139/ssrn.4833338](https://doi.org/10.2139/ssrn.4833338).
- [7] A. O. M. Maka and J. M. Alabid, « Solar energy technology and its roles in sustainable development », *Clean Energy*, vol. 6, n° 3, p. 476-483, June 2022, doi: [10.1093/ce/zkac023](https://doi.org/10.1093/ce/zkac023).
- [8] M. I. Blanco, « The economics of wind energy », *Renewable and Sustainable Energy Reviews*, vol. 13, n° 6-7, p. 1372-1382, aug.2009, doi: [10.1016/j.rser.2008.09.004](https://doi.org/10.1016/j.rser.2008.09.004).
- [9] A. M. Bagher, M. Vahid, M. Mohsen and D. Parvin, « Hydroelectric Energy Advantages and Disadvantages ». *American Journal of Energy Science*, april 2015; 2(2): 17-20.
- [10] T. Sharmin, N. R. Khan, M. S. Akram and M. M. Ehsan, « A State-of-the-Art Review on Geothermal Energy Extraction, Utilization, and Improvement Strategies: Conventional, Hybridized, and Enhanced Geothermal Systems », *International Journal of Thermofluids*, vol. 18, p. 100323, May 2023, doi: [10.1016/j.ijft.2023.100323](https://doi.org/10.1016/j.ijft.2023.100323).
- [11] E. E. Lora *et al.*, « Biomass electricity generation technologies: a review, technology selection procedure and power capacity calculation », in *Proceedings of the 25th International Congress of Mechanical Engineering*, ABCM, 2019. doi: [10.26678/ABCM.COBEM2019.COB2019-1628](https://doi.org/10.26678/ABCM.COBEM2019.COB2019-1628).
- [12] K. K. Jaiswal *et al.*, « Renewable and sustainable clean energy development and impact on social, economic and environmental health », *Energy Nexus*, vol. 7, p. 100118, sept. 2022, doi: [10.1016/j.nexus.2022.100118](https://doi.org/10.1016/j.nexus.2022.100118).
- [13] Q. Hassan, S. Algburi, A. Z. Sameen, H. M. Salman and M. Jaszczur, « A review of hybrid renewable energy systems: Solar and wind-powered solutions: Challenges, opportunities and policy implications », *Results in Engineering*, vol. 20, p. 101621, dec. 2023, doi: [10.1016/j.rineng.2023.101621](https://doi.org/10.1016/j.rineng.2023.101621).

- [14] F. Belhachat and C. Larbes, « Modeling, analysis and comparison of solar photovoltaic array configurations under partial shading conditions », *Solar Energy*, vol. 120, p. 399-418, oct. 2015, doi: [10.1016/j.solener.2015.07.039](https://doi.org/10.1016/j.solener.2015.07.039).
- [15] K. Lappalainen and S. Valkealahti, « Number of maximum power points in photovoltaic arrays during partial shading events by clouds », *Renewable Energy*, vol. 152, p. 812-822, june 2020, doi: [10.1016/j.renene.2020.01.119](https://doi.org/10.1016/j.renene.2020.01.119).
- [16] E. Paraskevadaki, S. Papathanassiou and G. Vokas, « Effects of Partial Shading on the PV Module Characteristic Curves », *MSF*, vol. 670, p. 391-398, dec. 2010, doi: [10.4028/www.scientific.net/MSF.670.391](https://doi.org/10.4028/www.scientific.net/MSF.670.391).
- [17] F. Bayrak, G. Ertürk and H. F. Oztop, « Effects of partial shading on energy and exergy efficiencies for photovoltaic panels », *Journal of Cleaner Production*, vol. 164, p. 58-69, oct. 2017, doi: [10.1016/j.jclepro.2017.06.108](https://doi.org/10.1016/j.jclepro.2017.06.108).
- [18] D. Craciunescu and L. Fara, « Investigation of the Partial Shading Effect of Photovoltaic Panels and Optimization of Their Performance Based on High-Efficiency FLC Algorithm », *Energies*, vol. 16, n° 3, p. 1169, jan. 2023, doi: [10.3390/en16031169](https://doi.org/10.3390/en16031169).
- [19] J. Ahmed and Z. Salam, « A critical evaluation on maximum power point tracking methods for partial shading in PV systems », *Renewable and Sustainable Energy Reviews*, vol. 47, p. 933-953, july 2015, doi: [10.1016/j.rser.2015.03.080](https://doi.org/10.1016/j.rser.2015.03.080).
- [20] F. Belhachat and C. Larbes, « A review of global maximum power point tracking techniques of photovoltaic system under partial shading conditions », *Renewable and Sustainable Energy Reviews*, vol. 92, p. 513-553, sept. 2018, doi: [10.1016/j.rser.2018.04.094](https://doi.org/10.1016/j.rser.2018.04.094).
- [21] D. Wang, D. Tan and L. Liu, « Particle swarm optimization algorithm: an overview », *Soft Comput*, vol. 22, n° 2, p. 387-408, jan. 2018, doi: [10.1007/s00500-016-2474-6](https://doi.org/10.1007/s00500-016-2474-6).
- [22] H. Chiroma *et al.*, « Bio-inspired computation: Recent development on the modifications of the cuckoo search algorithm », *Applied Soft Computing*, vol. 61, p. 149-173, dec. 2017, doi: [10.1016/j.asoc.2017.07.053](https://doi.org/10.1016/j.asoc.2017.07.053).
- [23] Y. Xiong, Z. Zou and J. Cheng, « Cuckoo search algorithm based on cloud model and its application », *Sci Rep*, vol. 13, n° 1, p. 10098, june 2023, doi: [10.1038/s41598-023-37326-3](https://doi.org/10.1038/s41598-023-37326-3).
- [24] N.-G. Park, M. Grätzel and T. Miyasaka, « *Organic-inorganic halide perovskite photovoltaics: from fundamentals to device architectures* », Cham: Springer, 2016.
- [25] R. W. Miles, K. M. Hynes and I. Forbes, « Photovoltaic solar cells: An overview of state-of-the-art cell development and environmental issues », *Progress in Crystal Growth and Characterization of Materials*, vol. 51, n° 1-3, p. 1-42, Jan. 2005, doi: [10.1016/j.pcrysgrow.2005.10.002](https://doi.org/10.1016/j.pcrysgrow.2005.10.002).
- [26] M. Eccher, A. Salemi, S. Turrini and R. S. Brusa, « Measurements of power transfer efficiency in CPV cell-array models using individual DC–DC converters », *Applied Energy*, vol. 142, p. 396-406, March 2015, doi: [10.1016/j.apenergy.2014.12.038](https://doi.org/10.1016/j.apenergy.2014.12.038).

- [27] R. Ramaprabha and B. L. Mathur, « A Comprehensive Review and Analysis of Solar Photovoltaic Array Configurations under Partial Shaded Conditions », *International Journal of Photoenergy*, vol. 2012, p. 1-16, 2012, doi: [10.1155/2012/120214](https://doi.org/10.1155/2012/120214).
- [28] S. Rühle, « Tabulated values of the Shockley–Queisser limit for single junction solar cells », *Solar Energy*, vol. 130, p. 139-147, June 2016, doi: [10.1016/j.solener.2016.02.015](https://doi.org/10.1016/j.solener.2016.02.015).
- [29] M. Ratner, « *The Physics of Solar Cells ; Third Generation Photovoltaics: Advanced Solar Energy Conversion* », *Physics Today*, vol. 57, n° 12, p. 71-72, dec. 2004, doi: [10.1063/1.1878345](https://doi.org/10.1063/1.1878345).
- [30] F. Dimroth *et al.*, « Four-Junction Wafer-Bonded Concentrator Solar Cells », *IEEE J. Photovoltaics*, vol. 6, n° 1, p. 343-349, Jan. 2016, doi: [10.1109/JPHOTOV.2015.2501729](https://doi.org/10.1109/JPHOTOV.2015.2501729).
- [31] R. M. Pujahari, « Solar cell technology », in *Energy Materials*, Elsevier, 2021, p. 27-60. doi: [10.1016/B978-0-12-823710-6.00007-8](https://doi.org/10.1016/B978-0-12-823710-6.00007-8).
- [32] L. Jiang, S. Cui, P. Sun, Y. Wang and C. Yang, « Comparison of Monocrystalline and Polycrystalline Solar Modules », in *2020 IEEE 5th Information Technology and Mechatronics Engineering Conference (ITOEC)*, Chongqing, China: IEEE, June 2020, p. 341-344. doi: [10.1109/ITOEC49072.2020.9141722](https://doi.org/10.1109/ITOEC49072.2020.9141722).
- [33] K. ElKhamisy, H. Abdelhamid, E.-S. M. El-Rabaie and N. Abdel-Salam, « A Comprehensive Survey of Silicon Thin-film Solar Cell: Challenges and Novel Trends », *Plasmonics*, vol. 19, n° 1, p. 1-20, Feb. 2024, doi: [10.1007/s11468-023-01905-x](https://doi.org/10.1007/s11468-023-01905-x).
- [34] G. Ganguly, « Improved sustainability of solar panels by improving stability of amorphous silicon solar cells », *Sci Rep*, vol. 13, n° 1, p. 10512, June 2023, doi: [10.1038/s41598-023-37386-5](https://doi.org/10.1038/s41598-023-37386-5).
- [35] M. A. Scarpulla *et al.*, « CdTe-based thin film photovoltaics: Recent advances, current challenges and future prospects », *Solar Energy Materials and Solar Cells*, vol. 255, p. 112289, June 2023, doi: [10.1016/j.solmat.2023.112289](https://doi.org/10.1016/j.solmat.2023.112289).
- [36] J. Ramanujam and U. P. Singh, « Copper indium gallium selenide based solar cells – a review », *Energy Environ. Sci.*, vol. 10, n° 6, p. 1306-1319, 2017, doi: [10.1039/C7EE00826K](https://doi.org/10.1039/C7EE00826K).
- [37] M. Khan *et al.*, « Improving the efficiency of dye-sensitized solar cells based on rare-earth metal modified bismuth ferrites », *Sci Rep*, vol. 13, n° 1, p. 3123, Feb. 2023, doi: [10.1038/s41598-023-30000-8](https://doi.org/10.1038/s41598-023-30000-8).
- [38] P. S. Pawar, P. A. Koyale, A. G. Dhodamani and S. D. Delekar, « Nanocrystalline metal oxide-based hybrids for third-generation solar cell technologies », in *Advances in Metal Oxides and Their Composites for Emerging Applications*, Elsevier, 2022, p. 263-286. doi: [10.1016/B978-0-323-85705-5.00018-X](https://doi.org/10.1016/B978-0-323-85705-5.00018-X).
- [39] M. M. Salah, A. Zekry, A. Shaker, M. Abouelatta, M. Mousa and A. Saeed, « Investigation of Electron Transport Material-Free Perovskite/CIGS Tandem Solar Cell », *Energies*, vol. 15, n° 17, p. 6326, Aug. 2022, doi: [10.3390/en15176326](https://doi.org/10.3390/en15176326).
- [40] M. A. Fikri *et al.*, « Recent progresses and challenges in cooling techniques of concentrated photovoltaic thermal system: A review with special treatment on phase change materials (PCMs)

based cooling », *Solar Energy Materials and Solar Cells*, vol. 241, p. 111739, July. 2022, doi: [10.1016/j.solmat.2022.111739](https://doi.org/10.1016/j.solmat.2022.111739).

[41] Felsberger, R.; Buchroithner, A.; Gerl, B.; Wegleiter, H. Conversion and Testing of a Solar Thermal Parabolic Trough Collector for CPV-T Application. *Energies* 2022, 13, 6142. <https://doi.org/10.3390/en13226142>

[42] A. Al Tarabsheh, M. Akmal and M. Ghazal, « Series Connected Photovoltaic Cells—Modelling and Analysis », *Sustainability*, vol. 9, n° 3, p. 371, March 2017, doi: [10.3390/su9030371](https://doi.org/10.3390/su9030371).

[43] H. Tian, F. Mancilla-David, K. Ellis, E. Muljadi and P. Jenkins, « A cell-to-module-to-array detailed model for photovoltaic panels », *Solar Energy*, vol. 86, n° 9, p. 2695-2706, Sept. 2012, doi: [10.1016/j.solener.2012.06.004](https://doi.org/10.1016/j.solener.2012.06.004).

[44] S. Bader, X. Ma and B. Oelmann, « One-diode photovoltaic model parameters at indoor illumination levels – A comparison », *Solar Energy*, vol. 180, p. 707-716, March 2019, doi: [10.1016/j.solener.2019.01.048](https://doi.org/10.1016/j.solener.2019.01.048).

[45] A. Padilla, C. Londoño, F. Jaramillo, I. Tovar, J. B. Cano and E. Velilla, « Photovoltaic performance assess by correcting the I-V curves in outdoor tests », *Solar Energy*, vol. 237, p. 11-18, May 2022, doi: [10.1016/j.solener.2022.03.064](https://doi.org/10.1016/j.solener.2022.03.064).

[46] V. Lo Brano and G. Ciulla, « An efficient analytical approach for obtaining a five parameters model of photovoltaic modules using only reference data », *Applied Energy*, vol. 111, p. 894-903, Nov. 2013, doi: [10.1016/j.apenergy.2013.06.046](https://doi.org/10.1016/j.apenergy.2013.06.046).

[47] A. R. Jordehi, « Parameter estimation of solar photovoltaic (PV) cells: A review », *Renewable and Sustainable Energy Reviews*, vol. 61, p. 354-371, Aug. 2016, doi: [10.1016/j.rser.2016.03.049](https://doi.org/10.1016/j.rser.2016.03.049).

[48] S. B. Prakash, G. Singh and S. Singh, « Modeling and Performance Analysis of Simplified Two-Diode Model of Photovoltaic Cells », *Front. Phys.*, vol. 9, p. 690588, Oct. 2021, doi: [10.3389/fphy.2021.690588](https://doi.org/10.3389/fphy.2021.690588).

[49] M. Hejri, H. Mokhtari, M. R. Azizian, M. Ghandhari and L. Soder, « On the Parameter Extraction of a Five-Parameter Double-Diode Model of Photovoltaic Cells and Modules », *IEEE J. Photovoltaics*, vol. 4, n° 3, p. 915-923, May 2014, doi: [10.1109/JPHOTOV.2014.2307161](https://doi.org/10.1109/JPHOTOV.2014.2307161).

[50] K. Tifidat and N. Maouhoub, « An efficient method for predicting PV modules performance based on the two-diode model and adaptable to the single-diode model », *Renewable Energy*, vol. 216, p. 119102, Nov. 2023, doi: [10.1016/j.renene.2023.119102](https://doi.org/10.1016/j.renene.2023.119102).

[51] N. M. Shannan, N. Z. Yahaya and B. Singh, « Two diode model for parameters extraction of PV module », in *2014 IEEE Conference on Energy Conversion (CENCON)*, Johor Bahru, Malaysia: IEEE, Oct. 2014, p. 260-264. doi: [10.1109/CENCON.2014.6967512](https://doi.org/10.1109/CENCON.2014.6967512).

[52] J. J. Soon, K.-S. Low and Shu Ting Goh, « Multi-dimension diode photovoltaic (PV) model for different PV cell technologies », in *2014 IEEE 23rd International Symposium on Industrial Electronics (ISIE)*, Istanbul, Turkey: IEEE, June 2014, p. 2496-2501. doi: [10.1109/ISIE.2014.6865012](https://doi.org/10.1109/ISIE.2014.6865012).



- [53] C. Caruana, « Power converters for renewable energy: solar », in *Encyclopedia of Electrical and Electronic Power Engineering*, Elsevier, 2023, p. 168-183. doi: [10.1016/B978-0-12-821204-2.00154-9](https://doi.org/10.1016/B978-0-12-821204-2.00154-9).
- [54] S. Harrison *et al.*, « Review of multiport power converters for distribution network applications », *Renewable and Sustainable Energy Reviews*, vol. 203, p. 114742, Oct. 2024, doi: [10.1016/j.rser.2024.114742](https://doi.org/10.1016/j.rser.2024.114742).
- [55] M. Ali, M. A. Koondhar, J. Ogale, A. Ali and B. Khan, « Intelligent hybrid energy system and grid integration using microcontrollers », *Computers and Electrical Engineering*, vol. 110, p. 108873, Sept. 2023, doi: [10.1016/j.compeleceng.2023.108873](https://doi.org/10.1016/j.compeleceng.2023.108873).
- [56] J. L. López, S. I. Seleme, P. F. Donoso, L. M. F. Morais, P. C. Cortizo and M. A. Severo, « Digital control strategy for a buck converter operating as a battery charger for stand-alone photovoltaic systems », *Solar Energy*, vol. 140, p. 171-187, Dec. 2016, doi: [10.1016/j.solener.2016.11.005](https://doi.org/10.1016/j.solener.2016.11.005).
- [57] A. Hayat, D. Sibtain, A. F. Murtaza, S. Shahzad, M. S. Jajja and H. Kilic, « Design and Analysis of Input Capacitor in DC–DC Boost Converter for Photovoltaic-Based Systems », *Sustainability*, vol. 15, n° 7, p. 6321, April 2023, doi: [10.3390/su15076321](https://doi.org/10.3390/su15076321).
- [58] J. Monteiro, V. F. Pires, D. Foito, A. Cordeiro, J. F. Silva and S. Pinto, « A Buck-Boost Converter with Extended Duty-Cycle Range in the Buck Voltage Region for Renewable Energy Sources », *Electronics*, vol. 12, n° 3, p. 584, Jan. 2023, doi: [10.3390/electronics12030584](https://doi.org/10.3390/electronics12030584).
- [59] A. M. Eltamaly, « Performance of MPPT Techniques of Photovoltaic Systems Under Normal and Partial Shading Conditions », in *Advances in Renewable Energies and Power Technologies*, Elsevier, 2018, p. 115-161. doi: [10.1016/B978-0-12-812959-3.00004-6](https://doi.org/10.1016/B978-0-12-812959-3.00004-6).
- [60] H. M. H. Farh, M. F. Othman, A. M. Eltamaly and M. S. Al-Saud, « Maximum Power Extraction from a Partially Shaded PV System Using an Interleaved Boost Converter », *Energies*, vol. 11, n° 10, p. 2543, Sept. 2018, doi: [10.3390/en11102543](https://doi.org/10.3390/en11102543).
- [61] L. Fialho, R. Melicio, V. M. F. Mendes, J. Figueiredo and M. Collares-Pereira, « Effect of Shading on Series Solar Modules: Simulation and Experimental Results », *Procedia Technology*, vol. 17, p. 295-302, 2014, doi: [10.1016/j.protcy.2014.10.240](https://doi.org/10.1016/j.protcy.2014.10.240).
- [62] Z. Salameh, « Photovoltaic », in *Renewable Energy System Design*, Elsevier, 2014, p. 33-113. doi: [10.1016/B978-0-12-374991-8.00002-7](https://doi.org/10.1016/B978-0-12-374991-8.00002-7).
- [63] K. Chen, S. Tian, Y. Cheng and L. Bai, « An Improved MPPT Controller for Photovoltaic System Under Partial Shading Condition », *IEEE Trans. Sustain. Energy*, vol. 5, n° 3, p. 978-985, July. 2014, doi: [10.1109/TSTE.2014.2315653](https://doi.org/10.1109/TSTE.2014.2315653).
- [64] K. Abdulmawjood, S. Alsadi, S. S. Refaat and W. G. Morsi, « Characteristic Study of Solar Photovoltaic Array Under Different Partial Shading Conditions », *IEEE Access*, vol. 10, p. 6856-6866, 2022, doi: [10.1109/ACCESS.2022.3142168](https://doi.org/10.1109/ACCESS.2022.3142168).
- [65] M. N. R. Nazeri, M. F. N. Tajuddin, T. S. Babu, A. Azmi, M. Malvoni and N. M. Kumar, « Firefly Algorithm-Based Photovoltaic Array Reconfiguration for Maximum Power Extraction during Mismatch Conditions », *Sustainability*, vol. 13, n° 6, p. 3206, March 2021, doi: [10.3390/su13063206](https://doi.org/10.3390/su13063206).

- [66] K. Chandrasekaran, S. Sankar and K. Banumalar, « Partial shading detection for PV arrays in a maximum power tracking system using the sine-cosine algorithm », *Energy for Sustainable Development*, vol. 55, p. 105-121, April 2020, doi: [10.1016/j.esd.2020.01.007](https://doi.org/10.1016/j.esd.2020.01.007).
- [67] F. Belhachat and C. Larbes, « Survey and Classification of Hybrid GMPPT Techniques for Photovoltaic System under Partial Shading Conditions », *ENPESJ*, vol. 2, n° 2, p. 31-46, Dec. 2022, doi: [10.53907/enpesj.v2i2.116](https://doi.org/10.53907/enpesj.v2i2.116).
- [68] N. Al-Tawalbeh, M. H. Zafar, M. A. M. Radzi, M. A. A. M. Zainuri and I. Al-Wesabi, « Novel initialization strategy: Optimizing conventional algorithms for global maximum power point tracking », *Results in Engineering*, vol. 22, p. 102067, June 2024, doi: [10.1016/j.rineng.2024.102067](https://doi.org/10.1016/j.rineng.2024.102067).
- [69] M. Seapan, Y. Hishikawa, M. Yoshita and K. Okajima, « Temperature and irradiance dependences of the current and voltage at maximum power of crystalline silicon PV devices », *Solar Energy*, vol. 204, p. 459-465, July. 2020, doi: [10.1016/j.solener.2020.05.019](https://doi.org/10.1016/j.solener.2020.05.019).
- [70] S. H. Hanzaei, S. A. Gorji and M. Ektesabi, « A Scheme-Based Review of MPPT Techniques With Respect to Input Variables Including Solar Irradiance and PV Arrays' Temperature », *IEEE Access*, vol. 8, p. 182229-182239, 2020, doi: [10.1109/ACCESS.2020.3028580](https://doi.org/10.1109/ACCESS.2020.3028580).
- [71] M. Q. Duong, G. N. Sava, G. Ionescu, H. Necula, S. Leva and M. Mussetta, « Optimal bypass diode configuration for PV arrays under shading influence », in *2017 IEEE International Conference on Environment and Electrical Engineering and 2017 IEEE Industrial and Commercial Power Systems Europe (EEEIC / I&CPS Europe)*, Milan, Italy: IEEE, June 2017, p. 1-5. doi: [10.1109/EEEIC.2017.7977526](https://doi.org/10.1109/EEEIC.2017.7977526).
- [72] O. Bozorg-Haddad, *Advanced Optimization by Nature-Inspired Algorithms*. In *Studies in Computational Intelligence*, vol. 720, Springer, 2018. doi: [10.1007/978-981-10-5221-7](https://doi.org/10.1007/978-981-10-5221-7).
- [73] A. E. Badoud, « Real-Time Experimental Analysis of Hybrid BG-FL Based MPPT Controller for a Photovoltaic System Under Partial Shading Conditions », in *2022 19th International Multi-Conference on Systems, Signals & Devices (SSD)*, Sétif, Algeria: IEEE, May 2022, p. 1409-1414. doi: [10.1109/SSD54932.2022.9955848](https://doi.org/10.1109/SSD54932.2022.9955848).
- [74] R. Vieira, F. De Araújo, M. Dhimish and M. Guerra, « A Comprehensive Review on Bypass Diode Application on Photovoltaic Modules », *Energies*, vol. 13, n° 10, p. 2472, May 2020, doi: [10.3390/en13102472](https://doi.org/10.3390/en13102472).
- [75] A. Bidram, A. Davoudi and R. S. Balog, « Control and Circuit Techniques to Mitigate Partial Shading Effects in Photovoltaic Arrays », *IEEE J. Photovoltaics*, vol. 2, n° 4, p. 532-546, Oct. 2012, doi: [10.1109/JPHOTOV.2012.2202879](https://doi.org/10.1109/JPHOTOV.2012.2202879).
- [76] P. K. Bonthagorla and S. Mikkili, « Performance analysis of PV array configurations ( SP , BL , HC and TT ) to enhance maximum power under non-uniform shading conditions », *Engineering Reports*, vol. 2, n° 8, p. e12214, Aug. 2020, doi: [10.1002/eng2.12214](https://doi.org/10.1002/eng2.12214).
- [77] O. Bingöl and B. Özkaya, « Analysis and comparison of different PV array configurations under partial shading conditions », *Solar Energy*, vol. 160, p. 336-343, Jan. 2018, doi: [10.1016/j.solener.2017.12.004](https://doi.org/10.1016/j.solener.2017.12.004).



- [78] V. Gautam, S. Khatoon, M. F. Jalil and R. C. Bansal, « Comparative analysis of various reconfiguration strategies of PV array in partial shading conditions: a review », *International Journal of Modelling and Simulation*, p. 1-34, Sept. 2024, doi: [10.1080/02286203.2024.2403008](https://doi.org/10.1080/02286203.2024.2403008).
- [79] G. Harish Kumar Varma, V. R. Barry and R. K. Jain, « A Novel Magic Square Based Physical Reconfiguration for Power Enhancement in Larger Size Photovoltaic Array », *IETE Journal of Research*, vol. 69, n° 7, p. 4644-4657, Sept. 2023, doi: [10.1080/03772063.2021.1944333](https://doi.org/10.1080/03772063.2021.1944333).
- [80] G. Meerimatha and B. L. Rao, « Novel reconfiguration approach to reduce line losses of the photovoltaic array under various shading conditions », *Energy*, vol. 196, p. 117120, April 2020, doi: [10.1016/j.energy.2020.117120](https://doi.org/10.1016/j.energy.2020.117120).
- [81] F. Belhachat and C. Larbes, « PV array reconfiguration techniques for maximum power optimization under partial shading conditions: A review », *Solar Energy*, vol. 230, p. 558-582, Dec. 2021, doi: [10.1016/j.solener.2021.09.089](https://doi.org/10.1016/j.solener.2021.09.089).
- [82] D. Sharma, M. F. Jalil, M. S. Ansari and R. C. Bansal, « A review of PV array reconfiguration techniques for maximum power extraction under partial shading conditions », *Optik*, vol. 275, p. 170559, March 2023, doi: [10.1016/j.ijleo.2023.170559](https://doi.org/10.1016/j.ijleo.2023.170559).
- [83] F. Belhachat and C. Larbes, « Photovoltaic array reconfiguration strategies for mitigating partial shading Effects: Recent advances and perspectives », *Energy Conversion and Management*, vol. 313, p. 118547, Aug. 2024, doi: [10.1016/j.enconman.2024.118547](https://doi.org/10.1016/j.enconman.2024.118547).
- [84] D. Yousri, D. Allam and Magdy. B. Eteiba, « Optimal photovoltaic array reconfiguration for alleviating the partial shading influence based on a modified harris hawks optimizer », *Energy Conversion and Management*, vol. 206, p. 112470, Feb. 2020, doi: [10.1016/j.enconman.2020.112470](https://doi.org/10.1016/j.enconman.2020.112470).
- [85] D. Li, H. Zhou, Y. Zhou, Y. Rao and W. Yao, « Atom Search Optimization-Based PV Array Reconfiguration Technique under Partial Shading Condition », *International Transactions on Electrical Energy Systems*, vol. 2023, p. 1-15, April 2023, doi: [10.1155/2023/8685976](https://doi.org/10.1155/2023/8685976).
- [86] Y. Wang and B. Yang, « Optimal PV array reconfiguration under partial shading condition through dynamic leader based collective intelligence », *Prot Control Mod Power Syst*, vol. 8, n° 1, p. 40, Dec. 2023, doi: [10.1186/s41601-023-00315-9](https://doi.org/10.1186/s41601-023-00315-9).
- [87] M. Mao, L. Cui, Q. Zhang, K. Guo, L. Zhou and H. Huang, « Classification and summarization of solar photovoltaic MPPT techniques: A review based on traditional and intelligent control strategies », *Energy Reports*, vol. 6, p. 1312-1327, Nov. 2020, doi: [10.1016/j.egyr.2020.05.013](https://doi.org/10.1016/j.egyr.2020.05.013).
- [88] H. Islam et al., « Performance Evaluation of Maximum Power Point Tracking Approaches and Photovoltaic Systems », *Energies*, vol. 11, n° 2, p. 365, Feb. 2018, doi: [10.3390/en11020365](https://doi.org/10.3390/en11020365).
- [89] H. H. H. Mousa, A.-R. Youssef and E. E. M. Mohamed, « State of the art perturb and observe MPPT algorithms based wind energy conversion systems: A technology review », *International Journal of Electrical Power & Energy Systems*, vol. 126, p. 106598, March 2021, doi: [10.1016/j.ijepes.2020.106598](https://doi.org/10.1016/j.ijepes.2020.106598).

- [90] A. Asnil, R. Nazir, K. Krismadinata and M. N. Sonni, « Performance Analysis of an Incremental Conductance MPPT Algorithm for Photovoltaic Systems Under Rapid Irradiance Changes », *TEM Journal*, p. 1087-1094, May 2024, doi: [10.18421/TEM132-23](https://doi.org/10.18421/TEM132-23).
- [91] D. Baimel, S. Tapuchi, Y. Levron and J. Belikov, « Improved Fractional Open Circuit Voltage MPPT Methods for PV Systems », *Electronics*, vol. 8, n° 3, p. 321, March 2019, doi: [10.3390/electronics8030321](https://doi.org/10.3390/electronics8030321)
- [92] H. P. Corrêa and F. H. T. Vieira, « Hybrid sensor-aided direct duty cycle control approach for maximum power point tracking in two-stage photovoltaic systems », *International Journal of Electrical Power & Energy Systems*, vol. 145, p. 108690, Feb. 2023, doi: [10.1016/j.ijepes.2022.108690](https://doi.org/10.1016/j.ijepes.2022.108690).
- [93] W. He, F. Liu, J. Ji, S. Zhang and H. Chen, « Safety Analysis of Solar Module under Partial Shading », *International Journal of Photoenergy*, vol. 2015, p. 1-8, 2015, doi: [10.1155/2015/907282](https://doi.org/10.1155/2015/907282).
- [94] M. A. Danandeh and S. M. Mousavi G., « Comparative and comprehensive review of maximum power point tracking methods for PV cells », *Renewable and Sustainable Energy Reviews*, vol. 82, p. 2743-2767, Feb. 2018, doi: [10.1016/j.rser.2017.10.009](https://doi.org/10.1016/j.rser.2017.10.009).
- [95] R. Eberhart and J. Kennedy, « A new optimizer using particle swarm theory », in *MHS'95. Proceedings of the Sixth International Symposium on Micro Machine and Human Science*, Nagoya, Japan: IEEE, 1995, p. 39-43. doi: [10.1109/MHS.1995.494215](https://doi.org/10.1109/MHS.1995.494215).
- [96] Rezk and A. M. Eltamaly, « A comprehensive comparison of different MPPT techniques for photovoltaic systems », *Solar Energy*, vol. 112, p. 1-11, Feb. 2015, doi: [10.1016/j.solener.2014.11.010](https://doi.org/10.1016/j.solener.2014.11.010).
- [97] M. Seyedmahmoudian *et al.*, « State of the art artificial intelligence-based MPPT techniques for mitigating partial shading effects on PV systems – A review », *Renewable and Sustainable Energy Reviews*, vol. 64, p. 435-455, Oct. 2016, doi: [10.1016/j.rser.2016.06.053](https://doi.org/10.1016/j.rser.2016.06.053).
- [98] R. Rahmani, R. Yusof, M. Seyedmahmoudian and S. Mekhilef, « Hybrid technique of ant colony and particle swarm optimization for short term wind energy forecasting », *Journal of Wind Engineering and Industrial Aerodynamics*, vol. 123, p. 163-170, Dec. 2013, doi: [10.1016/j.jweia.2013.10.004](https://doi.org/10.1016/j.jweia.2013.10.004).
- [99] A. Scaria, K. George and J. Sebastian, « An Artificial Bee Colony Approach for Multi-objective Job Shop Scheduling », *Procedia Technology*, vol. 25, p. 1030-1037, 2016, doi: [10.1016/j.protcy.2016.08.203](https://doi.org/10.1016/j.protcy.2016.08.203).
- [100] Y. Shaiek, M. Ben Smida, A. Sakly and M. F. Mimouni, « Comparison between conventional methods and GA approach for maximum power point tracking of shaded solar PV generators », *Solar Energy*, vol. 90, p. 107-122, April. 2013, doi: [10.1016/j.solener.2013.01.005](https://doi.org/10.1016/j.solener.2013.01.005).
- [101] A. A. Kulaksız et R. Akkaya, « A genetic algorithm optimized ANN-based MPPT algorithm for a stand-alone PV system with induction motor drive », *Solar Energy*, vol. 86, n° 9, p. 2366-2375, Sept. 2012, doi: [10.1016/j.solener.2012.05.006](https://doi.org/10.1016/j.solener.2012.05.006).

- [102] M. F. N. Tajuddin, S. M. Ayob, Z. Salam and M. S. Saad, « Evolutionary based maximum power point tracking technique using differential evolution algorithm », *Energy and Buildings*, vol. 67, p. 245-252, Dec. 2013, doi: [10.1016/j.enbuild.2013.07.085](https://doi.org/10.1016/j.enbuild.2013.07.085).
- [103] M. F. N. Tajuddin, S. M. Ayob and Z. Salam, « Tracking of maximum power point in partial shading condition using differential evolution (DE) », in *2012 IEEE International Conference on Power and Energy (PECon)*, Kota Kinabalu, Malaysia: IEEE, Dec. 2012, p. 384-389. doi: [10.1109/PECon.2012.6450242](https://doi.org/10.1109/PECon.2012.6450242).
- [104] M. I. Mosaad, M. O. Abed el-Raouf, M. A. Al-Ahmar and F. A. Banakher, « Maximum Power Point Tracking of PV system Based Cuckoo Search Algorithm; review and comparison », *Energy Procedia*, vol. 162, p. 117-126, Apr. 2019, doi: [10.1016/j.egypro.2019.04.013](https://doi.org/10.1016/j.egypro.2019.04.013).
- [105] S. Mohanty, B. Subudhi and P. K. Ray, « A New MPPT Design Using Grey Wolf Optimization Technique for Photovoltaic System Under Partial Shading Conditions », *IEEE Trans. Sustain. Energy*, vol. 7, n° 1, p. 181-188, Jan. 2016, doi: [10.1109/TSTE.2015.2482120](https://doi.org/10.1109/TSTE.2015.2482120).
- [106] M. V. Rocha, L. P. Sampaio and S. A. O. Da Silva, « Maximum Power Point Extraction in PV Array Under Partial Shading Conditions Using GWO-Assisted Beta Method », *RE&PQJ*, vol. 16, n° 4, Jan. 2024, doi: [10.24084/repqj16.346](https://doi.org/10.24084/repqj16.346).
- [107] X.-S. Yang, « Flower Pollination Algorithm for Global Optimization », in *Unconventional Computation and Natural Computation*, vol. 7445, J. Durand-Lose et N. Jonoska, Éd., in Lecture Notes in Computer Science, vol. 7445, Berlin, Heidelberg: Springer Berlin Heidelberg, 2012, p. 240-249. doi: [10.1007/978-3-642-32894-7\\_27](https://doi.org/10.1007/978-3-642-32894-7_27).
- [108] X.-S. Yang, « Firefly Algorithms for Multimodal Optimization », in *Stochastic Algorithms: Foundations and Applications*, vol. 5792, O. Watanabe et T. Zeugmann, Éd., in Lecture Notes in Computer Science, vol. 5792, Berlin, Heidelberg: Springer Berlin Heidelberg, 2009, p. 169-178. doi: [10.1007/978-3-642-04944-6\\_14](https://doi.org/10.1007/978-3-642-04944-6_14).
- [109] K. Sundareswaran, S. Peddapatil and S. Palani, « MPPT of PV Systems Under Partial Shaded Conditions Through a Colony of Flashing Fireflies », *IEEE Trans. Energy Convers.*, vol. 29, n° 2, p. 463-472, June 2014, doi: [10.1109/TEC.2014.2298237](https://doi.org/10.1109/TEC.2014.2298237).
- [110] K. Kaced, C. Larbes, N. Ramzan, M. Bounabi and Z. E. Dahmane, « Bat algorithm based maximum power point tracking for photovoltaic system under partial shading conditions », *Solar Energy*, vol. 158, p. 490-503, Dec. 2017, doi: [10.1016/j.solener.2017.09.063](https://doi.org/10.1016/j.solener.2017.09.063).
- [111] R. Bennis, C. Larbes and F. Belhachat, « Maximum Power Point Tracking Under Fast Changing Irradiance Using Hybrid Fuzzy-PO Algorithm », in *Artificial Intelligence and Heuristics for Smart Energy Efficiency in Smart Cities*, vol. 361, M. Hatti, Éd., in Lecture Notes in Networks and Systems, vol. 361, Cham: Springer International Publishing, 2022, p. 155-166. doi: [10.1007/978-3-030-92038-8\\_15](https://doi.org/10.1007/978-3-030-92038-8_15).
- [112] C. G. Villegas-Mier, J. Rodriguez-Resendiz, J. M. Álvarez-Alvarado, H. Rodriguez-Resendiz, A. M. Herrera-Navarro and O. Rodríguez-Abreo, « Artificial Neural Networks in MPPT Algorithms for Optimization of Photovoltaic Power Systems: A Review », *Micromachines*, vol. 12, n° 10, p. 1260, Oct. 2021, doi: [10.3390/mi12101260](https://doi.org/10.3390/mi12101260).

- [113] M. A. M. Shaheen, H. M. Hasanien and A. Alkuhayli, « A novel hybrid GWO-PSO optimization technique for optimal reactive power dispatch problem solution », *Ain Shams Engineering Journal*, vol. 12, n° 1, p. 621-630, March 2021, doi: [10.1016/j.asej.2020.07.011](https://doi.org/10.1016/j.asej.2020.07.011).
- [114] K. Sundareswaran, V. Vignesh Kumar and S. Palani, « Application of a combined particle swarm optimization and perturb and observe method for MPPT in PV systems under partial shading conditions », *Renewable Energy*, vol. 75, p. 308-317, March 2015, doi: [10.1016/j.renene.2014.09.044](https://doi.org/10.1016/j.renene.2014.09.044).
- [115] G. Calvino, J. Pombo, S. Mariano and M. D. Rosario Calado, « Design and Implementation of MPPT System Based on PSO Algorithm », in *2018 International Conference on Intelligent Systems (IS)*, Funchal - Madeira, Portugal: IEEE, Sept. 2018, p. 733-738. doi: [10.1109/IS.2018.8710479](https://doi.org/10.1109/IS.2018.8710479).
- [116] A. Ibrahim, R. Aboelsaud and S. Obukhov, « Improved particle swarm optimization for global maximum power point tracking of partially shaded PV array », *Electr Eng*, vol. 101, n° 2, p. 443-455, June 2019, doi: [10.1007/s00202-019-00794-w](https://doi.org/10.1007/s00202-019-00794-w).
- [117] M. Alshareef, Z. Lin, M. Ma and W. Cao, « Accelerated Particle Swarm Optimization for Photovoltaic Maximum Power Point Tracking under Partial Shading Conditions », *Energies*, vol. 12, n° 4, p. 623, Feb. 2019, doi: [10.3390/en12040623](https://doi.org/10.3390/en12040623).
- [118] M. H. Zafar *et al.*, « Group Teaching Optimization Algorithm Based MPPT Control of PV Systems under Partial Shading and Complex Partial Shading », *Electronics*, vol. 9, n° 11, p. 1962, Nov. 2020, doi: [10.3390/electronics9111962](https://doi.org/10.3390/electronics9111962).
- [119] M. L. Kathe, A. B. Makokha, S. O. Zachary and M. S. Adaramola, « A Comprehensive Review of Maximum Power Point Tracking (MPPT) Techniques Used in Solar PV Systems », *Energies*, vol. 16, n° 5, p. 2206, Feb. 2023, doi: [10.3390/en16052206](https://doi.org/10.3390/en16052206).
- [120] J. S. Koh, R. H. G. Tan, W. H. Lim and N. M. L. Tan, « A Modified Particle Swarm Optimization for Efficient Maximum Power Point Tracking Under Partial Shading Condition », *IEEE Trans. Sustain. Energy*, vol. 14, n° 3, p. 1822-1834, July. 2023, doi: [10.1109/TSTE.2023.3250710](https://doi.org/10.1109/TSTE.2023.3250710).
- [121] C. B. Nzoundja Fapi, H. Tchakounté, M. Ndje, P. Wira and M. Kamta, « Extraction of the Global Maximum Power for PV System under PSC Using an Improved PSO Technique », *Period. Polytech. Elec. Eng. Comp. Sci.*, vol. 68, n° 1, p. 64-73, Sept. 2023, doi: [10.3311/PPee.22254](https://doi.org/10.3311/PPee.22254).
- [122] C. Charin, D. Ishak, M. A. A. Mohd Zainuri, B. Ismail and M. K. Mohd Jamil, « A hybrid of bio-inspired algorithm based on Levy flight and particle swarm optimizations for photovoltaic system under partial shading conditions », *Solar Energy*, vol. 217, p. 1-14, March 2021, doi: [10.1016/j.solener.2021.01.049](https://doi.org/10.1016/j.solener.2021.01.049).
- [123] H. Li, D. Yang, W. Su, J. Lu and X. Yu, « An Overall Distribution Particle Swarm Optimization MPPT Algorithm for Photovoltaic System Under Partial Shading », *IEEE Trans. Ind. Electron.*, vol. 66, n° 1, p. 265-275, Jan. 2019, doi: [10.1109/TIE.2018.2829668](https://doi.org/10.1109/TIE.2018.2829668).
- [124] F. Keyrouz, « Enhanced Bayesian Based MPPT Controller for PV Systems », *IEEE Power Energy Technol. Syst. J.*, vol. 5, n° 1, p. 11-17, March 2018, doi: [10.1109/JPETS.2018.2811708](https://doi.org/10.1109/JPETS.2018.2811708).

- [125] L. Guo and N. M. M. Abdul, « Design and Evaluation of Fuzzy Adaptive Particle Swarm Optimization Based Maximum Power Point Tracking on Photovoltaic System Under Partial Shading Conditions », *Front. Energy Res.*, vol. 9, p. 712175, July. 2021, doi: [10.3389/fenrg.2021.712175](https://doi.org/10.3389/fenrg.2021.712175).
- [126] S. Chtita *et al.*, « A novel hybrid GWO–PSO-based maximum power point tracking for photovoltaic systems operating under partial shading conditions », *Sci Rep*, vol. 12, n° 1, p. 10637, June 2022, doi: [10.1038/s41598-022-14733-6](https://doi.org/10.1038/s41598-022-14733-6).
- [127] L. G. K. Chai, L. Gopal, F. H. Juwono, C. W. R. Chiong, H.-C. Ling and T. A. Basuki, « A novel global MPPT technique using improved PS-FW algorithm for PV system under partial shading conditions », *Energy Conversion and Management*, vol. 246, p. 114639, Oct. 2021, doi: [10.1016/j.enconman.2021.114639](https://doi.org/10.1016/j.enconman.2021.114639).
- [128] M. Seyedmahmoudian *et al.*, « Simulation and Hardware Implementation of New Maximum Power Point Tracking Technique for Partially Shaded PV System Using Hybrid DEPSO Method », *IEEE Trans. Sustain. Energy*, vol. 6, n° 3, p. 850-862, July. 2015, doi: [10.1109/TSTE.2015.2413359](https://doi.org/10.1109/TSTE.2015.2413359).
- [129] A. M. Eltamaly, H. M. H. Farh and A. G. Abokhalil, « A novel PSO strategy for improving dynamic change partial shading photovoltaic maximum power point tracker », *Energy Sources, Part A: Recovery, Utilization and Environmental Effects*, p. 1-15, May 2020, doi: [10.1080/15567036.2020.1769774](https://doi.org/10.1080/15567036.2020.1769774).
- [130] D. K. Mathi and R. Chinthamalla, « A hybrid global maximum power point tracking of partially shaded PV system under load variation by using adaptive salp swarm and differential evolution – perturb & observe technique », *Energy Sources, Part A: Recovery, Utilization and Environmental Effects*, vol. 43, n° 20, p. 2471-2495, Oct. 2021, doi: [10.1080/15567036.2020.1850927](https://doi.org/10.1080/15567036.2020.1850927).
- [131] D. K. Mathi and R. Chinthamalla, « Global maximum power point tracking technique based on adaptive salp swarm algorithm and P&O techniques for a PV string under partially shaded conditions », *Energy Sources, Part A: Recovery, Utilization and Environmental Effects*, p. 1-18, April 2020, doi: [10.1080/15567036.2020.1755391](https://doi.org/10.1080/15567036.2020.1755391).
- [132] S. Mohanty, B. Subudhi and P. K. Ray, « A Grey Wolf-Assisted Perturb & Observe MPPT Algorithm for a PV System », *IEEE Trans. Energy Convers.*, vol. 32, n° 1, p. 340-347, March 2017, doi: [10.1109/TEC.2016.2633722](https://doi.org/10.1109/TEC.2016.2633722).
- [133] K. Krishnaram, T. Suresh Padmanabhan, F. Alsaif and S. Senthilkumar, « Development of grey wolf optimization based modified fast terminal sliding mode controller for three phase interleaved boost converter fed PV system », *Sci Rep*, vol. 14, n° 1, p. 9256, April 2024, doi: [10.1038/s41598-024-59900-z](https://doi.org/10.1038/s41598-024-59900-z).
- [134] K. Guo, L. Cui, M. Mao, L. Zhou and Q. Zhang, « An Improved Gray Wolf Optimizer MPPT Algorithm for PV System With BFBIC Converter Under Partial Shading », *IEEE Access*, vol. 8, p. 103476-103490, 2020, doi: [10.1109/ACCESS.2020.2999311](https://doi.org/10.1109/ACCESS.2020.2999311).
- [135] M. Kumar, K. P. Panda, J. C. Rosas-Caro, A. Valderrabano-Gonzalez and G. Panda, « Comprehensive Review of Conventional and Emerging Maximum Power Point Tracking



Algorithms for Uniformly and Partially Shaded Solar Photovoltaic Systems », *IEEE Access*, vol. 11, p. 31778-31812, 2023, doi: [10.1109/ACCESS.2023.3262502](https://doi.org/10.1109/ACCESS.2023.3262502).

[136] C. Hussaian Basha, M. Palati, C. Dhanamjayulu, S. M. Muyeen and P. Venkatareddy, « A novel on design and implementation of hybrid MPPT controllers for solar PV systems under various partial shading conditions », *Sci Rep*, vol. 14, n° 1, p. 1609, Jan. 2024, doi: [10.1038/s41598-023-49278-9](https://doi.org/10.1038/s41598-023-49278-9).

[137] A. Chalh, R. Chaibi, A. E. Hammoumi, S. Motahhir, A. E. Ghzizal and M. Al-Dhaifallah, « A novel MPPT design based on the seagull optimization algorithm for photovoltaic systems operating under partial shading », *Sci Rep*, vol. 12, n° 1, p. 21804, Dec. 2022, doi: [10.1038/s41598-022-26284-x](https://doi.org/10.1038/s41598-022-26284-x).

[138] I. Al-Wesabi et al., « Cuckoo Search Combined with PID Controller for Maximum Power Extraction of Partially Shaded Photovoltaic System », *Energies*, vol. 15, n° 7, p. 2513, March 2022, doi: [10.3390/en15072513](https://doi.org/10.3390/en15072513).

[139] P. Qi, H. Xia, X. Cai, M. Yu, N. Jiang and Y. Dai, « Novel Global MPPT Technique Based on Hybrid Cuckoo Search and Artificial Bee Colony under Partial-Shading Conditions », *Electronics*, vol. 13, n° 7, p. 1337, April 2024, doi: [10.3390/electronics13071337](https://doi.org/10.3390/electronics13071337).

[140] B. S. Goud, P. S. Varma, B. L. Rao, M. S. K. Reddy, A. Pandian and Ch. R. Reddy, « Cuckoo Search Optimization based MPPT for Integrated DFIG-Wind Energy System », in *2020 International Conference on Decision Aid Sciences and Application (DASA)*, Sakheer, Bahrain: IEEE, Nov. 2020, p. 636-639. doi: [10.1109/DASA51403.2020.9317072](https://doi.org/10.1109/DASA51403.2020.9317072).

[141] M. Kumar and J. S. Lather, « Comparative Performance Analysis of PV module using PSO and CSA Techniques », in *2020 First IEEE International Conference on Measurement, Instrumentation, Control and Automation (ICMICA)*, Kurukshetra, India: IEEE, June 2020, p. 1-5. doi: [10.1109/ICMICA48462.2020.9242834](https://doi.org/10.1109/ICMICA48462.2020.9242834).

[142] D. A. Nugraha, K. L. Lian and Suwarno, « A Novel MPPT Method Based on Cuckoo Search Algorithm and Golden Section Search Algorithm for Partially Shaded PV System », *Can. J. Electr. Comput. Eng.*, vol. 42, n° 3, p. 173-182, 2019, doi: [10.1109/CJECE.2019.2914723](https://doi.org/10.1109/CJECE.2019.2914723).

[143] A. Harrison, N. H. Alombah and J. De Dieu Nguimfack Ndongmo, « Solar irradiance estimation and optimum power region localization in PV energy systems under partial shaded condition », *Heliyon*, vol. 9, n° 8, p. e18434, August 2023, doi: [10.1016/j.heliyon.2023.e18434](https://doi.org/10.1016/j.heliyon.2023.e18434).

[144] K. Ali, Q. Khan, S. Ullah, I. Khan and L. Khan, « Nonlinear robust integral backstepping based MPPT control for stand-alone photovoltaic system », *PLoS ONE*, vol. 15, n° 5, p. e0231749, May 2020, doi: [10.1371/journal.pone.0231749](https://doi.org/10.1371/journal.pone.0231749).

[145] M. Mohammadinodoushan, R. Abbassi, H. Jerbi, F. Waly Ahmed, H. Abdalqadir Kh Ahmed and A. Rezvani, « A new MPPT design using variable step size perturb and observe method for PV system under partially shaded conditions by modified shuffled frog leaping algorithm- SMC controller », *Sustainable Energy Technologies and Assessments*, vol. 45, p. 101056, June 2021, doi: [10.1016/j.seta.2021.101056](https://doi.org/10.1016/j.seta.2021.101056).

[146] M. H. Zafar, N. M. Khan, A. F. Mirza and M. Mansoor, « Bio-inspired optimization algorithms based maximum power point tracking technique for photovoltaic systems under partial

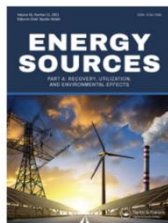
- shading and complex partial shading conditions », *Journal of Cleaner Production*, vol. 309, p. 127279, August 2021, doi: [10.1016/j.jclepro.2021.127279](https://doi.org/10.1016/j.jclepro.2021.127279).
- [147] A. F. Mirza, M. Mansoor, Q. Ling, B. Yin and M. Y. Javed, « A Salp-Swarm Optimization based MPPT technique for harvesting maximum energy from PV systems under partial shading conditions », *Energy Conversion and Management*, vol. 209, p. 112625, April 2020, doi: [10.1016/j.enconman.2020.112625](https://doi.org/10.1016/j.enconman.2020.112625).
- [148] M. Premkumar, C. Kumar, R. Sowmya and J. Pradeep, « A novel salp swarm assisted hybrid maximum power point tracking algorithm for the solar photovoltaic power generation systems », *Automatika*, vol. 62, n° 1, p. 1-20, Jan. 2021, doi: [10.1080/00051144.2020.1834062](https://doi.org/10.1080/00051144.2020.1834062).
- [149] R. Sridhar, C. Subramani and S. Pathy, « A grasshopper optimization algorithm aided maximum power point tracking for partially shaded photovoltaic systems », *Computers & Electrical Engineering*, vol. 92, p. 107124, June 2021, doi: [10.1016/j.compeleceng.2021.107124](https://doi.org/10.1016/j.compeleceng.2021.107124).
- [150] H. Deboucha, S. Mekhilef, S. Belaid and A. Guichi, « Modified deterministic Jaya (DM-Jaya)-based MPPT algorithm under partially shaded conditions for PV system », *IET power electron.*, vol. 13, n° 19, p. 4625-4632, Dec. 2020, doi: [10.1049/iet-pel.2020.0736](https://doi.org/10.1049/iet-pel.2020.0736).
- [151] Kulu. Amadu. Amalo, S. I. Birninkudu, B. B. Bukata, A. T. Salawudeen and A. A. Ahmad, « Cultured Bat Algorithm for Optimized MPPT Tracking Under Different Shading Conditions », in *2020 International Conference in Mathematics, Computer Engineering and Computer Science (ICMCECS)*, Ayobo, Ipaja, Lagos, Nigeria: IEEE, March 2020, p. 1-8. doi: [10.1109/ICMCECS47690.2020.246985](https://doi.org/10.1109/ICMCECS47690.2020.246985).
- [152] C. Y. Liao, R. K. Subroto, I. S. Millah, K. L. Lian and W.-T. Huang, « An Improved Bat Algorithm for More Efficient and Faster Maximum Power Point Tracking for a Photovoltaic System Under Partial Shading Conditions », *IEEE Access*, vol. 8, p. 96378-96390, 2020, doi: [10.1109/ACCESS.2020.2993361](https://doi.org/10.1109/ACCESS.2020.2993361).
- [153] M. V. Da Rocha, L. P. Sampaio and S. A. O. Da Silva, « Comparative analysis of MPPT algorithms based on Bat algorithm for PV systems under partial shading condition », *Sustainable Energy Technologies and Assessments*, vol. 40, p. 100761, Aug. 2020, doi: [10.1016/j.seta.2020.100761](https://doi.org/10.1016/j.seta.2020.100761).
- [154] S. Titri, C. Larbes, K. Y. Toumi and K. Benatchba, « A new MPPT controller based on the Ant colony optimization algorithm for Photovoltaic systems under partial shading conditions », *Applied Soft Computing*, vol. 58, p. 465-479, Sept. 2017, doi: [10.1016/j.asoc.2017.05.017](https://doi.org/10.1016/j.asoc.2017.05.017).
- [155] K. Sundareswaran, V. Vigneshkumar, P. Sankar, S. P. Simon, P. Srinivasa Rao Nayak and S. Palani, « Development of an Improved P&O Algorithm Assisted Through a Colony of Foraging Ants for MPPT in PV System », *IEEE Trans. Ind. Inf.*, vol. 12, n° 1, p. 187-200, Feb. 2016, doi: [10.1109/TII.2015.2502428](https://doi.org/10.1109/TII.2015.2502428).
- [156] L. L. Jiang and D. L. Maskell, « A uniform implementation scheme for evolutionary optimization algorithms and the experimental implementation of an ACO based MPPT for PV systems under partial shading », in *2014 IEEE Symposium on Computational Intelligence Applications in Smart Grid (CIASG)*, Orlando, FL, USA, Dec. 2014, p. 1-8, doi: [10.1109/CIASG.2014.7011560](https://doi.org/10.1109/CIASG.2014.7011560).

- [157] C. Gonzalez-Castano, C. Restrepo, S. Kouro and J. Rodriguez, « MPPT Algorithm Based on Artificial Bee Colony for PV System », *IEEE Access*, vol. 9, p. 43121-43133, 2021, doi: [10.1109/ACCESS.2021.3066281](https://doi.org/10.1109/ACCESS.2021.3066281).
- [158] A. soufyane Benyoucef, A. Chouder, K. Kara, S. Silvestre and O. A. sahed, « Artificial bee colony based algorithm for maximum power point tracking (MPPT) for PV systems operating under partial shaded conditions », *Applied Soft Computing*, vol. 32, p. 38-48, July. 2015, doi: [10.1016/j.asoc.2015.03.047](https://doi.org/10.1016/j.asoc.2015.03.047).
- [159] K. Sundareswaran, V. Vigneshkumar, S. P. Simon and P. S. R. Nayak, « Gravitational search algorithm combined with P&O method for MPPT in PV systems », in *2016 IEEE Annual India Conference (INDICON)*, Bangalore, India: IEEE, Dec. 2016, p. 1-5. doi: [10.1109/INDICON.2016.7838956](https://doi.org/10.1109/INDICON.2016.7838956).
- [160] Y.-P. Huang, M.-Y. Huang and C.-E. Ye, « A Fusion Firefly Algorithm With Simplified Propagation for Photovoltaic MPPT Under Partial Shading Conditions », *IEEE Trans. Sustain. Energy*, vol. 11, n° 4, p. 2641-2652, Oct. 2020, doi: [10.1109/TSTE.2020.2968752](https://doi.org/10.1109/TSTE.2020.2968752).
- [161] A. S. Joshi, O. Kulkarni, G. M. Kakandikar and V. M. Nandedkar, « Cuckoo Search Optimization- A Review », *Materials Today: Proceedings*, vol. 4, n° 8, p. 7262-7269, 2017, doi: [10.1016/j.matpr.2017.07.055](https://doi.org/10.1016/j.matpr.2017.07.055).
- [162] M. Hijjawi *et al.*, « Accelerated Arithmetic Optimization Algorithm by Cuckoo Search for Solving Engineering Design Problems », *Processes*, vol. 11, n° 5, p. 1380, May 2023, doi: [10.3390/pr11051380](https://doi.org/10.3390/pr11051380).
- [163] R. D. A.Almunem, D. H. Muhsen, H. T. Haider and T. Khatib, « A novel method for modeling of photovoltaic modules based on arithmetic optimization algorithm and cuckoo search », *Optik*, vol. 298, p. 171591, March 2024, doi: [10.1016/j.ijleo.2023.171591](https://doi.org/10.1016/j.ijleo.2023.171591).
- [164] B. H. Wijaya, R. K. Subroto, K. L. Lian and N. Hariyanto, « A Maximum Power Point Tracking Method Based on a Modified Grasshopper Algorithm Combined with Incremental Conductance », *Energies*, vol. 13, n° 17, p. 4329, Aug. 2020, doi: [10.3390/en13174329](https://doi.org/10.3390/en13174329).

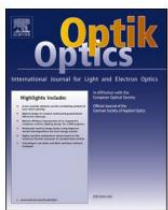


## Publications

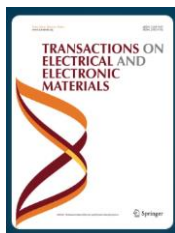
### Articles:



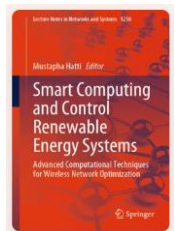
R. Bennia, F. Belhachat and C. Larbes, « Smart hybrid algorithm for global maximum power point tracking under partial shading conditions », *Energy Sources, Part A: Recovery, Utilization and Environmental Effects*, vol. 46, n° 1, p. 14779-14808, dec. 2024, doi: [10.1080/15567036.2024.2417089](https://doi.org/10.1080/15567036.2024.2417089).



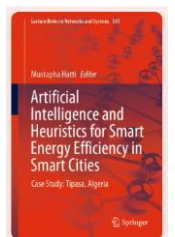
F. Belhachat, C. Larbes and R. Bennia, « Recent advances in fault detection techniques for photovoltaic systems: An overview, classification and performance evaluation », *Optik*, vol. 306, p. 171797, July. 2024, doi: [10.1016/j.ijleo.2024.171797](https://doi.org/10.1016/j.ijleo.2024.171797).



A. Yousfi, O Saidani, R. Bennia, F. Saad Saoud, L. Saidi, S. Bhattarai, Md. R. Islame, Md. F. Rahman, G. Sahoo., « Numerical Simulation of High-Efficiency Double-Absorber Layer Perovskite Solar Cells Using SCAPS- 1D and MATLAB PV Models », *Trans. Electr. Electron. Mater.*, avr. 2025, doi: [10.1007/s42341-025-00606-y](https://doi.org/10.1007/s42341-025-00606-y).



F. Belhachat, C. Larbes, & R. Bennia, « Empowering MPPT Efficiency in Partial Shading with Machine Learning Driven Metaheuristic Strategies: Recent Developments », in *Smart Computing and Control Renewable Energy Systems*, vol. 1238, M. Hatti, Éd., in Lecture Notes in Networks and Systems, vol. 1238. , Cham: Springer Nature Switzerland, 2025, p. 594-612. doi: [10.1007/978-3-031-80301-7\\_64](https://doi.org/10.1007/978-3-031-80301-7_64).



R. Bennia, C. Larbes and F. Belhachat, « Maximum Power Point Tracking Under Fast Changing Irradiance Using Hybrid Fuzzy-PO Algorithm », in *Artificial Intelligence and Heuristics for Smart Energy Efficiency in Smart Cities*, vol. 361, M. Hatti, Éd., in Lecture Notes in Networks and Systems, vol. 361. , Cham: Springer International Publishing, 2022, p. 155-166. doi: [10.1007/978-3-030-92038-8\\_15](https://doi.org/10.1007/978-3-030-92038-8_15).

### International and National Conferences

F. Belhachat, C. larbes, R. Bennia, « Empowering MPPT Efficiency in Partial - Shading with Machine Learning Driven Metaheuristic Strategies: Recent Developments », in the 8<sup>th</sup> international conference on Artificial Intelligence in Renewable Energetic Systems” ICAIRES 2024 – Tipasa

R. Bennia, F. Belhachat, C. Larbes, A. Yousfi & O. Saidani «Power Optimization in PV systems Subjected to Partial Shading Conditions using Soft Computing Techniques», in the Third International Conference on Materials, Energy & Environment (MEE'2025) ” April 21-22, 2025 in El Oued – Algeria.

F. Belhachat, R. Bennia & C. Larbes « Advanced Metaheuristic Strategies for Optimizing Power Output in Photovoltaic Systems under Partial Shading Conditions », in the Third International Conference on Materials, Energy & Environment (MEE'2025) ” April 21-22, 2025 in El Oued – Algeria.

F. Belhachat, R. Bennia & C. Larbes « Analysis of Fault Effects on Photovoltaic Array Configurations for Optimized System Efficiency », in the Third International Conference on Materials, Energy & Environment (MEE'2025) ” April 21-22, 2025 in El Oued – Algeria.

R. Bennia, F. Belhachat, C. Larbes, A. Yousfi, Okba, Saidani & R. Zerrougui , «Energy enhancement in PV arrays driven modern and conventional optimization techniques under mismatching conditions», in The First International Conference on Green Engineering. University Of Mohamed El Bachir El Ibrahimi of Bordj Bou Arreridj, Algeria. May 12-13, 2025.

F. Belhachat, R. Bennia & C. Larbes « Embedded Solutions for Optimizing Performance in Photovoltaic Systems », in The First International Conference on Green Engineering. University Of Mohamed El Bachir El Ibrahimi of Bordj Bou Arreridj, Algeria. May 12-13, 2025.

R. Bennia, F. Belhachat, C. Larbes, A. Yousfi & Okba Saidani «Performance Improvement of Partially Shaded PV Systems through Optimization Algorithms: Comparative Analysis of Classical and Recent Techniques », in The First National Conference on Renewable Energies and Advanced Electrical Engineering (NC-EAEE'25). Mohammed BOUDIAF University of M'Sila - May 06-07th, 2025

R. Bennia, C. Larbes, F. Belhachat & R. Zerrougui , «Energy Optimization in Photovoltaic Generation Systems Subjected to Partial Shading Conditions: a Bioinspired Approach», in the 2nd NATIONAL SEMINAR OF PHYSICS, CHEMISTRY AND THEIR APPLICATIONS (NSPCA'25). University Of Mohamed El Bachir El Ibrahimi of Bordj Bou Arreridj, Algeria. February 17th -18th, 2025

R. Bennia, F. Belhachat & C. Larbes «Maximum Power Point Tracking in Photovoltaic Systems Driven Conventional and Metaheuristic Techniques », in The The Third Algerian Symposium on Renewable Energy & Materials ASREM'25 . University of Medea, Ouzera University Campus, Medea, Algeria April 24th,2025, Medea- Algeria

F. Belhachat, R. Bennia & C. Larbes « Optimizing Photovoltaic System Efficiency under Partial Shading Using Metaheuristic Algorithms », in The The Third Algerian Symposium on Renewable Energy & Materials ASREM'25 . University of Medea, Ouzera University Campus, Medea, Algeria April 24th,2025, Medea- Algeria

R. Bennia, C. Larbes, F. Belhachat, « Optimum Power Monitoring in PV systems Subjected to Partial Shading Conditions: a Metaheuristic Approach», in The 2nd national conference on electronics,

electrical engineering, telecommunications and computer vision - (C3ETCV'24) - November 2024 - Mila, Algeria.

F. Belhachat, C. Larbes, R. Bennia, « Monitoring and Analysis of a Photovoltaic System Performance », in The 2nd national conference on electronics, electrical engineering, telecommunications and computer vision - (C3ETCV'24) - November 2024 - Mila, Algeria.

R. Bennia, C. Larbes, F. Belhachat, « Particle Swarm Optimization for Global Maximum power point tracking under partial shading conditions», in the 1<sup>st</sup> International Conference on Electronics Technology of Telecommunications Advanced Applications. 2ETA 2023, University of Bordj Bou Arréridj.

R. Bennia, C. Larbes and F. Belhachat, « Maximum Power Point Tracking Under Fast Changing Irradiance Using Hybrid Fuzzy-PO Algorithm », in *Artificial Intelligence and Heuristics for Smart Energy Efficiency in Smart Cities*, vol. 361, M. Hatti, Éd., in Lecture Notes in Networks and Systems, vol. 361., Cham: Springer International Publishing, 2022, p. 155-166. doi: [10.1007/978-3-030-92038-8\\_15](https://doi.org/10.1007/978-3-030-92038-8_15).

F. Belhachat, C. Larbes, R. Bennia, « Design and Comparison of Two Intelligent Controllers for Global Maximum Power Point Tracking of PV System under Partial Shading Conditions », in the Electrical Engineering International Conference (EEIC'19) 4-5 Dec, 2019, University of Bejaia.

S. khennouf, H. Sayoud, R. Bennia. « Automatic categorization system of old documents for author identification purpose », in the first national conference on electronics ( NCENT'2015) May 19-20, M'Sila, Algeria.